

**University of Alberta**

**An Examination of Linking and Blocking Procedures for Use  
in Deflection Cantilever Array-Based Protein Detection**

by

Remko van den Hurk

A thesis submitted to the Faculty of Graduate Studies and Research  
in partial fulfillment of the requirements for the degree of

Master of Science

in

Microsystems and Nanodevices

Electrical and Computer Engineering

©Remko van den Hurk

Fall 2011

Edmonton, Alberta

Permission is hereby granted to the University of Alberta Libraries to reproduce single copies of this thesis and to lend or sell such copies for private, scholarly or scientific research purposes only. Where the thesis is converted to, or otherwise made available in digital form, the University of Alberta will advise potential users of the thesis of these terms.

The author reserves all other publication and other rights in association with the copyright in the thesis and, except as herein before provided, neither the thesis nor any substantial portion thereof may be printed or otherwise reproduced in any material form whatsoever without the author's prior written permission.

# Abstract

In this project common linking and blocking procedures were examined for use in multiplexed deflection cantilever array-based detection of proteins. A human interferon gamma (INF- $\gamma$ ) enzyme-linked immunosorbent assay (ELISA) kit was used to evaluate the effectiveness of the linking and blocking procedures using fluorescence and ELISA assays. The most effective linking and blocking procedures were then implemented on arrays of deflection cantilevers. Separating the active and reference cantilever signals proved to be challenging due to varying deflection in buffer solution. Background subtractions were implemented which reduced the nonspecific buffer deflection. Following the background subtractions 16 out of 52 experiments produced one or more data sets with a clearly defined separation between all the active and reference signals. The most successful linkers, reference cantilever blockers and cantilever backside blockers were Prolinker B, glutaraldehyde and EDC/Sulfo-NHS; canine capture antibody and INF- $\gamma$ ; and a thermal PEG-silanization procedure and PEG-thiol, respectively.

# Acknowledgements

There are a number of people I would like to thank for their aid in completing this project. Firstly I would like to thank my advisor Dr. Stephane Evoy for his support and guidance and my parents Drs Sylvia and Jan van den Hurk for their encouragement and advice. I'd also like to thank several past and present group members for their advice and input including Sarang Dutt, Nick Glass, Nathan Nelson-Fitzpatrick, and Dr. Amit Singh. Additionally, I'd like to acknowledge the staff at the biology lab at the National Institute for Nanotechnology and the University of Alberta Nanofab facility for their training and advice. Finally, I'd like to recognize the National Sciences and Engineering Council of Canada and the Alberta Ingenuity fund for their financial support.

# Table of Contents

<b>Chapter 1: Introduction .....</b>	<b>1</b>
<b>Chapter 2: Background and Research Rationale .....</b>	<b>7</b>
2.1 Enzyme Linked ImmunoSorbent Assay .....	7
2.2 Fluorescence .....	12
2.3 Cantilever-Based Sensor Technology .....	14
2.3.1 Principles of Cantilever-Based Sensor Technology .....	15
2.3.2 A Review of Static Cantilever-Based Protein Detection .....	20
2.4 Research Rationale and Approach .....	29
<b>Chapter 3: Analysis of Linking and Blocking Procedures by Fluorescence and Enzyme Linked Immunosorbent Assays .....</b>	<b>31</b>
3.1 Materials and Solutions.....	33
3.1.1 Materials .....	33
3.1.2 Solutions .....	34
3.1.3 Linking and Blocking Procedures.....	35
3.2 R&D Systems Enzyme Linked Immunosorbent Assay Protocol .....	37
3.3 Examination of Interferon Gamma and Capture Antibody binding on gold surfaces by Fluorescence .....	39
3.3.1 Examination of Murine Antibody Density on Gold Chips with Fluorescent Rabbit Anti-Mouse Immunoglobulin G Antibodies.....	41
3.3.2 Examination of Human Interferon Gamma Density on Gold Chips with Fluorescent Mouse Anti-Human Interferon Gamma Antibodies .....	43
3.3.3 Discussion.....	46
3.4 Examination of the Effect of Experimental Conditions on Interferon Gamma Detection by Enzyme Linked Immunosorbent Assay.....	47
3.4.1 Examination of Prolinker A, Prolinker B and Protein A Conditions.....	48
3.4.2 Optimization of Capture Antibody and Protein A Concentrations .....	51
3.4.3 Examination of Protein Binding on Silicon Surfaces .....	53
3.4.4 Discussion.....	55

3.5 Comparison of Linking and Blocking Procedures by Enzyme Linked Immunosorbent Assay .....	57
3.5.1 Individual Linker Measurements .....	58
3.5.2 Simultaneous Linker Measurements .....	66
3.5.3 Examination of Blocking Efficiency .....	69
3.5.4 Discussion .....	72
3.6 Summary .....	76

## **Chapter 4: Deflection Cantilever Array-Based Detection of Interferon**

<b>Gamma</b> .....	<b>80</b>
4.1 Materials and Solutions .....	81
4.1.1 Materials .....	81
4.1.2 Solutions .....	81
4.1.3 Cantilever Sensing Platform and Functionalization Unit .....	81
4.2 Cantilever Drift and Potential Correction Methods .....	82
4.2.1 Cantilever Drift .....	83
4.2.2 Classification of Cantilever Deflection Results .....	86
4.2.3 Drift Corrections .....	86
4.3 Cantilever Deflection Results .....	89
4.3.1 Detection of INF- $\gamma$ Using Prolinker B as the Linker .....	89
4.3.2 Detection of INF- $\gamma$ Using Glutaraldehyde as the Linker .....	100
4.3.3 Detection of INF- $\gamma$ Using 1-Ethyl-3-[3-dimethylaminopropyl] carbodiimide/N-hydroxysulfosuccinimide as the Linkers .....	107
4.3.4 Detection of Biotin with Streptavidin and Hydrocarbon-thiols with Gold .....	108
4.4 A Discussion of the Experimental Conditions and their Effects on the Cantilever Measurements .....	111
4.4.1 Gold Coating .....	111
4.4.2 Buffers .....	112
4.4.3 Cantilever Blocking .....	114
4.4.3.1 Backside Blocking .....	114
4.4.3.2 Reference Cantilever Blocking .....	116

4.4.4	Linking Methods .....	116
4.4.5	Temperature and Sequential Deflection.....	119
4.4.6	INF- $\gamma$ Concentration .....	120
4.5	Summary .....	121
<b>Chapter 5: Summary and Recommendations .....</b>		<b>124</b>
<b>References .....</b>		<b>131</b>

## List of Tables

Table 3.1: Summation of the pixel values from representative fluorescence images of Alexa Fluor 350 rabbit anti-mouse IgG-labeled hC-Ab.....	43
Table 3.2: Summation of the pixel values from representative fluorescence images of human INF- $\gamma$ labeled by Alexa Fluor 488 mouse anti-human INF- $\gamma$ antibodies .....	45
Table 3.3: Summation of the pixel values from representative fluorescence images of human INF- $\gamma$ labeled by Alexa Fluor 488 mouse anti-human INF- $\gamma$ antibodies .....	46
Table 3.4: Summary of the examination of protein binding on silicon surfaces ..	54
Table 3.5: OD results from control chips of six linkers.....	68
Table 4.1: Summary of cantilever classification results .....	88

# List of Figures

Figure 2.1: Legend for ELISA and fluorescence schematic depictions.....	8
Figure 2.2: Schematic depiction of a direct ELISA .....	9
Figure 2.3: Schematic depiction of an Indirect ELISA assay .....	9
Figure 2.4: Schematic depiction of three different sandwich ELISAs .....	12
Figure 2.5: Simplified Jablonski diagram of electron states which cause fluorescence .....	12
Figure 2.6: Diagram of a cantilever array optical readout system.....	16
Figure 2.7: Resonance peak shift following mass loading. ....	18
Figure 3.1: OD results from the R&D Systems ELISA Protocol .....	39
Figure 3.2: Schematic representation of the measurement of C-Ab with a fluorescent anti-mouse antibody .....	40
Figure 3.3: Schematic representation of the measurement of INF- $\gamma$ with fluorescent anti-human INF- $\gamma$ antibody .....	41
Figure 3.4: Examination of Prolinker A, Prolinker B and Protein A linking conditions with ELISA. ....	50
Figure 3.5: Examination of Prolinker A, Prolinker B and Protein A linking conditions with ELISA. ....	51
Figure 3.6: The effect of increasing Protein A concentration on INF- $\gamma$ binding..	53
Figure 3.7: The effect of increasing C-Ab concentration on INF- $\gamma$ binding.....	53
Figure 3.8: Examination of protein adhesion to silicon and gold. ....	55
Figure 3.9: OD results from the DSP linking procedure in two separate experiments.....	60
Figure 3.10: OD results from the glutaraldehyde linking procedure in two separate experiments. ....	62
Figure 3.11: OD results from the Protein A linking procedure in two separate experiments. ....	63
Figure 3.12: OD results from the DSP-PEG linking procedure in two separate experiments. ....	64

Figure 3.13: OD results from the EDC/Sulfo-NHS linking procedure in two separate experiments.....	65
Figure 3.14: OD results from the Prolinker B linking procedure in two separate experiments.....	66
Figure 3.15: Empty well OD results from the direct comparison of six different linking procedures.....	67
Figure 3.16: Gold chip OD results from the direct comparison of six different linking procedures.....	68
Figure 3.17: Comparison of blocking efficiency using DSP .....	71
Figure 3.18: Comparison of blocking efficiency using Prolinker B.....	72
Figure 4.1: Examples of the deflection of cantilevers in water and buffer solution .....	84
Figure 4.2: Comparison of cantilever deflection based on the period in solution	85
Figure 4.3: A representative heat test .....	86
Figure 4.4: Cantilever deflection results with Prolinker B as the linker and including data classified as group I.....	93
Figure 4.5: Cantilever deflection results with Prolinker B as the linker and including data classified as group I.....	94
Figure 4.6: Cantilever deflection results with Prolinker B as the linker and including data classified as group I.....	95
Figure 4.7: Cantilever deflection results with Prolinker B as the linker and including data classified as group I.....	98
Figure 4.8: Cantilever deflection results with Prolinker B as the linker and including data classified as group I.....	99
Figure 4.9: Cantilever deflection results with glutaraldehyde as the linker and including data classified as group I.....	103
Figure 4.10: Cantilever deflection results with glutaraldehyde as the linker and including data classified as group I.....	104
Figure 4.11: Cantilever deflection results with glutaraldehyde as the linker and including data classified as group I.....	105

Figure 4.12: Cantilever deflection results with glutaraldehyde as the linker and including data classified as group I.....	106
Figure 4.13: Cantilever deflection results with EDC/Sulfo-NHS as the linker and including data classified as group I.....	108
Figure 4.14: Cantilever deflection caused by streptavidin binding to biotin linked to the surface with EZ-link and including data classified as group I.....	110
Figure 4.15: Effect of salt formation on cantilever deflection.....	113
Figure 4.16: Comparison of two identical EDC/Sulfo-NHS linking experiments. .....	119
Figure 4.17: Cantilever signals depicting the sequential order of deflection which is caused by crookedness of the cantilever array in the cartridge or holder. ....	120

# List of Abbreviations

AFM	Atomic Force Microscopy
APTES	3-aminopropyltriethoxysilane
Biotin-HPDP	(N-(6-(Biotinamido)hexyl)-3'-(2'-pyridyldithio)-propionamide
BSA	Bovine serum albumin
C-Ab	Capture antibody
cC-Ab	Canine capture antibody
CDK2	Cyclin-dependent protein kinase 2
CRP	Cardiac Reactive Protein
D-Ab	Detection antibody
DMSO	Dimethyl Sulfoxide
DNA	Dioxyrobonucleicacid
DSP	Dithiobis[succinimidyl propionate]
DSP-PEG	4,7,10,13,16,19,22,25,32,35,38,41,44,47,50,53-Hexadeca-oxa-28,29-dithiahexapentacontanedioic acid di-N-succinimidyl ester
DSU	Di-thio-bis-succinimidylundecanoate
DTSSP	Dithiobis(sulfosuccinimidylpropionate)
EDC	1-Ethyl-3-[3-dimethylaminopropyl] carbodiimide
ELISA	Enzyme linked immunosorbent assay
FBBMI	Fluorescent-Bead-Based Multiplex Immunoassay
FITC	Fluorescein isothiocyanate)
FWHM	Full width half maximum value)
GA	Glutaraldehyde)
gp120	Glycoprotein 120)
GST	Glutathione-S-transferase)
HAS	Human serum albumin
hC-Ab	Human Capture Antibody
hGH	Human growth hormone
HRP	Horseradish peroxidase
IgG	Immunoglobulin G

IL	Interleukin
INF- $\gamma$	Interferon gamma
MES	2-(N-morpholino)ethanesulfonic acid
MOSFETs	Metal-oxide semiconductor field-effect transistors
MS	Multiple Sclerosis
OD	Optical density
PBS	Phosphate buffered saline
PEG	Polyethylene glycol
PEG-Silane	2-[Methoxy(polyethyleneoxy)propyl]-trimethoxysilane
PEG-thiol	$\text{HO}(\text{CH}_2\text{CH}_2\text{O})_{11}\text{CH}_2\text{CH}_2\text{SH}$
PSA	Prostate Specific Antigen
PSD	Position sensitive detector
QCM	Quartz crystal microbalance
SAM	Self-assembled monolayer
SAW	Surface acoustic waves
SiN <sub>x</sub>	Silicon nitride
SPR	Silicon plasmon resonance
Sulfo-NHS	N-hydroxysulfosuccinimide
v/v	Percentage by volume solution

# Chapter 1

## Introduction

Proteins, in addition to nucleic acids, carbohydrates and lipids, are one of the major components of all living systems. Of these building blocks of living systems, proteins are particularly interesting because they are responsible for the vast majority of the chemical reactions which sustain, and sometimes destroy, life. Determining the concentration and location of proteins in cells and tissues is instrumental in a number of research fields and becomes especially critical for the diagnosis and treatment of diseases. Whether they are caused by internal sources like cancers, Alzheimer's, Multiple Sclerosis (MS) or cardiovascular disease or by external agents like viral and bacterial infections, all diseases involve proteins.

Biomarkers are substances which can be used to determine the state of a biological system. They may be used for the diagnosis of diseases, to determine the degree of disease progression, or to determine the effectiveness of treatment or preventative measures. Protein concentration, for example, can be used as a biomarker for a number of different diseases. Alzheimer's disease is thought to be caused by the build-up of plaque between nerve cells and the formation of tangles of twisted fibers in the brain. The plaque is made up of  $\beta$ -amyloid protein fragments while the fibers in the tangles are made up of Tau protein. A substantial amount of research has been performed into the use of  $\beta$ -amyloid and Tau protein concentrations in cerebral spinal fluid for the diagnosis of Alzheimer's disease and to determine the degree of disease progression. [1-4] Such research is important because early detection of disease can often improve treatment options. Also, enhanced knowledge of disease progression can lead to the development of new drugs to treat the disease.

In addition to Alzheimer's there are many other diseases where biomarkers have been used. Other examples of protein biomarkers include

Prostate Specific Antigen (PSA), Troponin C and Cardiac Reactive Protein (CRP). PSA is a biomarker for prostate cancer, while Troponin C and CRP are biomarkers for cardiovascular disease. Often single biomarkers are insufficient to accurately diagnose a disease or determine the degree of disease progression. This is because the proteins involved may not be generated specifically by the disease and their concentration may be elevated or decreased due to other causes. This is the case for MS where there are a host of identified biomarker proteins. Increased interferon gamma (INF- $\gamma$ ) concentration, for example, is a major indicator of relapse in MS patients. Interleukins (IL) 12 and 18 are therefore also of interest because they increase INF- $\gamma$  production. MS also illustrates how the measurement of protein concentration can result in new treatment approaches. Interferon beta-1a, one of the main drugs used to combat MS, leads to decreased INF- $\gamma$  production which as mentioned earlier increases in concentration during relapse.[5-7]

Many studies have been performed which sort through tens or even hundreds of proteins in order to determine biomarkers for a variety of conditions. Despite these studies, very few biomarkers are specific to a particular disease or condition. This is especially evident for ILs and other cytokines, as signaling molecules are of particular interest as biomarkers for many different diseases and conditions. IL-18, for example, is of interest as a biomarker for MS, cardiovascular disease, post-stroke depression, and other diagnostic applications.[7-9] This means that the concentration of IL-18 is unlikely to be a specific indicator for any of these diseases or conditions. This is but one case, but it exemplifies how the measurement of multiple biomarkers can improve medical diagnosis and prognosis, and it indicates the importance of multiplexing for the measurement of biomarkers. Measuring multiple biomarkers can be challenging with some techniques however, as the concentrations of biomarker proteins may vary significantly, from tens of pg/ml to tens of ug/ml.[10, 11] Despite the challenges, research continues to elucidate the changes in biomarker concentration in various diseases and conditions, allowing for more accurate medical prognosis and diagnosis.

In addition to their importance for biomarker studies, protein concentration measurements are also critical for vaccine development. Vaccines save millions of lives through the prevention of many major viral and bacterial infections.[12] Vaccines are composed of whole or partial virus or bacterial particles suspended in solution. Their purpose is to initiate a reaction which will produce a humoral immune response, a cell mediated immune response or both.[13, 14] The effectiveness of the humoral immune response can be determined from serum antibody concentration levels.

Genetic engineering is another area where protein concentration is important. This is because in many cases the purpose of alterations to the genetic code is to produce a particular protein. Wheat, for example, may be modified to produce proteins which make it resistant to certain herbicides. It is therefore important to verify that the quantity of herbicide resistance protein produced is sufficient to withstand the herbicide, but not so great as to decrease the rate of growth or nutritive value of the wheat.

Given the importance of accurate and specific detection and measurement of proteins, there are several methods which are regularly used to determine the protein concentration in a sample. The enzyme linked immunosorbent assay (ELISA) is most commonly used to determine the concentration of protein in a given sample. It is an invaluable technique and serves as a major diagnostic tool for various diseases and conditions including cancer, infections, allergies, and autoimmune conditions.[15] Recent developments have made it possible to measure multiple proteins in a single ELISA sample, but the process is relatively expensive.

A commonly used method to determine the location and concentration of proteins in tissues and cells is fluorescent labeling. The fluorescent label may either be attached to the protein of interest directly or to an antibody specific to the protein of interest. It is generally less sensitive and quantitative than the ELISA method. Given the difficulty involved with multiplexed ELISA experiments a different technique called the Fluorescent-Bead-Based Multiplex Immunoassay (FBBMI) was developed. It is a more complex fluorescence

method which can sensitively and specifically detect multiple proteins in a single sample.

In addition to the more commonly used biochemical techniques there are a variety of biosensor techniques which may be used to detect and quantify proteins. Biosensors are used to detect and measure nucleic acids and various other organic and inorganic analytes. What makes biosensors unique is that they incorporate biological or biomimetic materials, usually for the purpose of sensitive and specific interaction with the analyte of interest. Materials used for this purpose include tissues, cells, nucleic acids, biomimetic catalysts, molecular imprinted polymers, synthetic receptors, and a wide variety of proteins. Proteins used include enzymes, receptor proteins, antibodies, recombinant antibodies, and engineered proteins. In addition to the biological element, biosensors require a transducer or detector component to physiochemically convert the interaction between the biological element and the analyte into a measurable signal. Common transducing systems may be optical, piezoelectric, magnetic, micromechanical, thermometric, or electrochemical in nature. Some systems may also combine two or more of these transducing elements. The transducer component commonly produces an electrical signal which is proportional to the analyte concentration and with an appropriate standard curve can be used to determine the analyte concentration.

There are a number of common sensing platforms that can be readily converted into biosensors for protein measurements, including detection, quantification, interaction and structural studies. These platforms include silicon plasmon resonance (SPR), quartz crystal microbalance (QCM), cantilevers, surface acoustic waves (SAW), nanowires, optical gratings, ellipsometry, and interferometry. Further details can be found in the following reviews and papers.[16-22] These biosensors have some notable advantages over the more commonly used immunoassays discussed above.

One major advantage common to these biosensors is that they are label-free. This means that only one capture molecule is required to specifically bind the protein of interest to the sensor surface. The majority of the biochemical

techniques discussed previously require two antibodies. The label-free nature of these biosensors is advantageous for several reasons. Labeling can change the configuration of proteins, decreasing their binding effectiveness or inhibiting their activity. It can also be challenging to develop two antibodies which can simultaneously bind the protein of interest, particularly for smaller proteins. Thirdly, this property is useful for the measurement of new proteins, such as the proteins of new viruses, where multiple antibodies may not exist and where the development of an effective treatment or vaccine may be urgent.

A derivative property of the label-free aspect of biosensors is that the measurements can be performed actively in real time. This means that in situ measurements can be performed where the protein output or intake of cells is recorded over time. This theoretically makes it possible to actively record the reaction of cells, tissues or even patients to drug treatments. Another advantage of these biosensors is that they can be multiplexed to simultaneously detect several proteins.[23-28] Finally, these biosensors are also conducive to system integration with microfluidics, which would allow small sensitive testing kits for mobile applications.

Out of these biosensors some of the most sensitive measurements have been performed with cantilevers. One example was the detection of 0.23 attogram DNA strands by Ilic *et al.*[29] This sensitivity is what makes cantilever biosensors such a promising avenue of research. Unfortunately, cantilever sensitivity is dependent on specific measurement conditions. The experiment by Ilic *et al.* was performed in vacuum with resonance mode cantilevers. Biological experiments are frequently performed in aqueous solution however, and the sensitivity of resonant cantilevers decreases significantly in aqueous solutions. For this reason deflection cantilevers are often used for measurements performed in aqueous solution.

Deflection cantilevers are a promising platform for the detection and measurement of proteins for several reasons. Firstly, they can readily be used for multiplexing, which is valuable for the simultaneous measurement of multiple biomarker proteins. This is done by fabricating multiple cantilevers into a single

array and separately functionalizing the cantilevers to be specific for different biomarker proteins. This method was successfully demonstrated by Arntz *et al.* in 2003 through the simultaneous detection of cardiac biomarkers creatine kinase and myoglobin at a concentration of 20  $\mu\text{g/ml}$ . [28] The lowest protein concentration measured by deflection cantilevers was 0.2 ng/ml PSA by Wu *et al.*[30] While this detection limit is relatively high compared to the FBBMI, which may have a detection limit of 5 pg/mL or lower, new research continues to lead to improvements in detection sensitivity. Current research has focused almost exclusively on single protein detection however, even when cantilever arrays were used for the measurements. This means that the detection limit for the simultaneous measurement of proteins with deflection cantilevers has not improved since 2003.

Another major issue that becomes evident from a review of cantilever deflection based protein detection is that there is no standardization of measurement techniques. This is not unusual for an experimental technique, but it makes it difficult to accurately and reliably measure multiple proteins at different concentrations.

The goal of this project was to develop a method to reliably measure protein concentration using commercially available components including cantilever arrays, a cantilever deflection measurement platform and biological detection mechanism. Such a method should make it possible to readily measure multiple proteins with only minor adjustments to the biological detection system. Chapter 2 will introduce necessary background information concerning ELISAs, fluorescence assays, and cantilever technology. It will also relate the rationale behind and general approach to the experiments which are discussed in the following chapters. Chapter 3 presents the results from the fluorescence and ELISA experiments and what was discovered about the linking and blocking procedures which were tested. In Chapter 4, the results from the implementation of the linking and blocking procedures for the measurement of proteins with deflection cantilever arrays are discussed. Finally, in Chapter 5 all the experimental results and conclusions are summarized.

## Chapter 2

# Background and Research Rationale

The purpose of this chapter is to cover background information on several topics of relevance to the remainder of the thesis. The use of ELISA and fluorescence methods for detecting and measuring proteins is covered both because they are the most commonly employed methods and because they are important to the experimental approach. This is followed by a section describing the use of cantilevers as sensors as well as a section specifically reviewing the use of static/deflection cantilevers for protein detection. In the last section, the background information is related to the experimental approach in the following chapters, and the materials which were selected to perform the experiments are discussed.

### 2.1 Enzyme Linked ImmunoSorbent Assay

The Enzyme Linked ImmunoSorbent Assay (ELISA), also known as the Enzyme ImmunoAssay, was developed simultaneously by research groups in Sweden and the Netherlands.[31] In ELISAs, antibodies linked to enzymes are used to detect and measure proteins or other antigens. The antibody is used to specifically identify the antigen while the enzyme catalyzes a colourimetric, fluorescence or chemiluminescence reaction to quantify the antigen. The colourimetric reaction is most commonly used and the change in optical density (OD) of the substrate solution, which is catalyzed by the enzyme, is determined using an ELISA plate reader. A number of different enzymes may be used including  $\beta$ -galactosidase, acetylcholinesterase, catalase and most commonly horseradish peroxidase (HRP) or alkaline phosphatase. An ELISA is performed

on a surface to which the antigen or antibody adsorbs, also known as the solid phase. Ninety-six well polystyrene plates are commonly used for the solid phase as they readily allow the antibody or antigen to adsorb to the hydrophobic surfaces. In addition, the plates facilitate the separation of bound and unbound materials through washing. This is especially critical when the antigen is in a complex solution such as blood or serum.

There are various types of ELISAs that may be employed depending on the conditions and requirements of the assay. The legend used in all the ELISA and fluorescence schematics is shown in Figure 2.1.

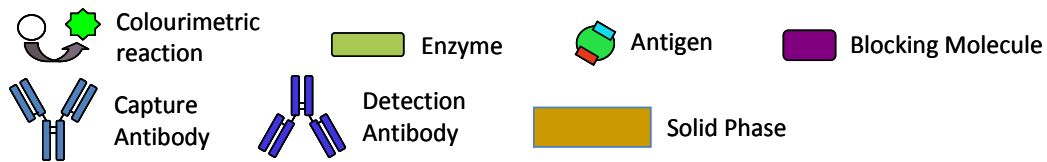


Figure 2.1: Legend for ELISA and fluorescence schematic depictions.

In direct ELISAs, the antigen is adsorbed directly to a solid phase and an enzyme-conjugated antibody is used to detect the antigen (Figure 2.2). Indirect ELISAs are similar to direct ELISAs except the primary detection antibody (D-Ab) is unconjugated and a secondary enzyme-conjugated D-Ab binds to the first D-Ab (Figure 2.3) Direct ELISAs are faster than indirect ELISAs and the probability of cross-reactivity is decreased since there is only one antibody step. Indirect ELISAs on the other hand provides greater flexibility because the primary D-Ab may be altered without changing the secondary D-Ab, which is species-specific. In addition, the binding efficiency of the primary D-Ab may be greater in the indirect ELISA, because in the direct ELISA the process of enzyme conjugation may cause deformation in the D-Ab.[32]

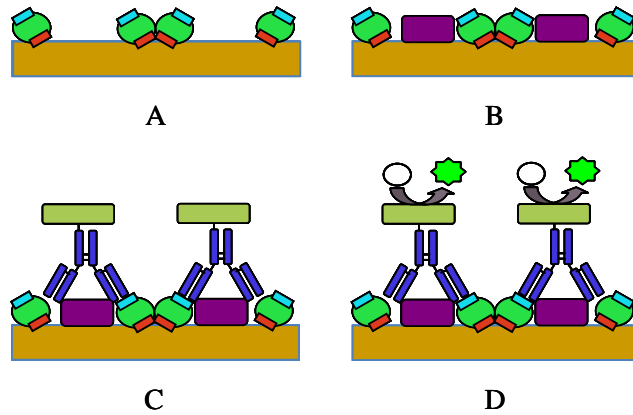


Figure 2.2: Schematic depiction of a direct ELISA. A - The antigen is adsorbed to the solid phase. B - A non-reactive molecule is optionally used to fill any open areas on the solid phase to decrease nonspecific reactions between the detection antibody and the solid phase. It is commonly known as the blocking step. C - The enzyme-conjugated detection antibodies bind to the antigen on the surface. D - The colourimetric solution is added to the wells and the enzyme reacts with the solution changing its colour.

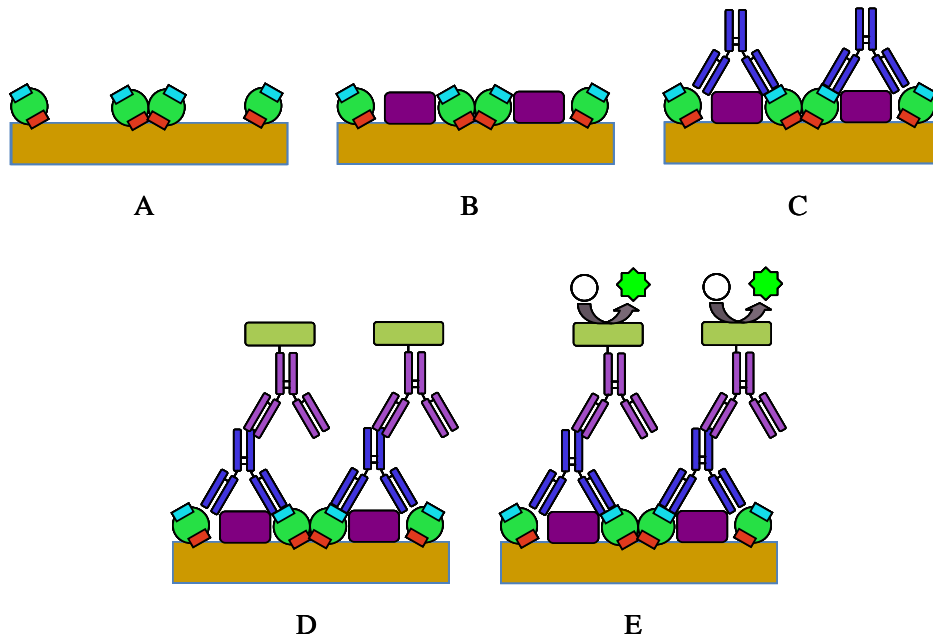


Figure 2.3: Schematic depiction of an Indirect ELISA. A - The antigen is adsorbed to the solid phase. B - The blocking molecule adsorbs to any uncoated surface on the solid phase. C - The unconjugated primary D-Ab binds to the antigen on the surface. D - The enzyme-conjugated secondary D-Ab binds to the primary detection antibody. E - The colourimetric solution is added to the wells and the enzyme reacts with the solution changing its colour.

The sandwich ELISA is characterized by the use of two antibodies: the capture antibody (C-Ab) which adsorbs to the solid phase to specifically capture the antigen of interest, and the D-Ab which binds to a different location on the antigen (Figure 2.4). As before, in direct sandwich ELISAs the D-Ab is conjugated to an enzyme while in indirect sandwich ELISAs the primary D-Ab is unconjugated and a secondary conjugated D-Ab binds to the primary D-Ab. Indirect sandwich ELISAs may also be altered such that the primary D-Ab is biotinylated, and enzyme-conjugated streptavidin is used instead of a conjugated secondary D-Ab. The advantage of a sandwich ELISA is the increased specificity for the antigen, while the drawback is the need for an additional antibody and the difficulty involved in properly targeting different locations on the surface of the antigen. In addition to these methods, there are many variations to the ELISA that are often employed, such as competition and inhibition ELISAs which may be used to measure how much an additional protein or other molecule interferes with the established ELISA protocol.[32]

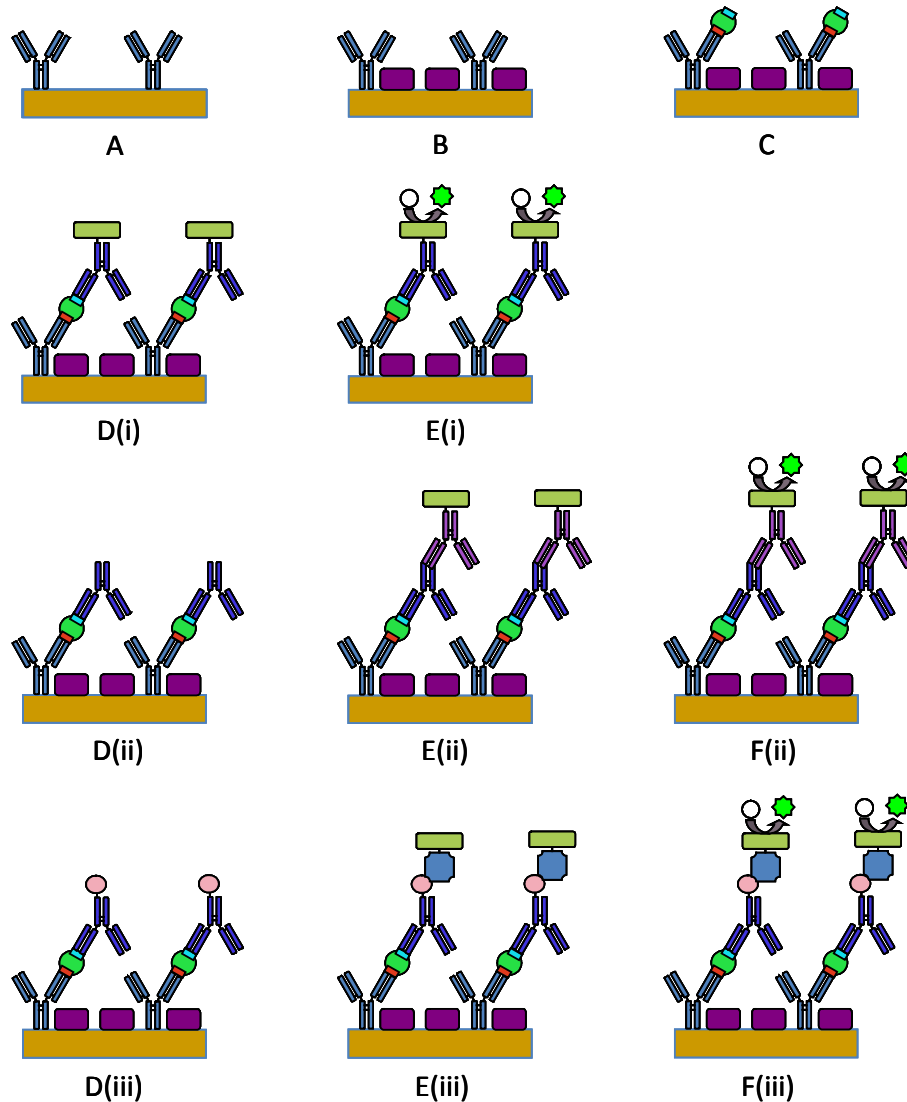


Figure 2.4: Schematic depiction of three different sandwich ELISAs. The first 3 steps A-C are common to all three procedures. The variations are represented by (i) for a direct assay, (ii) for an indirect assay with a secondary D-Ab, and (iii) for an indirect assay with biotin-streptavidin based enzyme conjugation. A - The capture antibody adsorbs to the solid phase. B - The blocking molecules prevent nonspecific binding to the solid phase. C - The antigen binds to the C-Ab. D - In the direct sandwich ELISA (i) the enzyme-conjugated D-Ab binds to the antigen, while in the first indirect sandwich ELISA (ii) an unconjugated D-Ab binds to the antigen, and in the second indirect sandwich ELISA (iii) a biotinylated D-Ab binds to the antigen. E - In the direct sandwich ELISA (i) the colourimetric solution is added, and the colour reaction takes place. In the first indirect sandwich ELISA (ii) the second enzyme-conjugated D-Ab binds to the first D-Ab, while in the second indirect sandwich ELISA (iii), enzyme-conjugated streptavidin binds to the biotinylated D-Ab. F - The direct sandwich ELISA is complete, while in the indirect sandwich ELISAs (ii) and (iii) the colourimetric solution is added, and the colour reaction takes place.

## 2.2 Fluorescence

Fluorescence methods are commonly used to determine the location and the quantity of proteins.[33] There are three main categories of fluorescent tags: small molecules like fluorescein, quantum dots and proteins like Green Fluorescent Protein. These fluorescent tags absorb light in a range of wavelengths, resulting in the excitation of electrons to a higher unstable energy state (Figure 2.5). The energy state is proportional to the frequency of the absorbed light and inversely proportional to the wavelength as given by Planck's Law below (equation 1.1).

$$E = h\nu = \frac{hc}{\lambda} \quad (1.1)$$

where  $E$  is the change in energy of the electron,  $h$  is Planck's constant ( $6.626068 \times 10^{-34} \text{ m}^2\text{kg/s}$ ),  $\nu$  is the frequency of the absorbed light,  $c$  is the speed of light and  $\lambda$  is the wavelength of the absorbed light. The electrons then undergo a vibrational relaxation step where energy is lost without light emission. Finally the electrons return to the ground state releasing a photon of light with less energy and a correspondingly lower wavelength.

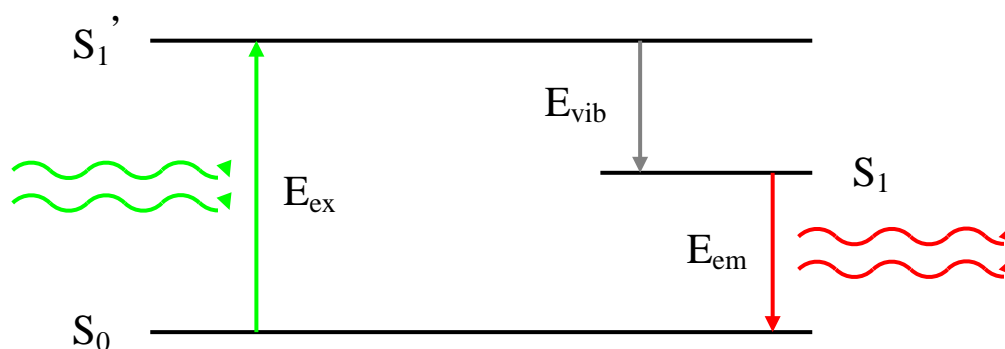


Figure 2.5: A simplified Jablonski diagram of the electron states which cause fluorescence. Incident light with excitation energy  $E_{ex}$ , in this case green, causes an electron to be excited from the stable ground state  $S_0$  to an unstable higher energy state  $S_1'$ . The electron then undergoes a vibrational relaxation from the  $S_1'$  state to the  $S_1$  state, with a corresponding loss of energy  $E_{vib}$ .  $S_1$  is also an unstable state, so the electron returns to the ground state  $S_0$ , releasing a photon with energy  $E_{em} < E_{ex}$ . The photon released has a correspondingly lower wavelength, in this case red.

Fluorescence imaging is commonly performed in cells, tissues and viruses in order to determine the presence and location of one or more proteins of interest. The fluorescent tag may be conjugated directly to the protein of interest or it may be linked to a D-Ab specific to the protein of interest. Fluorescent tags can also provide quantitative information by comparing the fluorescent intensity of a sample image to that of a control image. This can then be used to determine whether the protein or proteins of interest are present at a higher or lower concentration than in the control.

The Fluorescent-Bead-Based Multiplex Immunoassay (FBBMI) is commonly used to quantitatively measure protein concentration. While the ELISA is often used to determine the concentration of a single protein of interest, it is challenging and costly to extend this technique to measure many proteins simultaneously. Instead the FBBMI may be used for this purpose. In the FBBMI beads are impregnated with various ratios of two or more distinct fluorophores. The beads are then coated in C-Abs specific to individual proteins such that each fluorophore ratio corresponds to a distinct C-Ab. The fluorophore ratios are identified by their specific emission wavelength through laser excitation which is then used to determine which C-Ab is on a given bead. The sample is incubated with the beads, washed and incubated with biotinylated D-Abs specific to the proteins of interest. Next, streptavidin linked to a different fluorophore from those impregnating the beads is added to the beads. This fluorophore is excited by a different colour laser to quantitatively determine the number of proteins attached to a given bead. The beads are then separated in a thin capillary tube so that each bead is measured individually similarly to flow cytometry. The fluorescence from the beads identifies the protein bound on the surface of a given bead while the intensity of the fluorescence from the fluorophore bound to the D-Ab indicates the amount of antigen bound to the surface of the bead.[34]

While it is convenient to measure the concentration of proteins in cells or on beads, it is more challenging to use fluorescence to measure proteins on a flat surface. This is because the fluorescence is greatly diluted on a two-dimensional surface, which makes accurate measurement much more challenging. A new

modified ELISA using chemiluminescence makes measurement of multiple proteins on a two-dimensional surface possible. Roughly 25 C-Abs specific to different antigens may be spotted onto the bottom of each well in a 96-well plate. The sandwich ELISA procedure is then followed as described in section 2.1, though the standard curve must now include all the antigens for which the plate was spotted. The key to this method is that the chemiluminescent reaction amplifies the signal from each spot without significantly contaminating the reading of the other spots in a given well. The intensity from each sample spot is then compared to the standard to determine the concentration of the protein in the sample.[35] A similar method was developed by Meso Scale Discovery except that electrochemiluminescence was used instead of chemiluminescence. The D-Abs are labeled with Ruthenium (II) tris-bipyridine-(4-methylsulfonate)-*N*-hydroxysuccinimide ester which in conjunction with tripropylamine in an electric current leads to light production. The intensity of the resultant light, in conjunction with a standard curve, allows the proteins to be quantified.[36]

## 2.3 Cantilever-Based Sensor Technology

Atomic Force Microscopy (AFM) was first developed as a technique for surface imaging in 1986.[37] AFM may be divided into two main measurement methods, static mode and dynamic mode. During static mode measurements, the sharp cantilever tip scans across the material in direct contact with the surface. The recorded deflection of the AFM cantilever is then used to create a depth profile of the material. In dynamic mode measurements the cantilever is induced to oscillate at or near the fundamental resonance frequency or a higher harmonic. The amplitude, phase and frequency of the tip are influenced by various forces between the tip and the surface which allow for various imaging approaches. The field of AFM continues to advance, however, with the development of new sensing modes including capacitance and magnetic AFM. Furthermore, the technology has been exported for other applications such as the investigation of binding strength between biological molecules and the use of cantilevers for

various sensing applications.[38, 39] These sensors also operate in either static mode, where differential stress resulting in cantilever deflection is used to perform measurements, or dynamic mode, where changes in the resonant frequency of the cantilever are used to perform measurements. These cantilever sensors have been used to measure a variety of physical conditions including temperature and pH, various compounds including gasses, chemicals, proteins and DNA, as well as larger bodies including viruses, bacterial spores, yeast cells, and fungal spores.[28, 40-49]

### 2.3.1 Principles of Cantilever-Based Sensor Technology

Cantilever measurements are performed in either static mode or dynamic mode. In static mode measurements the physical condition or analyte of interest is detected through the surface stress induced on the functionalized surface of the cantilever or the resultant deflection caused by the induced stress. The relation between the induced stress and the resultant deflection of the cantilever is given by a variation of Stoney's equation (equation 1.2).[47, 50]

$$z = \frac{3\sigma(1-\nu)l^2}{Et^2} \quad (1.2)$$

where  $z$  is the deflection of the tip of the cantilever,  $l$  is the length of the cantilever,  $E$  is Young's modulus,  $t$  is the thickness of the cantilever,  $\sigma$  is the induced surface stress and  $\nu$  is the Poisson's ratio. Quantitative measurements are possible because the magnitude of the surface stress is dependent on physical conditions and the quantity of analyte bound to the cantilever surface.

Optical detection is a common method of reading cantilever deflection (Figure 2.6). A laser reflects off the tip of the cantilever beam and strikes a position sensitive detector (PSD). As the tip of the cantilever rises or falls the termination point of the laser similarly shifts upward or downward and this shift is recorded by the PSD. The PSD then provides an electrical output which is used to calculate the cantilever deflection. Using equation 1.2 the cantilever deflection

can then be directly related to the analyte concentration or the physical condition of interest, or indirectly related to the surface stress.[28]

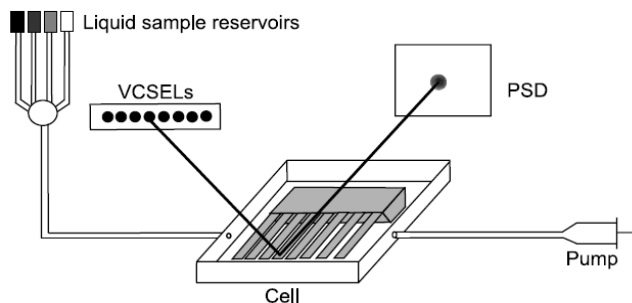


Figure 2.6: Diagram of a cantilever array optical readout system where VCSEL indicates the vertical cavity surface emitting lasers and the PSD designates a position sensitive detector. The pump is used to draw the sample solution through the measurement cell containing a deflection cantilever array. “Reprinted with permission from Arntz Y, Seelig JD, Lang HP, Zhang J, Hunziker P, Ramseyer JP, et al. Label-free protein assay based on a nanomechanical cantilever array. *Nanotechnology* 2003;14:86-90. Copyright 2003, IOP Publishing.”

Piezoresistive cantilevers are frequently used as an alternative to optical detection. Piezoresistive cantilevers have piezoresistors implanted into them during the fabrication process such that changes in the surface stress result in changes in the resistance of the piezoresistors. This resistance can then be calculated when a voltage is applied to the piezoresistor.[41] A third approach to measuring the cantilever stress is through metal-oxide semiconductor field-effect transistors (MOSFETs). The MOSFETs are fabricated such that the drain current is sensitive to changes in the cantilever surface stress. This means that the physical conditions or analyte concentration can be determined from the magnitude of the drain current.[51]

The most common materials used for deflection cantilevers are silicon and silicon nitride. In order to differentiate the active and passive surfaces of the cantilever, a gold layer is often deposited on one surface. This allows sulfide groups to bind to the gold surface, which simplifies the process of linking molecules to the surface.

From equation 1.2 it is evident that materials with a smaller Young's Modulus will make a more sensitive sensor.[39] Therefore, some researchers have been examining other materials with a lower Young's Modulus in order to increase the cantilever sensitivity. One such material is the polymer SU – 8 which has a Young's Modulus 40 times smaller than that of silicon or silicon nitride.[52] Other experiments have shown that under certain conditions SiO<sub>2</sub> cantilevers may exhibit an order of magnitude better deflection than silicon cantilevers.[53]

The actual source of the surface stress caused by analyte adsorption to the cantilever surface remains a hotly debated topic. Increased cantilever deflection was reported for increased alkanethiol length and concentration, which suggests that electrostatic repulsion is the primary source of stress for these molecules.[54] For DNA biosensors, however, steric, electrostatic and hydrophobic forces were suggested as the dominant source of surface stress.[55] Wu *et al.* disagree with this interpretation, however, because they observed compressive stress on the active cantilever surface following hybridization. They argue that configurational entropy can dominate the steric and electrostatic repulsion forces because ionic concentrations may cause charge shielding which then leads to changes in the molecular packing density.[56] Further studies by McKendry *et al.* indicate that ion concentration has a minimal effect on the DNA binding density, which suggests that steric repulsion is the dominant force.[57] These results are indicative of the challenges faced by any attempt at theoretically predicting the behavior of complex biomolecules. Proteins are substantially larger and more complex molecules than DNA, and are correspondingly more challenging to model accurately.

In dynamic mode measurements, the analyte of interest is detected by the shift in resonant frequency of the cantilever caused by the additional mass of the analyte when it binds to the surface. A cantilever beam may be modeled as a harmonic oscillator with resonant frequency  $f_0$ .

$$f_0 = \frac{1}{2\pi} \sqrt{\frac{k}{m}} \quad (1.3)$$

where  $k$  is the spring constant and  $m$  is the mass of the cantilever. For the added mass of the analyte  $\Delta m$ , there is a shift in the resonant frequency  $\Delta f = f - f_0$  where

$$\Delta f = -0.5 \frac{\Delta m}{m} f_0 \quad (1.4)$$

In a cantilever sensor, this shift in the resonant frequency can be used to determine the change in mass of the cantilever as an analyte is adsorbed to the cantilever surface (Figure 2.7).

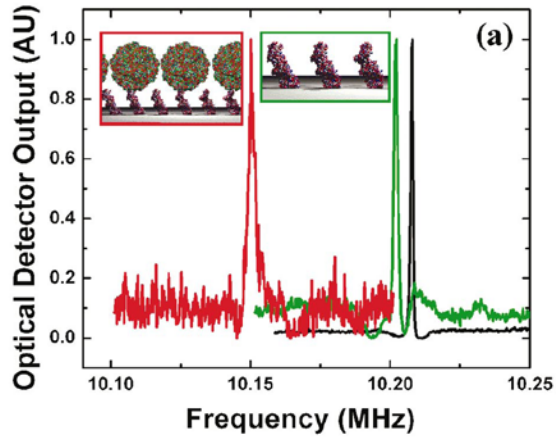


Figure 2.7: An example of the resonance peak shift which occurs after the addition of mass to the cantilever. The darkest right most peak is the initial resonance frequency, the central lightest peak is the resonance frequency after the adsorption of the antibodies to the cantilever surface and the left most peak is the resonance frequency after the binding of virus particles to the antibodies. “Reprinted with permission from Ilic B, Yang Y, Craighead HG. Virus Detection Using Nanoelectromechanical Devices. Applied Physics Letters 2004;85:2604-6. Copyright 2004, American Institute of Physics.”

The resonant frequency of the fundamental mode perpendicular to the cantilever surface is given by:

$$f_0 = \frac{3.515}{2\pi l^2} \sqrt{\frac{EI}{\rho A}} \quad (1.5)$$

where  $E$  is Young’s modulus,  $I$  is the moment of inertia,  $l$  is the length of the cantilever,  $\rho$  is the density of the cantilever and  $A$  is the cross-sectional area.[58]

For  $I \propto wt^3$  and  $A = wt$ , where  $w$  and  $t$  are the width and thickness of the cantilever respectively, then the frequency is linearly dependant on the thickness of the cantilever and independent of the width.

The quality factor ( $Q$ ) is an important value which affects the maximum mass sensitivity of dynamic cantilever sensors. The quality factor is defined as the quotient of the resonant frequency and the full width half maximum (FWHM) value of the resonance peak.

$$Q = \frac{f_0}{FWHM} \quad (1.6)$$

If a given fraction of the full width half maximum of a resonant peak can be resolved, then from equation 1.4  $\Delta f \propto f_0 Q^{-1}$  and with this approximation

$$\Delta m_{\min} \propto m Q^{-1} \quad (1.7)$$

where  $\Delta m_{\min}$  is the smallest mass that can be detected by the sensor.[39] Therefore, it is important to obtain sharp resonance peaks and to decrease the mass of the cantilever in order to increase the sensitivity of the sensor. This is why it is significantly simpler to achieve a high mass sensitivity in air or vacuum than in liquid, because  $Q$  values decrease substantially in solutions. To illustrate this, Wu *et al.* recorded a detection limit of 0.2 ng/mL prostate specific antigen (PSA) in buffer solution using deflection cantilevers while Hwang *et al.* recorded a detection limit of 1 ng/mL PSA in buffer solution using resonant cantilevers and Lee *et al.* recorded a detection limit of 10 pg/mL PSA using resonant cantilevers in air.[30, 59, 60] The most common materials used to fabricate resonance mode cantilevers are silicon and silicon nitride though other materials such as polysilicon and lead zirconate titanate are also used.

While dynamic-mode cantilever experiments have demonstrated outstanding mass sensitivity in vacuum and in atmospheric conditions, damping issues impair their applicability in fluids. Static mode cantilevers were selected to perform the protein measurements discussed in this work as they are better suited to a liquid environment. A thorough review of the literature on the use of static-mode cantilevers for the detection of proteins follows in the next subsection.

### 2.3.2 A Review of Static Cantilever-Based Protein Detection

Since this thesis is primarily concerned with the detection of proteins using deflection cantilevers, it is helpful to review all prior research concerning static cantilever detection of proteins. The deflection cantilevers used are commonly rectangular or v-shaped, and coated with gold on one side or on both sides. Since proteins readily adhere to gold and silicon surfaces, it is important to differentiate the active functionalized surface and the passive surface to prevent stress caused by nonspecific protein adhesion. For this reason the backsides of the cantilevers are often coated in a blocking molecule which inhibits protein binding. In most cases, the protein of interest binds to a specific receptor molecule linked to the active gold surface. Receptor molecules may be polypeptides, DNA or antibodies specific to the protein of interest. Thiol chemistry is frequently used to link the receptor molecule to the gold surface.

One of the most commonly used proteins in cantilever deflection experiments is PSA. Wu *et al.* made the most sensitive deflection cantilever measurements of PSA in 2001 using 200  $\mu\text{m}$  long v-shaped silicon nitride cantilevers coated in a 5 nm chromium adhesion layer and a 25 nm layer of gold. The 160  $\mu\text{g/ml}$  rabbit anti-human PSA antibodies were linked to the gold surface using Dithiobis(sulfosuccinimidylpropionate) (DTSSP), a thiol linked to an N-hydroxysuccinimide (NHS) ester. Nonspecific binding was blocked using bovine serum albumin (BSA) or human serum albumin (HAS), and the detection limit was 0.2 ng/ml.[30]

Separate measurements of PSA and CRP were performed by Wee *et al.* using composite rectangular piezoresistive cantilevers composed of multiple layers including: 500 nm silicon nitride ( $\text{SiN}_x$ ), 500 nm poly-silicon, 200 nm  $\text{SiO}_2$ , 300 nm  $\text{SiN}_x$  and evaporated layers of chromium and gold 25 nm and 45 nm thick respectively. A Calixcrown self-assembled monolayer (SAM) was used to link the antibodies to the surface and the surfaces were blocked with BSA. The layer of

silicon nitride on the backsides of the cantilevers was used to prevent nonspecific interactions. A background subtraction was performed internally using a wheatson bridge in conjunction with reference cantilevers. The detection limits were 10 ng/ml and 100 ng/ml for PSA and CRP respectively.[61]

Another measurement of PSA was performed using a chip filled with wells, each containing 4-8 deflection cantilevers. The silicon nitride cantilevers were 0.5  $\mu\text{m}$  thick, 40  $\mu\text{m}$  wide, and 200-400  $\mu\text{m}$  long and were coated with 25 nm of gold. Four different linking/blocking combinations were attempted in this study. In the first method DTSSP was used to link the C-Ab to the surface, while BSA was used to block the backside. A polyethylene glycol- silane (PEG-silane) molecule was used to block the backside of the cantilevers in the next three procedures. In the second method Sulfo-succinimidyl 2-(biotinamido)-ethyl-1,3-dithiopropionate (Sulfo-NHS-SS-Biotin) was incubated on the gold surface causing the disulfide bond to break and allowing subsequent binding of neutravidin to the free biotin and NHS groups. The biotinylated C-Ab then bound to the neutravidin on the surface. The third method employed DTSSP as the linker, while the fourth method used a mixed SAM of NHS-thiol (HS-[CH<sub>2</sub>]-11-[OCH<sub>2</sub>]-6-COO-NHS) and PEG-thiol (HS-[CH<sub>2</sub>]-11-[OCH<sub>2</sub>]-6-OH). Reasonably good results were observed from the cantilever deflection during the C-Ab linking process for the last two linkers, but the results for the first two methodologies were quite poor. The BSA blocking step in particular resulted in significant differences in deflection for identically functionalized cantilevers. For this reason BSA blocking was discarded as a viable option. The deflections of 50 cantilevers were recorded at various PSA concentrations with roughly linear results on a log-log plot of surface stress vs. PSA concentration. Two out of eight points in the plot did not fall within the linear fit however. The detection limit recorded was 1 ng/ml. [62]

A second measurement of CRP was performed by Chen *et al.* The v-shaped silicon nitride cantilevers were 600 nm thick, 200  $\mu\text{m}$  long, and 40  $\mu\text{m}$  wide. Gold with a chromium adhesion layer was deposited (the method of deposition was not given) on the top surface of the cantilevers. A carboxylic acid

terminated alkylthiol (SH-(CH<sub>2</sub>)<sub>7</sub>-COOH) SAM was formed on the gold surface and 1-Ethyl-3-[3-dimethylaminopropyl]carbodiimide Hydrochloride (EDC)/NHS chemistry was used to link the anti-CRP antibody to the SAM. Ethanolamine was used to block any remaining active sites after the EDC/NHS linking process. A CCD camera was used to align the laser beam on the cantilever tip and a PSD was used to measure the cantilever deflection. The silicon nitride backside seemed to adequately passivate the backside to avoid protein adhesion. The detection limit was not given. [63]

Vimentin is another cancer marker which was investigated. Amine-rich polyethyleneimine was used to link Vimentin-specific antibodies to the polysilicon microcantilevers through the free carboxylic acid groups on the antibody surface. Vimentin was successfully detected at a concentration of 90 ng/ml using optical detection. [64]

Dauksaite *et al.* made use of individual functionalized piezoresistive cantilevers, which allow for better use of reference cantilevers for background subtraction, to detect glutathione S-transferase (GST). Commercial cantilever arrays (CantiChip4), a commercial measurement unit (Cantilab) and a commercial ink-jet type functionalization unit (CantiSpot), all from Cantilab-NanoNord A/S, were used in their experiments. The rectangular cantilevers used were 480 nm thick including a 30 nm gold coating, 120 μm long and 50 μm wide. Again the method of gold deposition was not discussed. TCEP·HCl (Tris(2-Carboxyethyl) phosphine hydrochloride) was used to thiolate the antibodies allowing them to bind directly to the gold surface of the cantilevers. Goat anti-GST antibodies were linked to the two active cantilevers in the array, while the reference cantilevers were coated with reference goat IgG antibodies. The arrays were blocked with BSA and the limit of detection was determined to be 1 ng/ml. Interestingly, the absolute signals showed a significant downward trend, though the injection of GST showed a distinct separation between the active and control cantilevers.[41]

Some of the earliest cantilever array experiments, and the only ones found which demonstrate the simultaneous measurement of more than one protein, were performed by Arntz *et al.* The silicon cantilever arrays each had 8 cantilevers and

were fabricated at IBM in Zurich. The cantilevers were 500 nm thick, 500  $\mu\text{m}$  long, and 100  $\mu\text{m}$  wide and they were evaporated with 2 nm of titanium and 20 nm of gold. The myoglobin- and creatine kinase- specific antibodies were linked to the gold surface using di-thio-bis-succinimidylundecanoate (DSU). Glass capillaries 150  $\mu\text{m}$  wide were used to functionalize the active cantilevers with the antibody solution while the control cantilevers were blocked with ethanolamine. The linking process was tested using myoglobin, with mediocre results. This outcome was largely caused by the significant drift in cantilever deflection resulting from nonspecific binding to the cantilever surfaces. BSA blocking of the cantilever backsides significantly reduced the drift and improved the results. The same process was then used to simultaneously detect both myoglobin and creatine kinase, while BSA was used to block the entire surface of the reference cantilevers. Curiously, the cantilever deflection only took place while the sample solution was present in the measurement chamber. The cantilever deflection returned to zero as soon as buffer was pumped into the measurement chamber. The detection limit for both proteins was better than 20  $\mu\text{g}/\text{ml}$ . [28]

The first measurement of myoglobin was performed by Grogan *et al.* The silicon nitride cantilevers used were 600 nm thick, 190  $\mu\text{m}$  long and 20  $\mu\text{m}$  wide, and were coated with 30 nm of gold. The method of deposition was again not provided. Sulfosuccinimidyl 6-(3'-[2-pyridyldithio]-propionamido) hexanoate (Sulfo-LC-SPDP) was used to crosslink the C-Ab. The crosslinkages were then dissociated by breaking the disulfide bonds using dithiothreitol, leaving behind individual thiolated antibodies which readily adsorbed to the gold surface. Casein was used to block the cantilevers, and the reference cantilevers were coated in BSA. The magnitude of the differential deflection between the active and control cantilevers was comparatively small, only 10 nm over one hour, and there was a systemic downward deflection of the cantilevers. The detection limit was 85 ng/ml. Fluorescent antibodies were used to validate the binding of the capture antibody to the gold surface, and to show that there was limited C-Ab binding to the backside of the cantilevers. The binding pattern of the antibodies to the active surface was far from uniform however.[65]

Troponin C, a primary marker for myocardial injury, is another biomarker which has been investigated. The experimental approach and goals described in this paper were significantly different from the majority of the protein detection experiments. The purpose of the experiments was to investigate the interaction of the enzyme Troponin C with the substrate bee venom melittin using deflection cantilevers. Polyvinylidene fluoride-coated 2.5 mm x 0.8 mm aluminum cantilevers were used to examine the enzyme interaction. The concentrations used were in the tens of mg/ml, which is much greater than those used in other experiments. Also, the bee venom melittin and Troponin C were allowed to form a complex which was then applied to the cantilever surface. The resultant deflection pattern appeared to be similar even at different concentrations and was distinctly different from the deflection of plain Troponin C. In addition, the peak deflection increased reasonably linearly with the Troponin-melittin complex concentration. The detection limit was 1 mg/ml.[66] While informative, this method is not particularly useful for measurement of Troponin C in blood or serum samples because the bee venom will likely bind nonspecifically to other proteins, the detection limit is low, and the backsides of the cantilevers were not blocked.

The next paper was interesting because it investigates the aggregation of proteins, namely the growth of Amyloid proteins. The measurements were performed with individual v-shaped cantilevers and rectangular cantilever arrays. The silicon nitride v-shaped cantilevers, 220  $\mu\text{m}$  long and 0.6  $\mu\text{m}$  thick, were evaporated with 2 nm of chromium and 20 nm gold, and were blocked using a PEG-thiol in HCl. The backside was then identically coated in chromium and gold. The silicon cantilever arrays from IBM Zurich, with cantilevers 500  $\mu\text{m}$  long, 100  $\mu\text{m}$  wide and 1  $\mu\text{m}$  thick, were coated in 2 nm titanium and 20 nm gold. Seed fibrils were produced from processed bovine insulin and were used to coat the cantilevers. The individual cantilevers were functionalized using pipette tips and glass capillary tubes were used to functionalize the active cantilevers on the arrays. All the cantilevers were then blocked with PEG-thiol and were equilibrated in low molar HCl for 24-26 hours prior to the cantilever

measurements. The aggregation of the insulin fibrils continued for up to ten hours before individual v-shaped cantilevers were saturated. Since the backsides of the cantilevers in the arrays were not blocked, significant variation was observed from one reference cantilever to the next. [67]

Measurements with single-side gold coated cantilevers are susceptible to nonspecific deflection from temperature fluctuations due to the greater thermal expansion coefficient of the gold coating compared to the silicon substrate. Similarly, the greater sensitivity of the silicon substrate to ion concentration in aqueous solution can also cause nonspecific deflection. A different approach taken by Montserrat *et al.* made use of SU-8 photoresist cantilevers which were blocked on one side with a chemically inert fluorocarbon film. These materials are relatively inert to ions and have the potential for more sensitive protein detection due to the lower Young's modulus of SU-8. The cantilevers used were 200 nm long, 20  $\mu\text{m}$  wide and 4.5  $\mu\text{m}$  thick. The deflection due to temperature variation of the SU-8 cantilevers was about 3 times less than for comparable gold-coated silicon cantilevers. Furthermore, the deflection due to pH change was 6 times less between pH 7 and 11 and 50 times less between pH 7 and 2. The cantilevers were treated in piranha for 10 s to create free hydroxyl groups which allowed a thiol-silane to link to the surface. The heterobifunctional crosslinkers NHS and N-3-dimethylaminopropyl-N'-ethylcarbodiimide hydrochloride were used to link human growth hormone (hGH) antigen to the cantilever surface. Any remaining active linker sites were blocked with ethanolamine. A nonspecific antibody was used to test the blocking efficiency and no deflection was observed. The hGH antibody was successfully detected at a concentration of 5  $\mu\text{g}/\text{ml}$ . [68]

Aside from antibodies, a common method to detect proteins like enzymes or receptors is through the proteins or segments of proteins with which they normally react. Mukhopadhyay *et al.* used gold-coated piezoresistive silicon nitride cantilevers to determine the conformation of the human oestrogen receptor. The arrays used were commercial cantilever arrays (CantiChip4) from Cation A/S with 4 rectangular cantilevers per array. The cantilevers were 480 nm thick, 120  $\mu\text{m}$  long and 50  $\mu\text{m}$  wide. The measurements were performed using

the CantiLab system, also from Cation A/S. Alternating cantilevers were coated with one of two peptides, each of which was specific to one of the two conformations of the human oestrogen receptor. The conformation of the protein was identified by the cantilevers with the greatest deflection magnitude. The peptides were thiolated to facilitate linking to the gold surface and the backsides of the cantilevers were blocked using BSA. It is interesting to note that the two protein conformations resulted in cantilever deflection in opposite directions. In contrast to the majority of reported data on deflection cantilever detection of proteins, the results of a number of repetitions were presented, with reasonable consistency in cantilever deflection for 10 and 20 nM protein concentrations.[69]

Commonly, the measurement of proteins is performed in a plain buffer environment, because measurements in complex solutions are more prone to nonspecific binding. Shu *et al.*, however, successfully measured human cyclin-dependent protein kinase 2 (CDK2) in a complex solution derived from lysed cells. The silicon nitride cantilevers used were 600 nm thick, 220  $\mu\text{m}$  long and 22  $\mu\text{m}$  wide. Both cantilever surfaces were evaporated with 2 nm of chromium and 20 nm of gold and one surface was blocked with PEG-thiol. Since the chromium and gold layers were identical on both sides of the cantilever, deflection due to environmental conditions was significantly reduced when compared to single-side gold-coated cantilevers. A thiolated scaffold protein, Stefin A Triple Mutant, was used to link peptides specific to CDK2 to the gold surface. Any remaining open sites on the active gold surface were blocked with a PEG-thiol. CDK2 was measured at a concentration of 80 nM in cell lysate with an average deflection of 119 nm and a standard deviation of 37 nm over five measurements.[70]

While only applicable for a very select type of proteins, nucleic acid sequences can be used for specific protein detection. Eukaryotic RNA polymerase, for example, requires a TATA box DNA sequence to bind and initiate transcription. Savran *et al.* linked DNA sequences to a silicon nitride interdigitated cantilever sensor which was evaporated with 1 nm of titanium and 20 nm of gold. The active cantilever was functionalized with a DNA sequence specific to Taq DNA polymerase while the reference cantilever was blocked with

a random single-stranded DNA sequence. The DNA was linked to the surface through a thiol tag which was added to one end of the sequence. The Taq DNA polymerase was successfully detected in buffer and at a concentration of 50 pM in a dilute cell lysate solution.[71]

In another paper, antibodies were used to detect other antibodies using v-shaped cantilevers (200  $\mu\text{m}$  long, 40  $\mu\text{m}$  wide and 0.6  $\mu\text{m}$  thick) which were evaporated with 5 nm of chromium and 25 nm of gold. The carboxyl terminated thiol (SH-(CH<sub>2</sub>)<sub>7</sub>-COOH) mentioned earlier was used to form a SAM on the gold surface, and EDC/NHS chemistry was used to link the anti-IgG1 antibodies to the carboxylated surface. Any remaining active sites after the linking procedure were inactivated by ethanolamine. The sensors successfully detected IgG1 antibodies at a concentration of 50  $\mu\text{g/ml}$ . Unsurprisingly, it was found that higher antibody concentrations during the incubation step led to a higher antibody concentration on the gold surface. The interesting aspect of the experiments was however, that an electric field was used to attract the C-Ab to the cantilever surface. It was found that an electric field could be used to increase the relative C-Ab density on the cantilever surface, thus reducing the C-Ab concentration required in the functionalization solution and reducing the cost of the biosensor. [72]

In addition to performing antibody measurements, deflection cantilevers can also be used to measure viral proteins. This could potentially be used to diagnose infection or for research purposes. In the following report glycoprotein 120 (gp120) from human immunodeficiency virus type 1 was measured using monoclonal antibodies on AFM cantilevers. A SAM of 16-mercaptohexadecanoic acid was formed on the surface of the commercial gold-coated AFM cantilevers (600 nm thick, 196  $\mu\text{m}$  long and 18  $\mu\text{m}$  wide). The cantilevers were then incubated with EDC and NHS. In some of the experiments the antibodies were then linked directly to the surface. In others, an additional PEG incubation step was inserted into the procedure after the first EDC/NHS treatment and a second EDC/NHS step was used to link the antibody to the PEG on the surface. The gp120 was successfully detected, and further verification of detection was provided by the deflection caused by the addition of a secondary monoclonal

antibody specific to gp120. Interestingly, the addition of a PEG spacer molecule significantly decreased deflection from gp120 binding. [73]

An interesting method for improving protein detection was presented by Backmann *et al.* Instead of whole antibodies, thiolated single-chain antibody fragments were used to capture peptides. The eight cantilever (500 nm thick) silicon cantilever arrays were blocked with 2-[methoxypoly(ethyleneoxy)propyl]trimethoxysilane and following the silanization step the active cantilever surfaces were evaporated with 2 nm of titanium and 20 nm of gold. The active cantilevers were coated with a C11L34 antibody fragment specific to peptide GCN4(7P14P) which comes from yeast transcription factor GCN4. The control cantilevers were coated with a G9 antibody fragment which binds a peptide from amyloid protein PrP and the arrays were blocked with casein. A heat test was performed to determine the homogeneity of the functionalized cantilever deflection. The temperature was raised 2°C, and the maximum deflection was recorded. Only those cantilevers with the same maximum deflection were used in the peptide measurements. The detection limit reached was 20 ng/ml. [74]

Biotin-streptavidin binding experiments performed by Shu *et al.* lead to some interesting results concerning the effects of linking methods. The v-shaped cantilevers (220 μm long and 0.6 μm thick) were evaporated with 2 nm of chromium and 20 nm of gold, and one side was passivated using a PEG-thiol. Biotin was linked to the other gold surface in three different configurations as follow. The disulfide bond in (N-(6-(Biotinamido)hexyl)-3'-(2'-pyridyldithio)-propionamide (Biotin-HPDP) breaks apart upon contact with gold, leaving free biotin and pyridine molecules linked to the surface. Incubation with Biotin-polyethylene glycol disulfide (biotin-PEG) leaves free biotin molecules linked to the gold surface through a PEG spacer arm. Incubation with Biotin-SS-NHS also causes the disulfide bond to break upon contact with gold, leaving free NHS and biotin molecules linked to the cantilever surface. Interestingly, upon injection of 10 nM streptavidin into the measurement chamber, the biotin-HPDP cantilevers deflected towards the biotin coated surface, the biotin-PEG cantilevers were unresponsive and the Biotin-SS-NHS cantilevers deflected away from the biotin-

coated surface. The detection limit was found to be between 1 and 10 nM. [75] This result indicates that the linking method used can have a significant effect on the direction and magnitude of cantilever deflection.

The final three experiments of interest were characterized by microstructured cantilevers, MOSFET embedded cantilevers and protein adsorption to gold-coated cantilevers respectively. In the first paper, dealloyed nanostructured cantilevers were used to measure human interleukin-1 beta. The measurement sensitivity was 10 parts per billion or roughly 100 ng/ml, and the coefficient of variation was 10%. The antibodies were linked to the cantilevers using 2-aminoethanethiol hydrochloride and glutaraldehyde. The cantilever dimensions were not given. [76]

MOSFET-embedded gold-coated cantilevers were used in the second paper. The cantilever arrays produced each had 50 cantilevers (200 to 300  $\mu\text{m}$  long and 1.5 to 2  $\mu\text{m}$  thick) and streptavidin linked to the gold coated cantilever surface with DTSSP was used to measure biotin in buffer solution. A second experiment was performed where rabbit anti-goat antibodies linked to the gold surface with DTSSP were used to detect goat antibodies. The detection limit was not given. [51]

Finally, some of the earliest protein detection experiments were performed by Moulin *et al.* Instead of specific protein measurements, the deflection caused by the adsorption and deformation of BSA and antibodies on a bare gold surface was demonstrated. The silicon side of gold-coated AFM cantilevers was blocked with PEG-thiol. Interestingly the adsorption of antibodies caused compressive stress while the adsorption of BSA caused tensile stress.[77]

## 2.4 Research Rationale and Approach

It is evident from the review of deflection cantilever array-based protein detection, presented in section 2.3.2, that there are a number of valid approaches to the measurement of proteins using deflection cantilevers. Three main approaches were used to specifically bind the protein of interest to the cantilever

surface: DNA interactions, specific binding protein interactions and antibody-antigen interactions. While DNA interactions and protein-protein (or protein-peptide) interactions are undoubtedly useful, in most cases the protein of interest does not bind to DNA and frequently no specific protein-protein interactions exist. This leaves antibody-antigen interaction as the most convenient specific method for protein detection.

The review in Section 2.3.2 also illustrates the large number of valid linking and blocking procedures available and that these procedures can significantly affect the cantilever deflection results. Therefore the linking and blocking efficiency of a number of different procedures was investigated in detail. Because of the high cost of cantilever arrays, however, the procedures were first investigated using fluorescence and ELISA measurements. The reagents from a commercial human INF- $\gamma$  ELISA kit were used to test the linking and blocking procedures on gold and silicon surfaces in order to evaluate their effectiveness for the cantilever array-based detection of proteins. The experimental results from these experiments are described and discussed in Chapter 3.

Following the investigation of the linking and blocking procedures, the methods which were deemed most effective were implemented on the cantilever arrays, again using the reagents from the human INF- $\gamma$  ELISA kit. Certain blocking procedures were used to block the backsides of the cantilevers while others were used to coat the active surface of the reference cantilevers. The reference cantilevers were used to remove nonspecific deflection signals from the sensing cantilevers in the array experiments. The results from the cantilever experiments are described and discussed in Chapter 4. This is followed, in Chapter 5, with a general summary and recommendations for future work.

## Chapter 3

# Analysis of Linking and Blocking Procedures by Fluorescence and Enzyme Linked Immunosorbent Assays

Effective linking and blocking procedures are critical for many protein detection and measurement techniques. The goal of these procedures is to maximize sensitivity and minimize nonspecific and background signals. This is equally true for the measurement of proteins with antibody coated deflection cantilevers, the central topic of this thesis. More specifically, for this method of protein measurement the linking and blocking methods should meet the following requirements: i) The linker should maximize the antibody density on the active surface of the cantilevers and should ideally orient the active sites of the antibodies away from the cantilever surface. ii) The control blocker used on the active surface of the reference cantilevers should behave similarly to the antibodies on the sensing cantilevers but be inert to the antigenic protein. The reference cantilevers are used to account for any signal generated by nonspecific reactions due to environmental conditions. iii) The blocker used to passivate the backside of both the active and reference cantilevers should prevent molecular adsorption and binding. This blocker reduces nonspecific deflection due to induced surface stress by preventing molecules from adhering to the backside of the cantilevers. iv) An optional blocker may be used following the antibody-linking step to block any remaining open sites on the active surface of the cantilever. The purpose of the ELISA and fluorescence measurements was to examine linking and blocking methodologies and, based on the above criteria, determine which would be the most effective for the cantilever experiments.

ELISAs are generally much more sensitive than fluorescence imaging due to the amplifying effect of the enzyme. The human INF- $\gamma$  ELISA kit that was selected to test the linking and blocking procedures has a useful detection range of approximately 50 to 1000 pg/ml. While in principle the ELISA kit may be used at higher INF- $\gamma$  concentrations, the effective range would likely remain small and all the reagent concentrations would have to be adjusted to produce a proper standard curve. The C-Ab and INF- $\gamma$  concentrations used in the fluorescence experiments were significantly greater than those used in the ELISA experiments. This was necessary in order to generate sufficient fluorescence to differentiate the sample and control images. The greater concentrations also closely approximated those used in the cantilever experiments. In addition, the fluorescence images could be used to examine the level of homogeneity produced by the linking procedures. The ELISA method on the other hand, was more sensitive, accurate, convenient and reproducible and was therefore used for the majority of the linking and blocking experiments.

A commercial INF- $\gamma$  ELISA kit was selected for these experiments for a number of reasons. Firstly, using a kit ensures that the antibodies used are compatible and have a strong affinity for the INF- $\gamma$ . This is crucial because INF- $\gamma$  antibodies and the INF- $\gamma$  itself may vary depending on a number of factors, including the DNA sequence of the antigenic INF- $\gamma$ , the cell line used to produce the antibodies and the screening method used to select the antibodies. In addition, the human INF- $\gamma$  kit contains mouse antihuman INF- $\gamma$  C-Ab type IgG2a. This is convenient because Protein A has a strong affinity for mouse IgG2a type antibodies. In addition, this also simplified the selection of a control antibody for the reference cantilevers, because the canine INF- $\gamma$  ELISA kit from the same company contained mouse anti-canine INF- $\gamma$  C-Ab type IgG2a which has low cross-reactivity with human INF- $\gamma$ .

The following chapter is divided into six sections. The first section contains a list of all the materials and solutions that were used, as well as a brief description of the linking and blocking procedures which were examined. The original protocol upon which all the ELISA experiments were based is presented

in the second section. The third section relates the results from the fluorescent antibody experiments. The ELISA results are divided into two sections. Section 3.4 deals with the effects of experimental conditions on the ELISA results while section 3.5 presents the results from the examination of the linking and blocking procedures. The last section contains a brief summary of all the results and conclusions from both the fluorescence and ELISA experiments.

## 3.1 Materials and Solutions

### 3.1.1 Materials

**BD Falcon:** 96-well plates, BD 353072

**Fisher Scientific:** 1-Ethyl-3-[3-dimethylaminopropyl]carbodiimide Hydrochloride (EDC), PI-22980; *N*-hydroxysulfosuccinimide (Sulfo-NHS), PI-24510

**Gelbst:** 2-[Methoxy(polyethyleneoxy)propyl]-trimethoxysilane (PEG-Silane) 90%, SIM6492.7

**Millipore:** MilliQ water purification system; all water used except during the piranha cleaning and evaporation steps was purified by this machine

**NINT Biology Lab:** Microplate reader; Olympus IX81 Inverted Fluorescence Microscope; Nitrogen gas

**Polypure:** 98% pure HO(CH<sub>2</sub>CH<sub>2</sub>O)<sub>11</sub>CH<sub>2</sub>CH<sub>2</sub>SH (PEG-thiol)

**Proteogen:** Prolinker A; Prolinker B

**R&D Systems:** Canine IFN-gamma DuoSet ELISA, DY781; Human IFN-gamma DuoSet ELISA, DY285; Recombinant human IFN-gamma, CF 285-IF-100/CF; Stop solution sulfuric acid, DY994; Substrate reagent pack, DY999

**Sigma-Aldrich:** 2-(*N*-morpholino)ethanesulfonic acid (MES); 3-aminopropyltriethoxysilane (APTES) A3648; 4, 7, 10, 13, 16, 19, 22, 25, 32, 35, 38, 41, 44, 47, 50, 53-Hexadecaoxa-28, 29-dithiahexapentacontanedioic acid di-*N*-succinimidyl ester, 671630 (DSP-PEG); Acetone 95% pure; Albumin from

bovine serum (BSA), A3059; Alexa Fluor 350 rabbit anti-mouse IgG (H+L) 2 mg/ml, A-21062; Anhydrous chloroform 99% pure; Cysteamine hydrochloride, M6500; Dimethyl sulfoxide (DMSO); Dithiobis[succinimidyl propionate] (DSP), D3669; Cysteamine hydrochloride, M6500; Disodium hydrogen phosphate ( $\text{Na}_2\text{HPO}_4$ ); Hydrogen peroxide ( $\text{H}_2\text{O}_2$ ); Fluorescein isothiocyanate (FITC)-Streptavidin; Methanol (95%); Monopotassium phosphate ( $\text{KH}_2\text{PO}_4$ ); Mouse Anti-Human Interferon gamma Alexa Fluor 488, MHCIFG20; Potassium chloride (KCl); Protein A from *Staphylococcus aureus*, P6031; Sodium azide ( $\text{NaN}_3$ ), Sodium chloride (NaCl); Trizma base; Tween 20

**University of Alberta Chemistry Stores:** 95% Ethanol (this was used unless otherwise indicated); 99% pure Ethanol; 95% Isopropyl alcohol

**University of Alberta Nanofabrication Facility:** Chromium target; Distilled clean-room water; Gold target; 30% Hydrogen peroxide ( $\text{H}_2\text{O}_2$ ); Planar magnetron sputter system; 86% Sulfuric acid ( $\text{H}_2\text{SO}_4$ ); Titanium target; Water cooled bell-jar cryo-pumped four pocket evaporator

**University Wafer:** 100mm P(100) 1-100 ohm-cm 500um DSP Test Silicon Wafer both single and side polished and dual sided polished

### 3.1.2 Solutions

**2-(N-morpholino)ethanesulfonic acid saline (MES) buffer:** 0.1 M 2-(N-morpholino)ethanesulfonic acid and 0.5 M NaCl pH 6.0;

**Blocking Buffer:** 1% BSA in Phosphate buffered saline (PBS);

**Concentrated PBS:** 1 M NaCl, 270 mM KCl, 810 mM  $\text{Na}_2\text{HPO}_4$ , 150 mM  $\text{KH}_2\text{PO}_4$ , pH 7.2 - 7.4, 0.2  $\mu\text{m}$  filtered;

**PBS:** 137 mM NaCl, 2.7 mM KCl, 8.1 mM  $\text{Na}_2\text{HPO}_4$ , 1.5 mM  $\text{KH}_2\text{PO}_4$ , pH 7.2 - 7.4, 0.2  $\mu\text{m}$  filtered;

**Piranha:** 3:1 v/v 86%  $\text{H}_2\text{SO}_4$ :30%  $\text{H}_2\text{O}_2$ ;

**Reagent Diluent:** 0.1% BSA, 0.05% Tween 20 in Tris-buffered saline (20 mM Trizma base, 150 mM NaCl) pH 7.2 - 7.4, 0.2  $\mu\text{m}$  filtered;

**Stop Solution:** 2 N  $\text{H}_2\text{SO}_4$  from the stop solution pack;

**Substrate Solution:** 1:1 mixture of Color reagent A (H<sub>2</sub>O<sub>2</sub>) and Color reagent B (Tetramethylbenzidine) from the substrate reagent pack;

**Wash Buffer:** 0.05% Tween 20 in PBS, pH 7.2 - 7.4

### 3.1.3 Linking and Blocking Procedures

As the examination of linking and blocking procedures is integral to this Chapter and to Chapter 4, it is valuable to briefly examine the linking methodologies which were used. The seven linkers and blockers that were examined are described below.

Prolinker B is a calixcrown chemical linker which binds to proteins through free amine groups and has two free thiols which link it to gold surfaces. It also vertically orients the antibodies and performed better than other common linkers like Protein A and superaldehyde in a fluorescence test.[78, 79] The orientation of the C-Abs ensures that the active sites face away from the surface so that they can capture the antigen. This should increase the binding capacity of the cantilevers as well as the attractive or repulsive forces between the antigen molecules when they bind to the C-Abs on the cantilever surface, thus increasing the detection sensitivity. In addition, the results from Lam *et al.* [73] suggest that shorter linkers like Prolinker B also increase the sensitivity of cantilever detection.

Protein A is a protein found in *Staphylococcus aureus* bacteria which specifically binds and orients certain antibody isotypes, including rabbit IgG2a, the isotype of the C-Abs used in the experiments below. In addition, the side opposite to the binding domain adheres to various surfaces, including gold and silicon surfaces. Protein A is commonly used in biosensors and other applications to link antibodies to these surfaces in an oriented manner. [80, 81]

Succinimidyl and water-soluble sulfo-succinimidyl groups are leaving groups which react with free amines, and are often used in linkers to create covalent bonds between the linker and proteins. Three of the linking methods tested make use of succinimidyl/amine substitution reactions. Dithiobis

[succinimidyl propionate] (DSP) is a crosslinker with two succinimidyl groups which are connected by a water-insoluble disulfide bond. Upon contact with gold, the disulfide bond breaks apart and the thiols link the succinimidyl groups to the gold surface. 4, 7, 10, 13, 16, 19, 22, 25, 32, 35, 38, 41, 44, 47, 50, 53-Hexadeca-2,8,14-trithiahexapentacontanedioic acid di-N-succinimidyl ester (DSP-PEG) is identical to regular DSP apart from a polyethylene oxide spacer group between each succinimidyl group and the disulfide bond. *N*-hydroxysulfosuccinimide (Sulfo-NHS) is a water-soluble linker which is often used in conjunction with EDC to crosslink a free amine and a carboxyl group together. The EDC binds a carboxyl group, which binds the Sulfo-NHS, which then binds an amine group. After binding the carboxyl group the EDC may also bind a free amine directly and create a stable amide bond instead, however, which means that the bonding in this linking method is heterogeneous. In order to bind the proteins to the surface the EDC/Sulfo-NHS was incubated with the C-Ab first and then the aminated gold surface was incubated with the EDC/Sulfo-NHS C-Ab solution.

The two other linkers which were tested also require an aminated surface. Glutaraldehyde is a chemical crosslinker with two aldehyde groups which link to free amines. Prolinker A is identical to Prolinker B except that instead of two free thiols to link to a gold surface, it has two free aldehyde groups which link it to amines on the surface. These two linkers were tested on silicon or gold surfaces that were aminated using 3-aminopropyltriethoxysilane (APTES) or cysteamine respectively.

Five main blocking agents were evaluated. The protein BSA is commonly used in ELISAs to inhibit nonspecific binding to the surface of the wells. A canine C-Ab (cC-Ab) similar to the normal C-Ab but inert to the protein of interest was used to coat the reference cantilevers. Polyethylene glycol (PEG) is a hydrophilic molecule which has been shown to inhibit protein adsorption. 2-[Methoxy(polyethyleneoxy)propyl]-trimethoxysilane (PEG-Silane) and HO(CH<sub>2</sub>CH<sub>2</sub>O)<sub>11</sub>CH<sub>2</sub>CH<sub>2</sub>SH (PEG-thiol) are PEG-based blocking agents with demonstrated anti-protein adsorption properties.[74, 82] The last blocking agent

used was ethanolamine. It is also a hydrophilic molecule and it was mainly used to decrease nonspecific binding by inactivating any remaining free linking sites after the C-Ab linking step.

## 3.2 R&D Systems Enzyme Linked Immunosorbent Assay Protocol

Before any other experiments were performed it was critical to verify that the ELISA kit worked as specified. A transcript of the ELISA instructions supplied by the manufacturer is shown below. These instructions were used as a base for all the other experiments which followed. The procedure is essentially identical to the indirect ELISA shown in Figure 1.4 (iii). The dilute C-Ab concentration was 4 µg/ml in PBS, the Blocking Buffer was as listed in the materials and solutions but with the addition of 0.05% Sodium Azide, the standard consisted of seven twofold dilutions of 1 ng/ml INF-γ in reagent diluent, the dilute Detection Antibody was 50 ng/ml in reagent diluent, the dilute HRP-streptavidin was 1:200 v/v stock solution: reagent diluent.

### **General ELISA Protocol**

#### **Plate Preparation**

1. Dilute the Capture Antibody to the working concentration in PBS without carrier protein. Immediately coat a 96-well microplate with 100 µL per well of the diluted Capture Antibody. Seal the plate and incubate overnight at room temperature.
2. Aspirate each well and wash with Wash Buffer, repeating the process two times for a total of three washes. Wash by filling each well with Wash Buffer (400 µL) using a squirt bottle, manifold dispenser, or autowasher. Complete removal of liquid at each step is essential for good performance. After the last wash, remove any remaining Wash Buffer by aspirating or by inverting the plate and blotting it against clean paper towels.

3. Block plates by adding 300  $\mu\text{L}$  of Block Buffer to each well. Incubate at room temperature for a minimum of 1 hour.
4. Repeat the aspiration/wash as in step 2. The plates are now ready for sample addition.

### **Assay Procedure**

1. Add 100  $\mu\text{L}$  of sample or standards in Reagent Diluent, or an appropriate diluent, per well. Cover with an adhesive strip and incubate 2 hours at room temperature. Prepare Detection Antibody.
2. Repeat the aspiration/wash as in step 2 of Plate Preparation.
3. Add 100  $\mu\text{L}$  of the Detection Antibody, diluted in Reagent Diluent, to each well. Cover with a new adhesive strip and incubate 2 hours at room temperature.
4. Repeat the aspiration/wash as in step 2 of Plate Preparation.
5. Add 100  $\mu\text{L}$  of the working dilution of Streptavidin-HRP to each well. Cover the plate and incubate for 20 minutes at room temperature. Avoid placing the plate in direct light.
6. Repeat the aspiration/wash as in step 2.
7. Add 100  $\mu\text{L}$  of Substrate Solution to each well. Incubate for 20 minutes at room temperature. Avoid placing the plate in direct light.
8. Add 50  $\mu\text{L}$  of Stop Solution to each well. Gently tap the plate to ensure thorough mixing.
9. Determine the OD of each well immediately, using a microplate reader set to 450 nm. If wavelength correction is available, set to 540 nm or 570 nm. If wavelength correction is not available, subtract readings at 540 nm or 570 nm from the readings at 450 nm. This subtraction will correct for optical imperfections in the plate. Readings made directly at 450 nm without correction may be higher and less accurate.[83]

The ELISA kit procedure was tested using the above procedure with INF- $\gamma$  concentrations of 1000, 500, 250, 125, 62.5, 31.25, 15.625, and 0 pg/ml in reagent diluent. The results (Figure 3.1) exhibit the linearity of the standard curve.

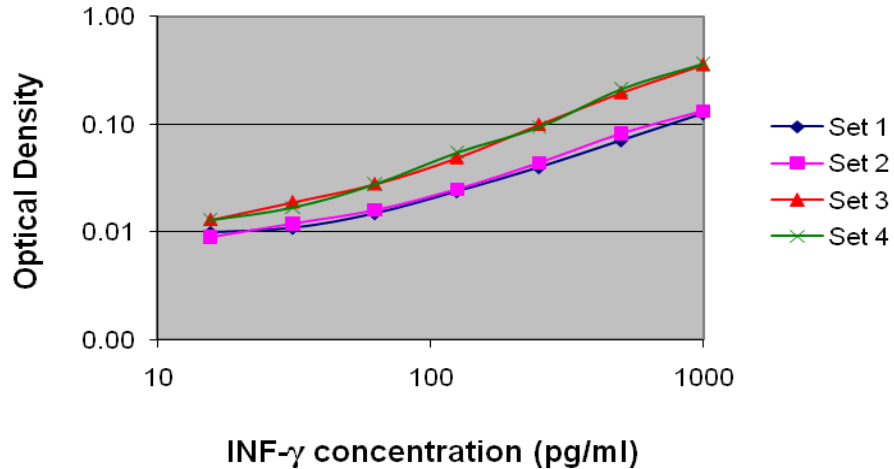


Figure 3.1: Log-log plot of OD vs. INF- $\gamma$  concentration. Set 1 and set 2 were tested on one occasion while set 3 and set 4 were performed on a separate occasion. The 0  $\mu\text{g/ml}$  INF- $\gamma$  values were 0.008, 0.007, 0.010, and 0.010 for Set 1 through Set 4 respectively.

### 3.3 Examination of Interferon Gamma and Capture Antibody binding on gold surfaces by Fluorescence

The initial purpose of the fluorescence experiments was to verify that the INF- $\gamma$  was binding properly to the gold surface. These tests were performed with silicon chips sputtered with gold. The ELISA procedure outlined in the General ELISA Protocol (section 2.2) was followed up to the HRP-Streptavidin incubation step which was replaced with a fluorescent Fluorescein isothiocyanate (FITC)-Streptavidin incubation step. The chips were then investigated under the fluorescence microscope. The low intensity of the fluorescence made visual inspection of the chips unfeasible and was likely a result of the fluorescence quenching which occurs when a fluorophore is near a metal surface.[84]

In order to improve the quality of the fluorescence images the procedure was altered to decrease the background emission, and increase the surface fluorescence. When a large chain of proteins is used, like in an ELISA, it is

possible that some proteins may break off during the washing steps. Alexa Fluor 488 mouse anti-human INF- $\gamma$  and Alexa Fluor 350 rabbit anti-mouse IgG antibodies were purchased to reduce the number of links in the molecular chain. The Alexa fluors should also produce more intense fluorescence per unit than the FITC. In addition, the two fluorescent antibodies allowed the C-Ab and INF- $\gamma$  densities to be examined separately. Finally, the C-Ab and INF- $\gamma$  concentrations were increased significantly both to increase the fluorescence signal and to more closely approximate the conditions used during the cantilever experiments. Schematic representations of the two processes are shown in Figures 3.2 and 3.3.

Despite these changes, the signal of both the active and control chips remained very weak. Since the gamma correction of the images was 1.0, the relationship between the fluorescent intensity and the pixel values recorded by the camera was linear. Consequently, instead of examining the images purely from a visual perspective, the summation of the pixel values in the image files were used to give a numerical value to the fluorescent intensity of each representational image. These were then used to determine the relative effectiveness of the linking procedures.

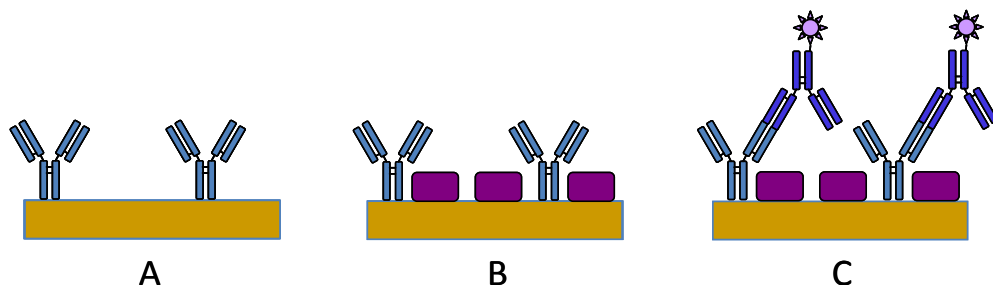


Figure 3.2: Schematic diagram of the measurement of C-Ab linked to the surface of gold chips. A - The C-Ab is linked to the surface. B - Blocking molecules fill in any remaining open spaces after the linking step. C - The fluorescent anti-mouse antibody binds to the C-Ab on the surface.

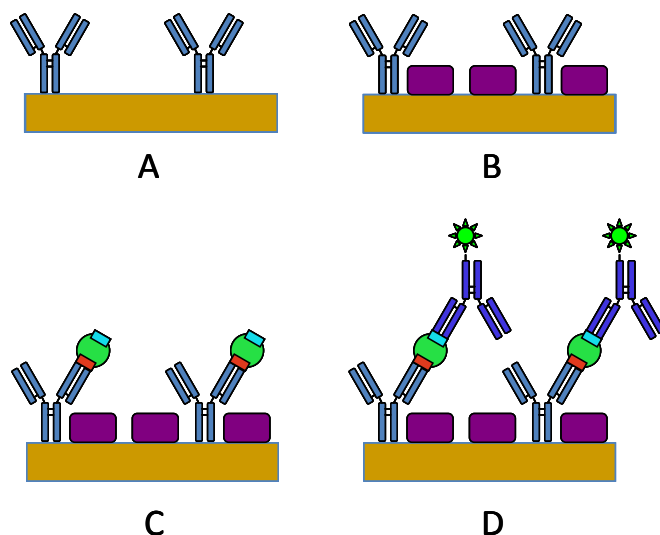


Figure 3.3: Schematic diagram of the measurement of INF- $\gamma$  linked to antibodies on the surface of gold chips. A - The C-Ab is linked to the surface. B - Blocking molecules fill in any remaining open spaces after the linking step. C - The INF- $\gamma$  binds to the C-Ab. D - The fluorescent anti-human INF- $\gamma$  antibody binds to the INF- $\gamma$  on the surface.

### 3.3.1 Examination of Murine Antibody Density on Gold Chips with Fluorescent Rabbit Anti-Mouse Immunoglobulin G Antibodies

The purpose of this experiment was to examine the binding of the murine C-Ab to the gold chips with Alexa Fluor 350 rabbit anti-mouse IgG fluorescent antibodies (Figure 3.2). Polished silicon wafers were cleaned in piranha, isopropyl alcohol (IPA), and water and were dried with nitrogen. The wafers were then evaporated with 3 nm of titanium and 40 nm of gold and were diced into 5x7 mm chips. Evaporation was selected over sputtering because evaporation should provide better stress conduction on the cantilever arrays due to larger grain size and lower surface roughness. This preparation of the gold chips was followed for all the remaining fluorescence experiments.

The chips were used to perform a simultaneous measurement of six linkers: Prolinker B, Protein A, DSP, DSP-PEG, glutaraldehyde, and EDC/Sulfo-NHS. The chips were sonicated in acetone and then washed in IPA and water. The

Prolinker B chips were washed 2x in chloroform and incubated in 1 mM Prolinker B for one hour. Subsequently they were washed in chloroform, IPA, water and PBS. The Protein A chips were incubated in 100 µg/ml Protein A in PBS for 1.5 hours and washed 3x in PBS. The DSP and DSP-PEG chips were washed 3x in DMSO and incubated in 4 mg/ml DSP and DSP-PEG in DMSO respectively for 30 minutes. Subsequently, they were washed in DMSO, water and 3x in PBS. The glutaraldehyde chips were incubated overnight in 10 mM cysteamine in PBS, washed 3x in PBS, placed in 10% (v/v) glutaraldehyde in PBS for 1.5 hours, and washed again 3x in PBS.

All the sample chips except the EDC/Sulfo-NHS sample chip were placed in 100 µg/ml hC-Ab in PBS. For the Prolinker B, DSP, DSP-PEG and glutaraldehyde chips the incubation time was 1 hour and for the Protein A chip the incubation time was overnight, due to nonspecific binding issues which will be discussed in the ELISA sections. The EDC/Sulfo-NHS chips were incubated in 10 mM Cysteamine in PBS overnight and washed 3x in PBS. Solutions of 2 mM EDC and 5 mM Sulfo-NHS in MES buffer, with 100 µg/ml hC-Ab and 0 µg/ml hC-Ab for the active and control chips respectively, were allowed to react for 15 minutes. The EDC reactions were then halted with the addition of 2-mercaptoethanol to a final concentration of 20 mM. To activate the Sulfo-NHS the pH was raised to above 7.0 with the addition of 20% v/v concentrated PBS. The chips were then left to incubate in this solution for 1 hour. Finally, the chips were washed 3x in PBS and placed in 7% ethanolamine in PBS for 15 minutes to inactivate the Sulfo-NHS.

The control chips were all incubated in blocking buffer for 1 hour. Subsequently, the control and sample chips were all washed 3x in PBS and incubated in blocking buffer for 1 hour. After a 3x wash in wash buffer the chips were placed in 8-fold diluted Alexa Fluor 350 rabbit anti-mouse IgG in PBS for 1 hour. The chips were again washed 3x in wash buffer and fluorescent images were taken in reagent diluent. The results are shown in Table 3.1. There is a clear difference between the sample and control in each case, which suggests that the antibodies were successfully linked to the gold surface. The EDC Sulfo-NHS

experiment showed significant variation in fluorescence intensity between the representative images. The Prolinker B procedure yielded a stronger signal than the other linkers, as well as the largest differential signal, though the Protein A procedure also performed well.

Table 3.1: Summation of the pixel values from representative fluorescence images of Alexa Fluor 350 rabbit anti-mouse IgG-labeled hC-Ab. Six different linkers were used to bind the C-Ab to the gold surface. The difference between the sample and control values indicates the efficacy of a given linking procedure for binding hC-Ab to the gold surface.

	DSP	EDC/Sulfo-NHS	Glutaraldehyde	DSP-PEG	Prolinker B	Protein A
Sample 1 ( $\times 10^7$ )	3.650	3.545	3.722	3.601	3.762	3.720
Sample 2 ( $\times 10^7$ )	3.640	3.673	3.717	3.591	3.765	3.682
Sample 3 ( $\times 10^7$ )	3.635	3.569	3.706	3.589	3.777	3.705
Average ( $\times 10^7$ )	<b>3.642</b>	<b>3.596</b>	<b>3.715</b>	<b>3.593</b>	<b>3.768</b>	<b>3.702</b>
Std. Dev. ( $\times 10^7$ )	0.008	0.068	0.009	0.007	0.008	0.019
Control 1 ( $\times 10^7$ )	3.556	3.522	3.630	3.555	3.602	3.540
Control 2 ( $\times 10^7$ )	3.554	3.519	3.625	3.545	3.593	3.542
Control 3 ( $\times 10^7$ )	3.550	3.521	3.623	3.554	3.590	3.535
Average ( $\times 10^7$ )	<b>3.553</b>	<b>3.521</b>	<b>3.626</b>	<b>3.551</b>	<b>3.595</b>	<b>3.539</b>
Std. Dev. ( $\times 10^7$ )	0.003	0.002	0.004	0.005	0.006	0.003
Difference ( $\times 10^7$ )	<b>0.089</b>	<b>0.075</b>	<b>0.089</b>	<b>0.042</b>	<b>0.173</b>	<b>0.163</b>

### 3.3.2 Examination of Human Interferon Gamma Density on Gold Chips with Fluorescent Mouse Anti-Human Interferon Gamma Antibodies

Since the linking methods appeared to be successfully binding hC-Ab, the next step was to examine how much INF- $\gamma$  was captured by the C-Abs. Alexa

Fluor 488 mouse anti-human INF- $\gamma$  antibody was selected for this purpose. Three separate measurements were performed using the DSP, EDC/Sulfo-NHS, and glutaraldehyde linking methods. These individual linker experiments were performed with some different concentrations and conditions than the simultaneous linking experiment (Table 3.3), which led to some interesting conclusions. The procedures used previously (Table 3.1) were repeated, but with a number of alterations. The procedure for the control chips was identical to that of the active chips except cC-Ab was used instead of hC-Ab, and the cC-Ab and hC-Ab concentrations for the EDC/Sulfo-NHS and glutaraldehyde linking procedures was 50  $\mu\text{g/ml}$  in PBS. The glutaraldehyde linker incubation period was 1 hour while the C-Ab incubation period for the glutaraldehyde chips was 1.5 hours. The Alexa Fluor 350 rabbit anti-mouse IgG step was replaced by a 2 hour incubation in 3  $\mu\text{g/ml}$  INF- $\gamma$  in PBS. The chips were then washed 3x in wash buffer and incubated for one hour in 8-fold diluted Alexa Fluor 488 mouse anti-human INF- $\gamma$  antibody in PBS, except that the incubation period for the glutaraldehyde chips was 1.5 hours. After a final 3x wash in wash buffer the images were taken with the fluorescence microscope. The results in Table 3.2 clearly show the difference between the sample and the control chips. Again there is more variation in the EDC/Sulfo-NHS pixel summations than for the other two linking procedures, however.

Following the individual linker experiments, a direct comparison of all six linkers was performed (Table 3.3). All the chips were sonicated in acetone, washed in IPA, washed in water, sonicated in chloroform and washed in chloroform. The Prolinker B chips were then incubated for 1 hour in 1 mM Prolinker B. Subsequently they were washed in chloroform, IPA, water and 3x in PBS. The DSP and DSP-PEG chips were washed in water and 3x DMSO. They were then placed in 4  $\mu\text{g/ml}$  of DSP and 21  $\mu\text{g/ml}$  DSP-PEG respectively for 30 minutes and were washed in DMSO, water and PBS. The Protein A, EDC/Sulfo-NHS and glutaraldehyde chips were all washed in water and PBS. The Protein A chips were placed in 100  $\mu\text{g/ml}$  Protein A in PBS overnight and the EDC/Sulfo-NHS and glutaraldehyde chips were placed in 10 mM cysteamine overnight. Both

sets of chips were then washed 3x in PBS. The EDC/Sulfo-NHS linking procedure was the same as was described previously (Table 3.2), except that 25 µg/ml C-Ab in PBS was used. The decreased C-Ab concentration was necessary for larger experiments using cC-Ab because it is supplied at the same price but one fourth the concentration of the hC-Ab. The glutaraldehyde chips were incubated in 10% v/v glutaraldehyde in PBS for 1.5 hours and then washed 3x in PBS.

Table 3.2: Summation of the pixel values from representative fluorescence images of human INF-γ labeled by Alexa Fluor 488 mouse anti-human INF-γ antibodies. DSP, EDC/Sulfo-NHS and glutaraldehyde were used to bind C-Ab to the gold surface. The difference between the sample and control values indicates the efficacy of a given linking procedure for sensitive and specific detection of INF-γ.

	DSP	EDC/Sulfo-NHS	Glutaraldehyde
Sample 1 (x 10 <sup>7</sup> )	3.398	3.479	3.819
Sample 2 (x 10 <sup>7</sup> )	3.392	3.421	3.817
Sample 3 (x 10 <sup>7</sup> )	n/a	3.415	3.787
Average (x 10 <sup>7</sup> )	<b>3.395</b>	<b>3.438</b>	<b>3.807</b>
Std. Dev. (x 10 <sup>7</sup> )	0.004	0.036	0.018
Control 1 (x 10 <sup>7</sup> )	3.23	3.281	3.589
Control 2 (x 10 <sup>7</sup> )	3.214	3.279	3.647
Control 3 (x 10 <sup>7</sup> )	n/a	3.299	3.62
Average (x 10 <sup>7</sup> )	<b>3.222</b>	<b>3.286</b>	<b>3.618</b>
Std. Dev. (x 10 <sup>7</sup> )	0.012	0.011	0.029
Difference (x 10 <sup>7</sup> )	<b>0.173</b>	<b>0.152</b>	<b>0.189</b>

All but the EDC/Sulfo-NHS chips were then placed in 25 µg/ml C-Ab (human and canine respectively for the active and control chips) in PBS for 1 hour except for the Protein A chips which were incubated in C-Ab for 4 hours. All the chips were then washed 3x in PBS and the rest of the procedure used to generate the Table 3.2 results was followed, except that the Alexa Fluor 488 mouse anti-human INF-γ antibody incubation period for all the chips was 2 hours. The results

are shown in Table 3.3. The effectiveness of the linkers was determined by the difference between the sample and control chip signals. The most effective linker by a significant margin was Prolinker B, followed by DSP-PEG and then Protein A. The other linkers were less effective, with a considerable decrease in the DSP, EDC/Sulfo-NHS and glutaraldehyde effectiveness as compared to Table 3.2.

Table 3.3: Summation of the pixel values from representative fluorescence images of human INF- $\gamma$  labeled by Alexa Fluor 488 mouse anti-human INF- $\gamma$  antibodies. Six different linkers were used to bind the C-Ab to the gold surface. The difference between the sample and control values indicates the efficacy of a given linking procedure for sensitive and specific detection of INF- $\gamma$ .

	DSP	EDC/Sulfo-NHS	Glutaraldehyde	DSP-PEG	Prolinker B	Protein A
Sample 1 ( $\times 10^7$ )	3.580	3.547	3.666	3.679	3.687	3.866
Sample 2 ( $\times 10^7$ )	3.620	3.509	3.697	3.792	3.695	3.647
Sample 3 ( $\times 10^7$ )	3.549	3.558	3.662	3.760	3.777	3.812
Sample 4 ( $\times 10^7$ )	n/a	n/a	3.678	3.741	3.739	3.826
Average ( $\times 10^7$ )	<b>3.583</b>	<b>3.538</b>	<b>3.676</b>	<b>3.743</b>	<b>3.725</b>	<b>3.788</b>
Std. Dev. ( $\times 10^7$ )	0.035	0.025	0.016	0.048	0.042	0.097
Control 1 ( $\times 10^7$ )	3.513	3.536	3.526	3.439	3.317	3.671
Control 2 ( $\times 10^7$ )	3.494	3.491	3.550	3.559	3.286	3.563
Control 3 ( $\times 10^7$ )	3.503	3.527	3.590	3.474	3.281	3.620
Control 4 ( $\times 10^7$ )	n/a	n/a	3.617	3.439	3.319	3.645
Average ( $\times 10^7$ )	<b>3.503</b>	<b>3.518</b>	<b>3.571</b>	<b>3.478</b>	<b>3.301</b>	<b>3.625</b>
Std. Dev. ( $\times 10^7$ )	0.010	0.024	0.040	0.057	0.020	0.046
Difference ( $\times 10^7$ )	<b>0.080</b>	<b>0.020</b>	<b>0.105</b>	<b>0.266</b>	<b>0.424</b>	<b>0.163</b>

### 3.3.3 Discussion

Table 3.1 shows that the highest antibody concentrations were achieved with Protein A and Prolinker B, with Prolinker B performing slightly better than

Protein A. The examination of the INF- $\gamma$  binding rate also demonstrated the greater effectiveness of Prolinker B as compared to the other linkers. The DSP-PEG was the second most effective linker because like Prolinker B it had a lower control signal, indicating little nonspecific binding. This is not surprising as the PEG in the spacer arm should serve to reduce nonspecific binding. The reduction in signal for the DSP, EDC/Sulfo-NHS and glutaraldehyde linkers from Table 3.2 to Table 3.3 was likely caused by the considerable decrease in C-Ab concentration. Also, the increase in the DSP-PEG signal was likely caused by the increase of the linker concentration, and the length of the fluorescent antibody incubation step. This suggests that the C-Ab concentration plays a major role in the effectiveness of INF- $\gamma$  capture, but that at least in the case of the DSP-PEG, this difference can be offset by increasing the linker concentration used. In addition, the large sample and control signals from the Protein A chips suggest that greater care must be taken to reduce nonspecific binding to optimize the Protein A linking procedure. Overall however, Prolinker B was considerably more effective than the other linkers tested.

### 3.4 Examination of the Effect of Experimental Conditions on Interferon Gamma Detection by Enzyme Linked Immunosorbent Assay

The initial ELISA experiments were mainly concerned with the use of Protein A and Prolinker B. These linkers were the most likely candidates for cantilever stress measurements because they orient the C-Ab on the gold surface and performed well in the fluorescence experiments. Ideally, the ELISA experiments would have been performed in 96-well plates, but unfortunately the width to depth ratio was too small to allow the sides of the wells to be completely evaporated with gold. Therefore, chips were again used, though the 96-well plates were used during the final colorimetric reaction to allow the OD to be read by the plate reader.

### 3.4.1 Examination of Prolinker A, Prolinker B and Protein A Conditions

In the first experiments the efficiency of Prolinker A and B using two reported solvents for the linker incubation were investigated. As mentioned earlier, Prolinker A is identical to Prolinker B except that it links to amines on the surface. Two different solvent solutions were tested; chloroform, which was recommended by the manufacturer, and a 1:199 chloroform:methanol solution used in [85]. Also, while the Protein A procedure was reasonably effective in the fluorescence experiments, the results in Table 3.3 showed a nonspecific signal from the control chip which was greater than that of any of the other linking procedures. Since Protein A binds specifically to certain antibody types there was a strong possibility that the BSA blocking was ineffective. Therefore, a Protein A experiment examining the blocking effectiveness of the BSA was performed. All the experiments discussed in section 3.4.1 were performed using 5 mm x 7 mm single side polished silicon chips, some of which were sputtered with a 3 nm chromium adhesion layer and a 40 nm layer of gold.

In the first experiment (Figure 3.4), gold and silicon chips were washed in acetone, IPA, and ethanol. The Protein A chips were then washed in water and PBS, and two were placed in 100 µg/ml Protein A in PBS overnight while the control chip where the linker was omitted was left in PBS overnight. The silicon Prolinker A chips were placed in 1% APTES in acetone for one hour, and washed in acetone. Half the Prolinker A and half the Prolinker B chips were washed in chloroform while the others were washed in a 1:199 solution of chloroform:methanol. Next the Prolinker A chips were placed in 3 mM Prolinker A, and the Prolinker B chips were placed in 1 mM Prolinker B overnight. The solvent solutions used were the same as those used in the washing step and the Prolinker concentrations used were recommended by the manufacturer. The chips were again washed in the same solutions in which the linker was dissolved. Subsequently, the Protein A chips were washed 2x in PBS and the Prolinker chips

were washed in acetone, IPA, ethanol, water and PBS. All the chips but the Protein A control chip where the C-Ab step was omitted were washed 3x in PBS and placed in 4 µg/ml hC-Ab overnight. The control chip was left in PBS overnight. The chips were washed again 3x in PBS and placed in 1% BSA in PBS for one hour. Each of the following reagent steps was separated by a 3x wash in wash buffer. The Prolinker sample chips and all the Protein A chips were incubated for two hours in 2 ng/ml INF- $\gamma$  in PBS and then all the chips were placed in 100 ng/ml D-Ab in PBS. The chips were submerged in 1:100 dilute Streptavidin-HRP in reagent diluent for 20 minutes and then placed in separate wells in a 96-well plate. The wells were filled with 200 µl of substrate solution and the chips were left to incubate for 20 minutes. Next, 100 µl of stop solution was added to each well and the chips were removed for the OD measurement in the plate reader.

The difference between the sample and control signals indicates that the solvent solution and Prolinker used do not have a significant impact on the quantity of INF- $\gamma$  binding to the surface. Also, the chloroform-methanol solution led to the formation of an undesirable white precipitate. Therefore, chloroform was used in further experiments as it was recommended by the manufacturer.

The goal of the Protein A experiment was to better elucidate the binding specificity of proteins involved in the ELISA. The relatively strong signal from the control where the C-Ab step was removed indicates that significant nonspecific binding takes place despite the BSA blocking step. Furthermore, the very large signal from the other control chip where the linking step was omitted could be the result of a number of different causes. It may be that in the absence of a linker a great amount of nonspecific binding takes place, the Prolinkers and Protein A are relatively ineffective at binding C-Ab to the gold surface, the C-Ab aggregates on the surface, leading to a great deal of bound INF- $\gamma$ , or it could be a combination of these factors.

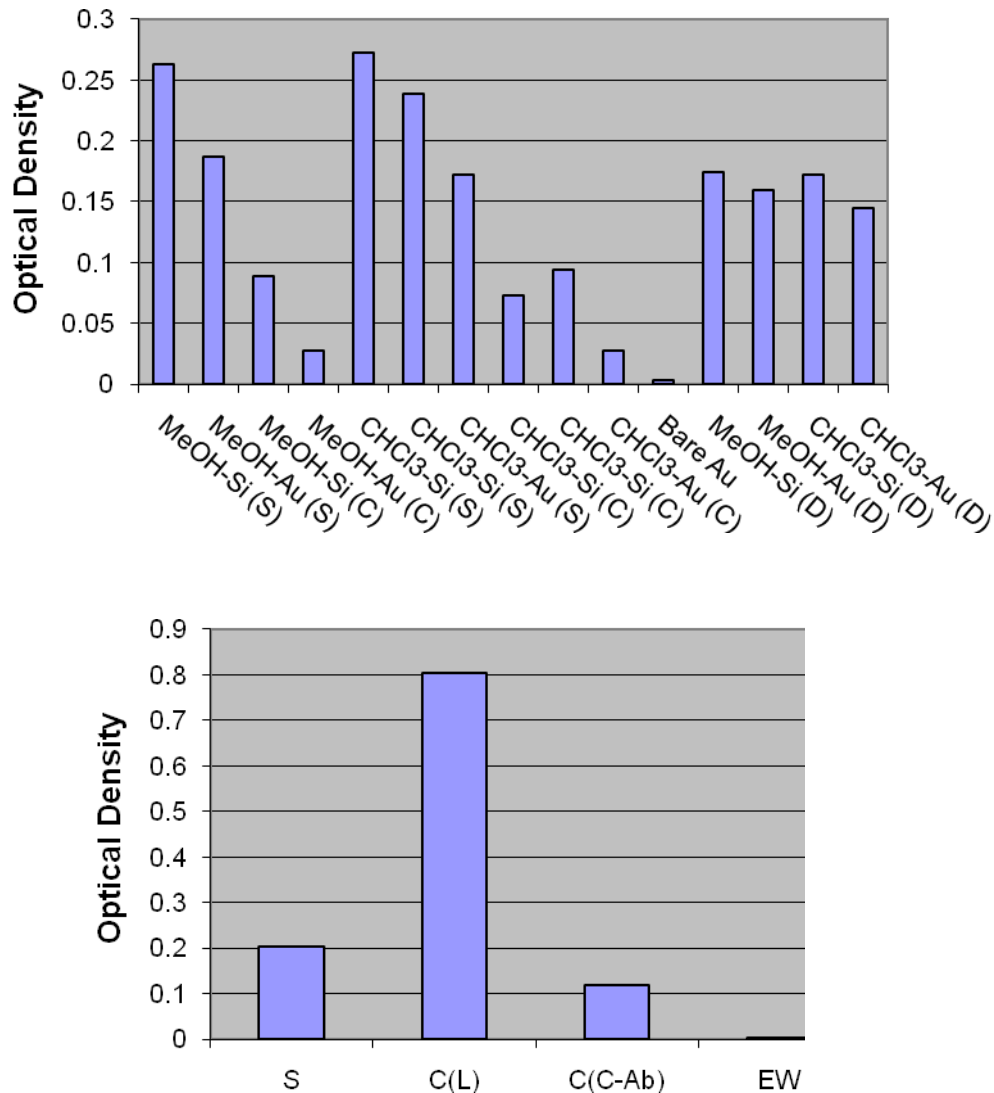


Figure 3.4: Examination of Prolinker A, Prolinker B and Protein A linking conditions with ELISA. Both experiments were performed simultaneously, but are shown separately due to the magnitude of the No Protein A control. The OD was measured at 450 nm. The silicon chips linked with Prolinker A are indicated by Si, the gold chips linked with Prolinker B are indicated by Au, chloroform is indicated by CHCl<sub>3</sub> while the chloroform/methanol solution is denoted by MeOH. S indicates the sample chips while C indicates the control chips which were not incubated in INF- $\gamma$ . The difference between the sample and control chip data is indicated by a D. On the bottom graph L indicates the control where the linking step was omitted, C-Ab indicates the control where the C-Ab step was omitted and EW indicates the well which was filled with substrate solution but was not filled with any chip.

The previous experiment was repeated with a 6 hour C-Ab incubation time and 3.5 hour INF- $\gamma$  incubation time but without the chips incubated in methanol

(Figure 3.5). The advantage of the shorter C-Ab incubation time is that less nonspecific binding or aggregation should take place. This was supported by the relatively lower signals in the absence of Protein A and INF- $\gamma$  as compared to Figure 3.4. In Figure 3.4 the Prolinker results are roughly equivalent while in Figure 3.5 the Prolinker B results were superior, which suggests that Prolinker B is equivalent or superior to Prolinker A. Therefore, Prolinker B was used in later experiments.

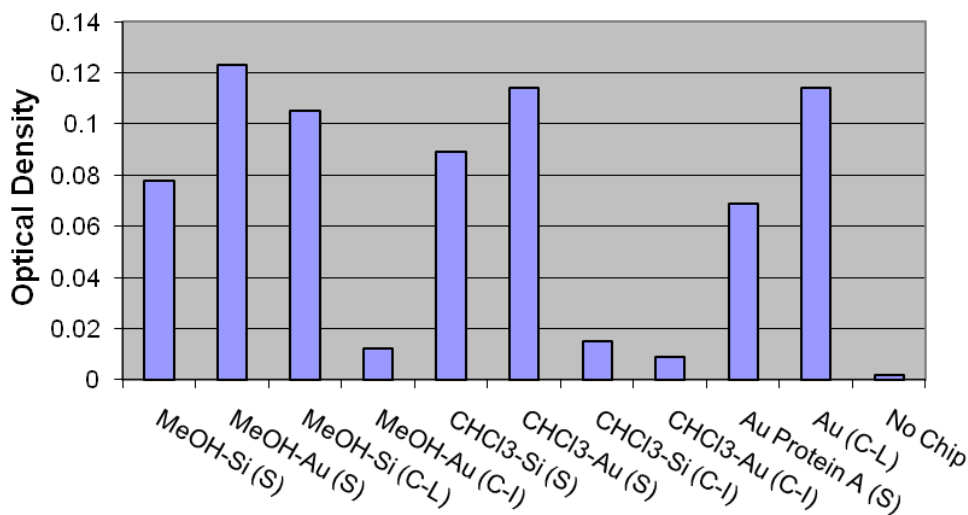


Figure 3.5: Examination of Prolinker A, Prolinker B and Protein A linking conditions with ELISA. The OD at 450 nm is shown. The sample chips are indicated by an S while C denotes the control chips where C-I means the INF- $\gamma$  step was removed and C-L means the linker step was removed. Note that the Protein A (C-L) control had no linker but was otherwise performed identically to the Protein A (S) sample chip. The difference between the sample and control chip data is indicated by a D.

### 3.4.2 Optimization of Capture Antibody and Protein A Concentrations

While in some cases the Prolinker A and Prolinker B linking procedures led to better INF- $\gamma$  binding than the Protein A procedure (Figures 3.4 and 3.5), the Prolinkers proved difficult to store as they must be kept in chloroform. Protein A, however, is soluble in PBS, which makes it considerably more convenient to use

and store. Additionally, it is likely that the Protein A and C-Ab concentrations used were not ideal for INF- $\gamma$  capture. Therefore, several experiments were performed using various concentrations of C-Ab and Protein A to augment the specific binding of INF- $\gamma$  on the chip surface.

In the first experiment the procedure used to produce the Protein A results in Figure 3.4 was repeated with the following alterations. The gold chips were sonicated in acetone in order to improve the cleanliness of the gold surface. They were then incubated in 0, 10, 25, 50, 100 and 500  $\mu\text{g/ml}$  Protein A overnight to determine the ideal concentration of Protein A and 4  $\mu\text{g/ml}$  C-Ab was used. The results (not shown) indicated that 25  $\mu\text{g/ml}$  Protein A maximizes INF- $\gamma$  binding. This procedure was repeated with 20, 25, 30, 500 and 1000  $\mu\text{g/ml}$  Protein A to determine whether 25  $\mu\text{g/ml}$  Protein A produces a local or absolute maximum quantity of INF- $\gamma$  binding. The second experiment suggests that higher concentrations of Protein A significantly increase the amount of INF- $\gamma$  binding (Figure 3.6). It seems unlikely, however, that the signal is from specific antibody-antigen interactions. The C-Ab concentration used was only 4  $\mu\text{g/ml}$ , and 7 mg of C-Ab can bind to every 1 mg of Protein A and earlier experiments (Figure 3.4) suggest that this free Protein A is not fully blocked by BSA and may bind other proteins in the ELISA.

Several experiments were performed with constant Protein A concentration and increasing C-Ab concentration. In each case there was evidence of increasing INF- $\gamma$  binding with increasing C-Ab concentration, but the most patent result is shown in Figure 3.7. The procedure was the same as for the earlier experiment (Figure 3.6), except that the Protein A concentration was held constant at 25  $\mu\text{g/ml}$  and the C-Ab concentration was varied as shown. The experiment shows the INF- $\gamma$  binding rate nearly doubling as the C-Ab concentration is doubled.

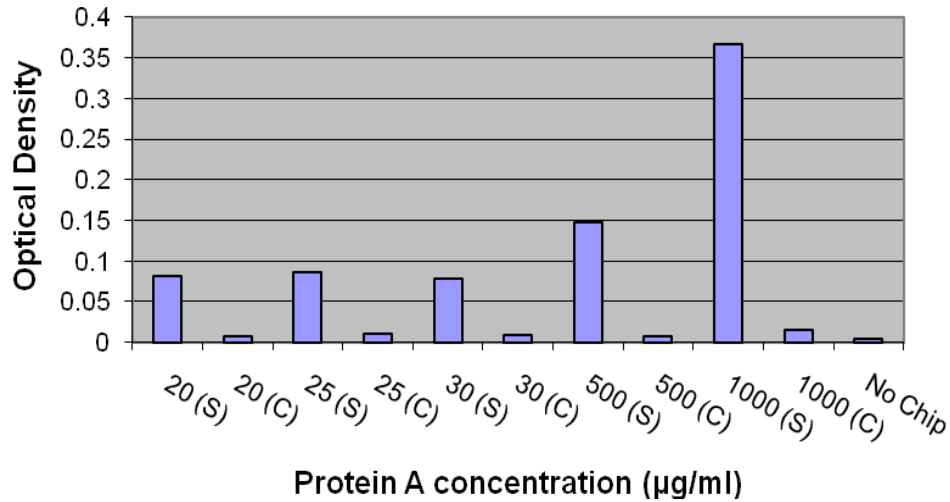


Figure 3.6: The effect of increasing Protein A concentration on INF- $\gamma$  binding where S indicates the sample chips and C indicates the control chips without INF- $\gamma$ . The OD at 450 nm is shown.

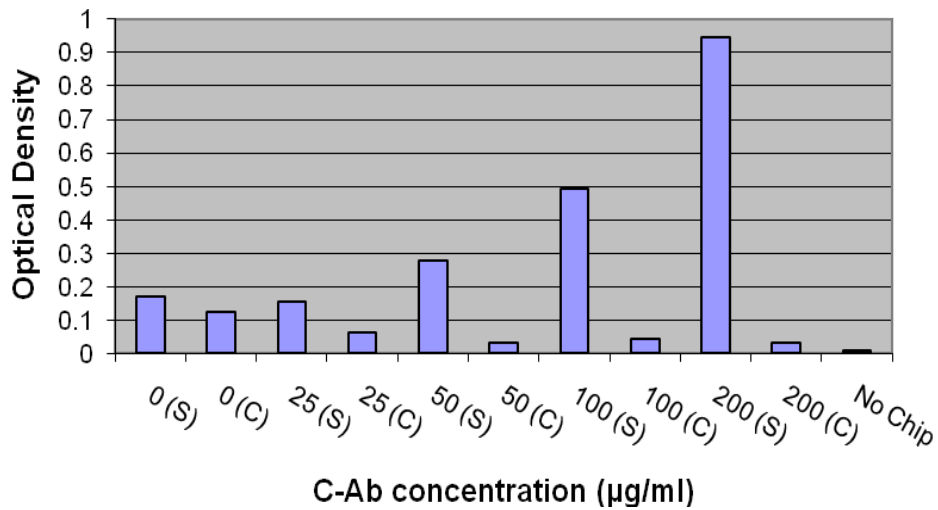


Figure 3.7: The effect of increasing C-Ab concentration on INF- $\gamma$  binding where S indicates the sample chips and C indicates the control chips without INF- $\gamma$ . The OD at 450 nm is shown.

### 3.4.3 Examination of Protein Binding on Silicon Surfaces

An important issue that arose from the protein binding investigation and an examination of the literature was that proteins will freely adsorb to unblocked silicon surfaces as well as to gold surfaces. Riquelme *et al.*, for example, used

antibodies which were adsorbed to a silicon surface to measure an antigen.[86] This is significant because the binding of Protein A and/or C-Ab to the silicon backside of the gold coated chips was unrestricted, likely leading to significant INF- $\gamma$  binding. This is also a major issue for deflection cantilever measurements because the deflection is dependent on the difference in surface stress between the two surfaces, and this stress is affected by the adsorption of proteins to the silicon backside of the cantilevers. For this reason the adsorption of the proteins to bare silicon chips was investigated.

The chips were sonicated in acetone, washed in mQ water, dried, and UV ozone cleaned. They were then washed in IPA, ethanol, and mQ water. The remainder of the procedure from the Protein A step onward was performed as per the results shown in Figure 3.4. The C-Ab concentration used was 40  $\mu\text{g/ml}$ , however, and alterations were made as necessary to the Protein A concentrations and the INF- $\gamma$  step to produce the results shown in Figure 3.8. The steps in the procedure for each chip are shown in Table 3.4. The results demonstrate that the proteins definitely adsorb to the silicon surface, and the SiC(L, I) control shows that the D-Ab and Streptavidin-HRP do not adsorb to the silicon surface after the C-Ab step. Also, the Protein A on gold sample chips produced a greater signal than the Protein A on silicon sample chips or the control where only the linking step was omitted.

Table 3.4: Summary of the examination of protein binding on silicon surfaces. This indicates whether the surface used was gold or silicon and which steps that were taken for each chip listed in Figure 3.8.

	Silicon	Gold	Protein A	C-Ab	INF- $\gamma$	D-Ab	Streptavidin-HRP
Si C (L)	+			+	+	+	+
Si C (L, I)	+			+		+	+
Au S		+	+	+	+	+	+
Si S	+		+	+	+	+	+
Au C (I)		+	+	+		+	+
Si C (I)	+		+	+		+	+

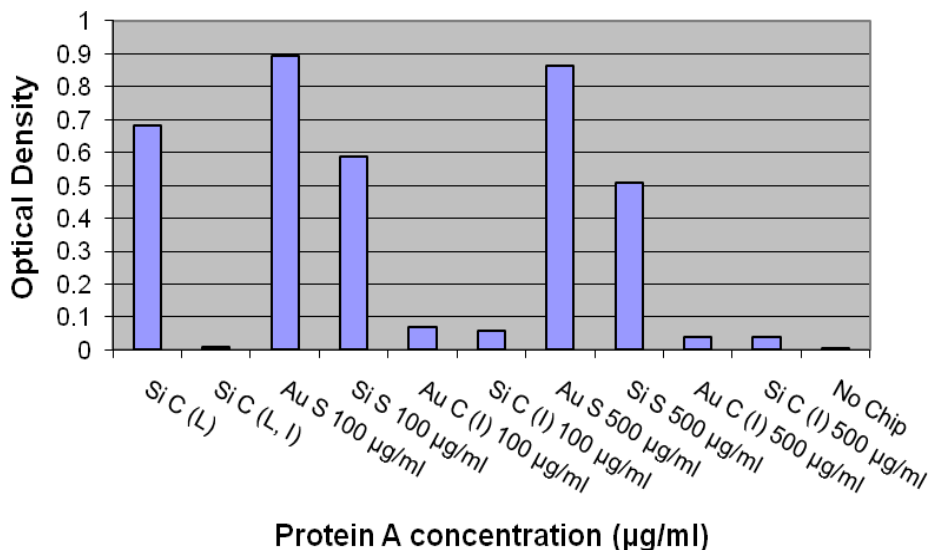


Figure 3.8: Examination of protein adhesion to silicon and gold. The concentrations refer to the Protein A concentration. Si denotes that a bare silicon chip was used while Au indicates that a one-side gold sputtered chip was used. S indicates the sample chips while C indicates the control chips where L denotes no linker and I denotes no INF- $\gamma$ . The OD at 450 nm is shown.

### 3.4.4 Discussion

Firstly, it is evident from Figure 3.1 that the ELISA is working properly. The difference between the two set of data also illustrates the difficulty in comparing ELISA results that are not performed simultaneously. This is why it is critical in ELISA experiments that controls are used to analyze the data. A comparison of the Prolinker results in Figures 3.4 and 3.5 suggests that under the right conditions Prolinker B is more effective than Prolinker A. These experiments also showed little difference between the two solvents tested, so chloroform was used in further experiments because it was recommended by the manufacturer. The results in Figures 3.4 and 3.5 also showed evidence of considerable protein binding to the bare chip surface.

In the next set of experiments, the concentrations of C-Ab and Protein A were varied to increase INF- $\gamma$  binding. It was found that increasing the C-Ab concentration can significantly increase the INF- $\gamma$  binding as shown in Figure 3.7.

Also, there was considerable binding of proteins to the Protein A on the surface when the C-Ab step was removed. This was evident from the results in Figures 3.4, 3.5 and 3.7 where the C-Ab step was omitted and in other experimental results which are not shown. Furthermore, the 0  $\mu\text{g/ml}$  C-Ab control in Figure 3.7 suggests that a significant portion of the signal is caused by nonspecific binding from the ELISA proteins other than the INF- $\gamma$ . Also, the pattern of decreasing control signal with increasing C-Ab concentration seen in Figure 3.7 was a recurring pattern seen in several similar experiments whose data are not shown. This pattern suggests that at low concentrations the C-Ab does not fully saturate the available Protein A binding locations and that INF- $\gamma$  and the D-Ab or streptavidin-HRP bind to these free binding domains. This conclusion was supported by a further experiment investigating the ELISA protein binding (data not shown).

Upon initial inspection, the results in Figure 3.6 suggest that the quantity of INF- $\gamma$  binding continues to increase with Protein A concentrations as high as 1 mg/ml. This is unrealistic however, since the quantity of C-Ab binding to the Protein A is unlikely to increase at a comparative rate, especially since the C-Ab concentration was only 4  $\mu\text{g/ml}$ . It is more likely that the increasing signal was caused by nonspecific binding of INF- $\gamma$  and the D-Ab or streptavidin-HRP to the free Protein A binding domains.

The nonspecific adhesion of proteins to silicon surfaces was investigated in Figure 3.8 and compared to the signal from gold chips. It was evident that there is considerable adsorption to the silicon surface both with and without Protein A. The chips which were used for the experiments in Figures 3.4-3.7 were only coated with gold on one surface. Protein adsorption to silicon therefore resulted in substantial nonspecific signal from the uncoated silicon backside of the chips. Fortunately the silicon chip signals were lower than the gold chip signals. For the previous Protein A experiments this means that while there was a signal from the Protein A and C-Ab on the silicon backside of the chips, it was less than the signal from the gold side, so the trends that were observed in Figures 3.4 - 3.7 should hold true. Furthermore, in Figure 3.8 the signal from the silicon control

chip without a linker was less than either of the gold sample chip signals. Similarly in Figure 3.5 the Protein A gold sample signal was less than those of the Prolinker B samples, the trends discussed for this figure should remain true. The same is likely true for the Figure 3.4 results. The signal from the silicon control chip without the linker in Figure 3.8 is slightly less than 80% of the Protein A gold sample chip signals. If this difference is applied to the Protein A sample chip signal in Figure 3.4, then the predicted OD for a pure silicon chip without a linker would be about 0.16, which is less than that of either of the Prolinker B chips. This means that the trends noted for these experiments should be unaffected except that the Prolinker B linking procedure was actually more effective relative to the Prolinker A linking procedure. This is because Prolinker A coated both sides of the silicon chips which were incubated with it, while Prolinker B only coated the gold side of the chips which were incubated with it and the silicon side was coated with C-Ab, which produces a weaker signal than C-Ab bound to Prolinker A or B.

For the cantilever experiments the important point is that INF- $\gamma$  can bind to the silicon surface either through Protein A or the C-Ab, causing stress on the silicon side of the cantilever, likely decreasing the sensitivity of detection. This means that appropriate blocking of the silicon backside of the cantilevers significantly increases the sensitivity of the sensor. In addition it shows that BSA blocking after the C-Ab step is insufficient to prevent nonspecific protein adsorption on the silicon backside, and that protein binding to the gold surface is greater than to the silicon surface.

### 3.5 Comparison of Linking and Blocking Procedures by Enzyme Linked Immunosorbent Assay

The following ELISA measurements were performed to compare the gold linking procedures and the blocking procedures. In order to eliminate the nonspecific signal experienced in the previous experiments dual side polished and

gold coated silicon chips were used. The wafers were washed in piranha for 20 minutes, washed in water and dried. They were then evaporated with 3 nm titanium and 40 nm gold on both surfaces, and diced into 5 mm x 7 mm rectangles. As mentioned earlier, ELISAs are usually performed by creating a standard curve and comparing the sample of interest to the standard to determine the protein concentration. The standard curve should be roughly linear on a log-log plot of OD vs. protein concentration over the range of interest as shown in Figure 3.1. A standard curve was created to evaluate the effectiveness of each linking and blocking strategy. In addition, to further control the conditions of the ELISA and improve the precision of the measurements, all possible steps were performed in 96-well plates. Naturally the chloroform solution steps were performed in glass containers as chloroform causes polystyrene to dissolve. The chips were washed by pipetting into the wells and aspirating from the wells. The chips were transferred by grasping the silicon edges to avoid damaging the proteins on the gold surfaces.

### 3.5.1 Individual Linker Measurements

Each of the linkers was initially examined individually to determine the linearity of the standard curve and the quantity of INF- $\gamma$  binding. All the steps following the linking procedure were held constant, save the C-Ab incubation period and the manner of C-Ab incubation for the EDC/Sulfo-NHS procedure. All the C-Ab, BSA, INF- $\gamma$ , D-Ab and HRP-Streptavidin were held constant. DSP was the first linker tested. The gold chips were sonicated in acetone and washed in IPA, water and 3x in DMSO. The chips were then incubated for 30 minutes in 4 mg/ml DSP in DMSO and washed in DMSO, water, and 3x in PBS. Each of the following steps was succeeded by a 3x wash with wash buffer. The gold chips were incubated in 4  $\mu$ g/ml hC-Ab for one hour and blocking buffer for one hour. The chips were then incubated in: 1000, 500, 250, 125, 62.5, 31.25, 15.625, or 0 pg/ml INF- $\gamma$  for 2 hours, followed by 2 hours in 50 ng/ml D-Ab and 20 minutes in 1:200 diluted HRP-Streptavidin. Following the washing step the chips were

moved to new empty wells. This is necessary because the proteins bind to both the chips and the surface of the wells. The original wells and the new wells were then filled with 200  $\mu$ l Substrate Solution. After 20 minutes 100  $\mu$ l of Stop Solution was added to each well, the chips were removed from the new empty wells and the optical density of the wells was recorded. The results are shown in Figure 3.9. For this and the following ELISA experiments the “Empty” data series refer to the empty wells in which ELISA procedure was performed before the colorimetric step. Similarly, the “Gold” data series refer to the new wells where the colorimetric and stopping steps were performed with the chips. The results are generally linear although lower INF- $\gamma$  concentration points in the first experiment and one 125 ng/ml point in the second data set are off.

Glutaraldehyde was the second linker examined. The same initial wash was performed as for the DSP linker, but the DMSO washes were replaced by PBS washes. The chips were then placed in 10 mM cysteamine in PBS overnight, and washed 3x in PBS. Subsequently, the chips were incubated in 10% glutaraldehyde in PBS for 1 hour, washed 3x in PBS and incubated for 1.5 hours in 4  $\mu$ g/ml hC-Ab. The remainder of the ELISA procedure was performed identically to the previous experiment and the results are shown in Figure 3.10. In the first test, there were a few points that deviated from the linear curve in the empty well data. In order to improve the linearity of the OD data, the cleaning procedure for the second data set, shown on the bottom in Figure 3.10, included additional steps. Between the water wash and the 3x PBS wash in the original cleaning procedure, the chips were sonicated in chloroform, washed in chloroform and washed in water. Again the linking was successful and the linearity appears to be better than for the DSP experiment, though the magnitude of the optical density at 1000 pg/ml INF- $\gamma$  concentration was greater for the DSP linker.

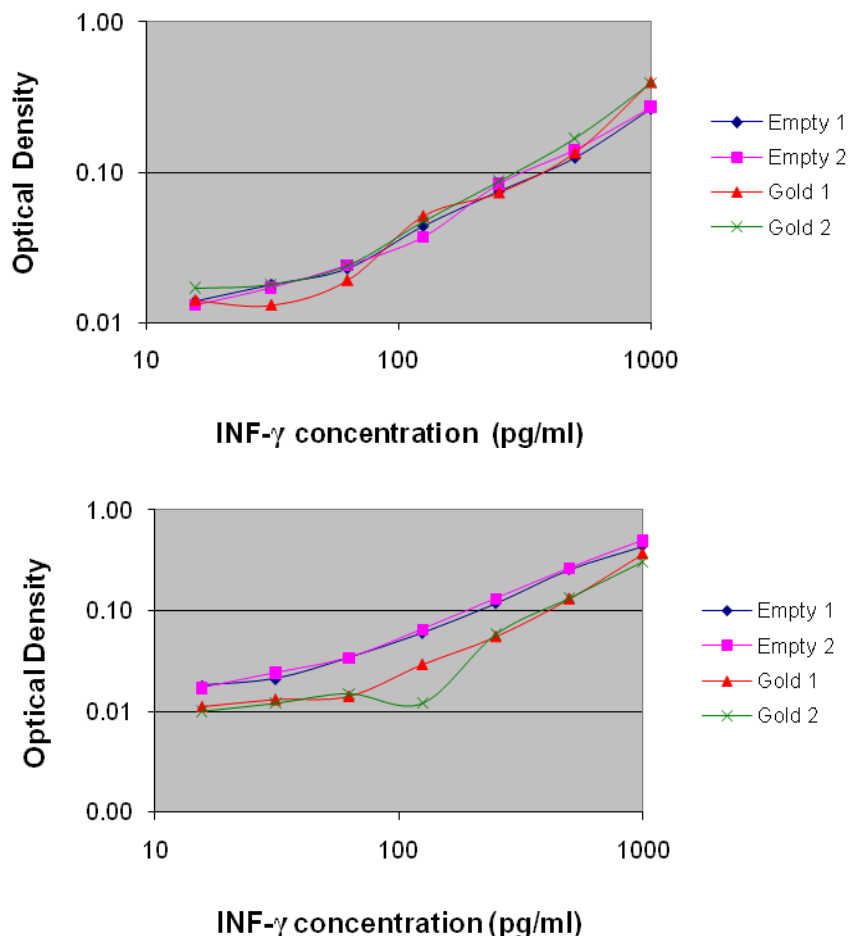


Figure 3.9: OD results from the DSP linking procedure in two separate experiments. The 0  $\mu\text{g/ml}$  INF- $\gamma$  control values for the Empty 1, Empty 2, Gold 1 and Gold 2 series were 0.011, 0.012, 0.013, 0.021 for the top graph and 0.014, 0.013, 0.012, 0.009 for the bottom graph respectively.

The third linker tested was Protein A. For the first data set on the top in Figure 3.11 the chips were washed as in the second glutaraldehyde experiment, and were placed in 100  $\mu\text{g/ml}$  Protein A for 1 hour. The chips were then washed 3x in wash buffer and incubated with 4  $\mu\text{g/ml}$  hC-Ab for one hour. The rest of the steps were performed as outlined in the DSP experiment, except that an additional 2000 pg/ml INF- $\gamma$  point was added to the INF- $\gamma$  standard curve. Unfortunately, there was some significant variation in the “Empty” series data. In addition, it is evident that there was considerable nonspecific binding to the gold chips at the lower INF- $\gamma$  concentrations. This may have been caused by the low C-Ab concentration and the short Protein A and C-Ab incubation times. For the second

data set on the bottom (Figure 3.11) a number of improvements were made to the procedure in order to reduce the nonspecific reaction. Firstly, the Protein A incubation time was increased to 1.5 hours and the hC-Ab incubation was performed overnight. The nonspecific signal was vastly reduced, but was still much larger than in Figures 3.9 and 3.10. Also 20  $\mu\text{g/ml}$  hC-Ab was tested with 1000  $\text{pg/ml}$  INF- $\gamma$  in addition to the normal 4  $\mu\text{g/ml}$  C-Ab chips to determine if this led to an improvement. There was little change, though the Empty and Gold signals were all slightly lower than those of the 4  $\mu\text{g/ml}$  C-Ab chips at 1000  $\text{pg/ml}$ . Higher C-Ab concentration would likely produce better results, but the cost of the reagents made such experiments unfeasible.

The fourth linker tested was DSP-PEG (Figure 3.12). The procedure was identical to that of the DSP experiment except the DSP was replaced by 3.6  $\text{mg/ml}$  DSP-PEG in DMSO. Again, there is considerable variation in the signal, though the results were more linear than for Protein A. As expected there was little nonspecific binding at low INF- $\gamma$  concentration. In fact, the signal at 1000  $\text{pg/ml}$  was lower than for any of the other linkers.

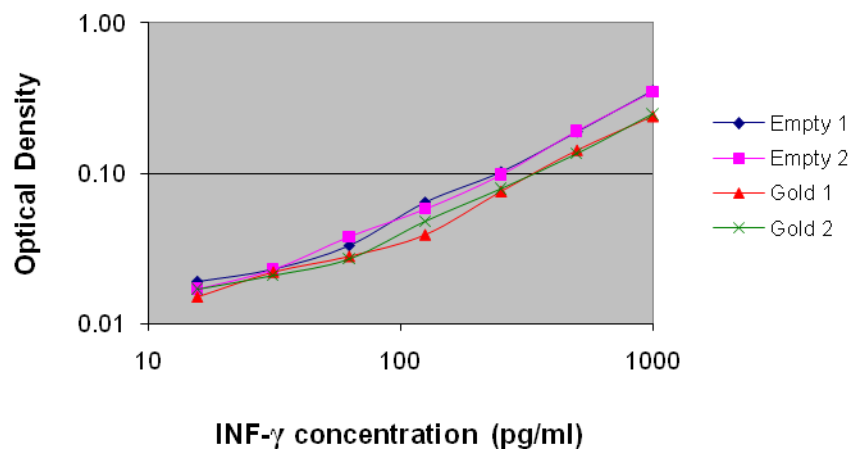
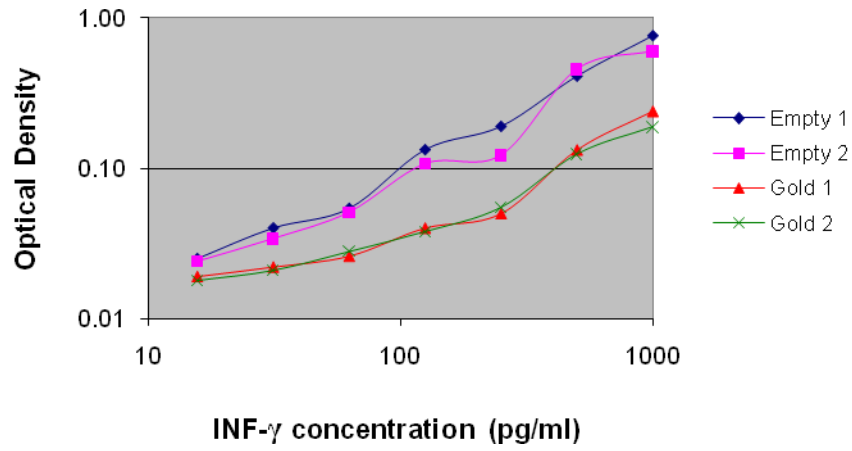


Figure 3.10: OD results from the glutaraldehyde linking procedure in two separate experiments. The 0  $\mu\text{g/ml}$  INF- $\gamma$  control values for the Empty 1, Empty 2, Gold 1 and Gold 2 series were 0.012, 0.012, 0.016, 0.017 for the top graph and 0.013, 0.012, 0.015, 0.015 for the bottom graph respectively.

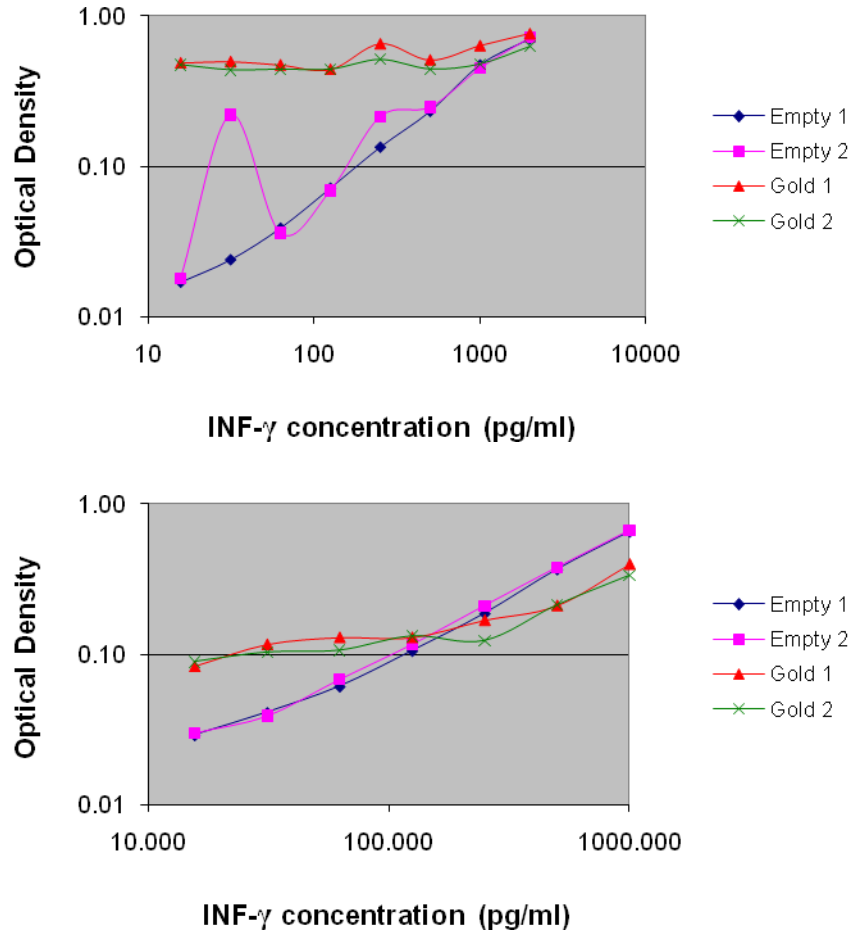


Figure 3.11: OD results from the Protein A linking procedure in two separate experiments. The 0  $\mu\text{g/ml}$  INF- $\gamma$  control values for the Empty 1, Empty 2, Gold 1 and Gold 2 series were 0.015, 0.010, 0.454, 0.381 for the top graph and 0.018, 0.019, 0.118, 0.099 for the bottom graph respectively. The 20  $\mu\text{g/ml}$  hC-Ab results were 0.612, 0.651, 0.334 and 0.329 respectively.

The fifth procedure tested was the EDC/Sulfo-NHS linking method. The initial wash was performed as for the second glutaraldehyde experiment, and the chips were washed 3x with water and placed in 10 mM cysteamine in water overnight. They were then washed once in water and 3x in PBS. Subsequently, 2 mM EDC and 5 mM Sulfo-NHS were incubated with 4  $\mu\text{g/ml}$  hC-Ab in MES buffer for 15 minutes. After 15 minutes 20 mM 2-mercaptoethanol was added to the solution to inactivate the EDC, and the pH was raised above 7.0 through the addition of 20% by volume concentrated PBS. After the solution was mixed, it was added to the aminated gold surface and left to incubate for 1 hour. The chips

were washed 3x in PBS and the remainder of the ELISA procedure was followed as in the DSP experiment, except that for the experiment on the bottom in Figure 3.13 an additional blocking step was performed with 7% ethanolamine in PBS before the usual blocking step. The results in Figure 3.13 show that there is considerable deviation from linearity in the linking procedure while the empty well series were comparatively smooth and linear. Also, there appears to be nonspecific binding occurring on the surface at the lower INF- $\gamma$  concentrations, though less than in the Protein A linking procedure. The additional ethanolamine blocking step was performed in order to improve these issues but it was unsuccessful.

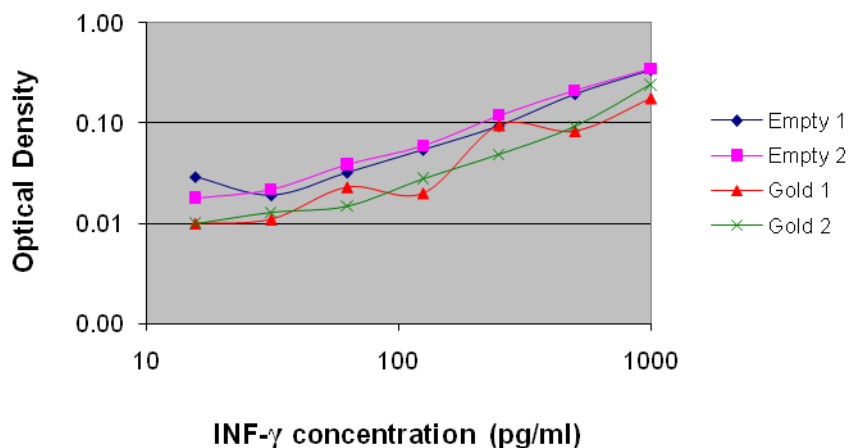


Figure 3.12: OD results from the DSP-PEG linking procedure in two separate experiments. The 0  $\mu\text{g/ml}$  INF- $\gamma$  control values for the Empty 1, Empty 2, Gold 1 and Gold 2 series were 0.012, 0.012, 0.009, and 0.010.

Prolinker B was the last linker investigated. The chips were sonicated in acetone, washed in IPA and water, sonicated in chloroform and placed in 1 mM Prolinker B for 1 hour. They were then washed in chloroform, IPA, water, and 3x in PBS. The remainder of the procedure was identical to that used for the DSP experiment (Figure 3.9). The results are shown in Figure 3.14. It is evident from these results that Prolinker B is clearly superior to the other linkers. There is very little nonspecific adsorption of the proteins to the surface as is evident from the low 0  $\text{pg/ml}$  INF- $\gamma$  control values and the points are linear. Contrary to all the other linkers tested the optical density for the chips was significantly greater than for the empty wells, and the results from the experiments were nearly identical.

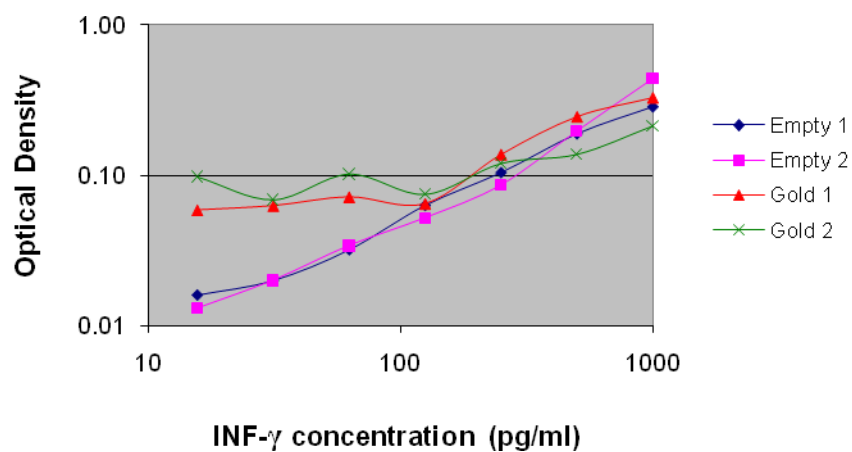
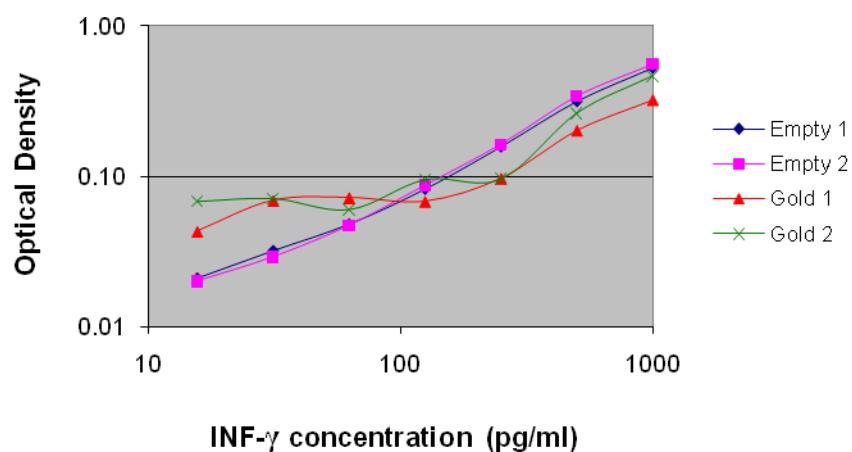


Figure 3.13: OD results from the EDC/Sulfo-NHS linking procedure in two separate experiments. The 0  $\mu\text{g/ml}$  INF- $\gamma$  control values for the Empty 1, Empty 2, Gold 1 and Gold 2 series were 0.015, 0.015, 0.053, 0.054 for the top graph and 0.010 0.010 0.036, 0.081 for the bottom graph respectively.

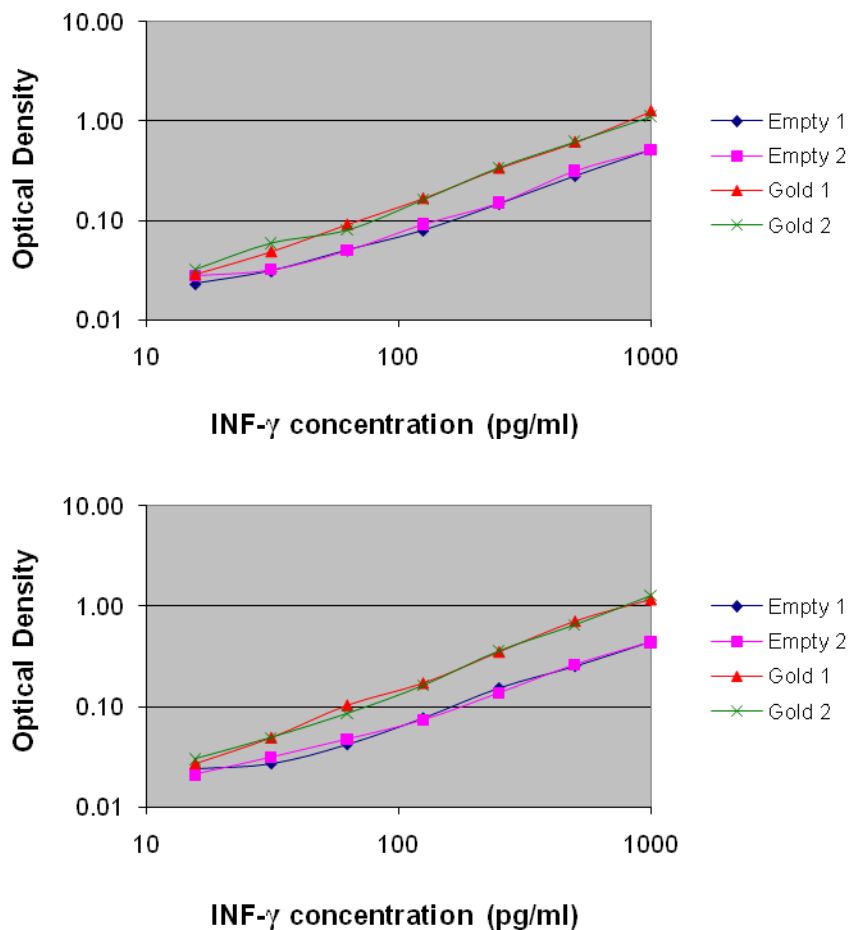


Figure 3.14: OD results from the Prolinker B linking procedure in two separate experiments. The 0  $\mu\text{g/ml}$  INF- $\gamma$  control values for the Empty 1, Empty 2, Gold 1 and Gold 2 series were 0.016, 0.017, 0.014, 0.012 for the top graph and 0.014, 0.013, 0.011, 0.011 for the bottom graph respectively.

### 3.5.2 Simultaneous Linker Measurements

In order to verify the individual linker results, the six linking procedures were compared directly using a reduced standard curve with 0, 62.5, 250 and 1000 pg/ml INF- $\gamma$  concentrations. The number of points in the standard curve was reduced to allow for the increased number of chips involved in the experiment. The chips were sonicated in acetone, washed in IPA and water, sonicated in chloroform and washed in chloroform. Each chip was then washed 3x in the solvent of their respective linkers (except Prolinker B) and the procedures were followed as outlined in the individual linker experiments in section 3.5.1.

Wherever there were changes to the procedure the steps for the second experiment (shown on the bottom in the Figures) were used. The results are shown in Figure 3.15, Figure 3.16 and Table 3.5. The empty well data were all linear or nearly linear, which shows that the ELISA was performed correctly.

The Protein A data was non-linear just like the data in Figure 3.11, though the nonspecific binding seen in the 0 pg/ml INF- $\gamma$  control data was much less than before. The glutaraldehyde results were reasonably linear and the two data sets were quite similar. The DSP-PEG data sets were also reasonably linear but their slopes were quite different. The DSP results were linear and were more similar than the DSP-PEG results. Prolinker B performed significantly better than the other linking procedures yet again. The two sets of data were linear, nearly identical and the 0 pg/ml control signals were the second lowest. In addition, the OD values were superior to those of all the other linkers aside from three points at 62.5 pg/ml which were likely the result of nonspecific binding. Though the results were reasonably linear, the EDC Sulfo-NHS linking procedure had the greatest rate of non-specific binding, as shown by the 0 pg/ml INF- $\gamma$  control results in Table 3.5.

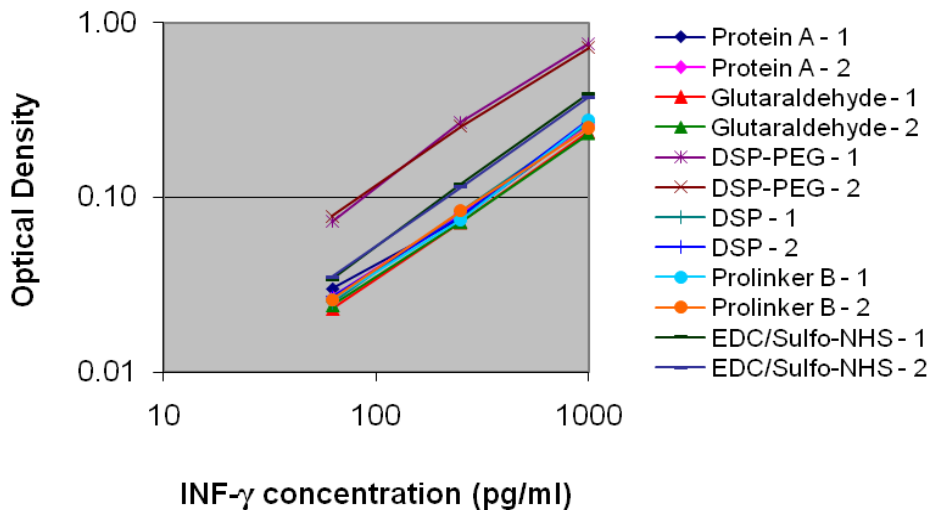


Figure 3.15: OD results from the direct comparison of six different linking procedures. Replicas are indicated by 1 and 2. These results are from the Empty wells in which the protein binding steps of the ELISA were performed.

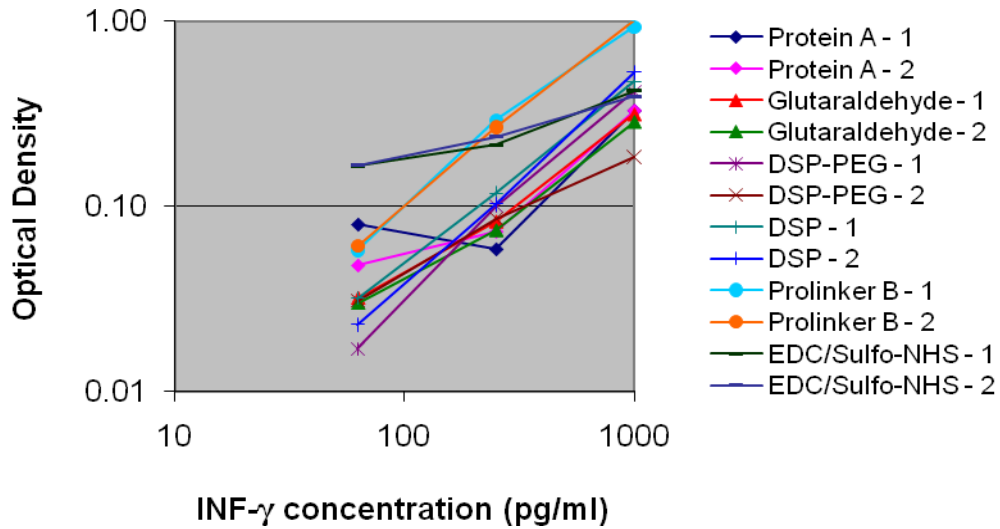


Figure 3.16: OD results from the direct comparison of six different linking procedures. Replicas are indicated by 1 and 2. These results are from the gold chips to which the C-Ab was linked.

Table 3.5: OD results from the direct comparison of six different linking procedures. Replicas are indicated by 1 and 2. These results are from the 0  $\mu\text{g/ml}$  INF- $\gamma$  control chips.

Linker	Empty Well OD	Gold Chip OD
Protein A - 1	0.011	0.043
Protein A - 2	0.012	0.030
Glutaraldehyde - 1	0.01	0.014
Glutaraldehyde - 2	0.011	0.015
DSP-PEG - 1	0.016	0.010
DSP-PEG - 2	0.016	0.009
DSP - 1	0.011	0.010
DSP - 2	0.011	0.012
Prolinker B - 1	0.013	0.010
Prolinker B - 2	0.011	0.010
EDC/Sulfo-NHS - 1	0.011	0.157
EDC/Sulfo-NHS - 2	0.012	0.161

### 3.5.3 Examination of Blocking Efficiency

The following two experiments examine the effectiveness of PEG-silane and PEG-thiol at blocking protein adsorption to silicon and gold surfaces. Furthermore, the effectiveness of BSA at reducing nonspecific INF- $\gamma$  binding and cC-Ab as a negative control for the hC-Ab were examined. The first experiment was performed with DSP, while the second was performed with Prolinker B.

In the DSP experiment four variations of the ELISA procedure were tested in addition to the normal ELISA: substitution of hC-Ab for cC-Ab, removal of hC-Ab step, the addition of a PEG-blocking step before the hC-Ab step and the addition of a silane blocking step to the silicon chips before the hC-Ab step. All the chips were cleaned by sonicating in acetone and washing in IPA and water. The silicon chips were then washed 3x in 100% ethanol, placed in 2% PEG-silane in 100% ethanol for 1 hour, and were washed in 100% ethanol. The gold evaporated PEG-thiol chips were washed in 100% ethanol and 3x in water. They were then placed in 50  $\mu\text{g/ml}$  PEG-thiol in PBS for 1 hour and washed in wash buffer. The other gold chips were washed 3x in DMSO, were placed in 4 mg/ml DSP in DMSO for 30 minutes, and were washed in DMSO. All the chips were then washed in water and 3x in PBS. The Normal ELISA gold chips and PEG blocked chips were incubated in 4  $\mu\text{g/ml}$  hC-Ab for 2 hours while the cC-Ab gold chips were incubated for 1 hour in 4  $\mu\text{g/ml}$  cC-Ab. They were then washed 3x in PBS. The subsequent steps were all followed by a 3x wash in wash buffer. The Normal hC-Ab, cC-Ab and BSA chips were blocked for 1 hour with 1% BSA in PBS and washed 3x with wash buffer. The remaining ELISA steps were performed with all the chips as seen in the DSP individual linker experiment in Section 3.5.1. The INF- $\gamma$  concentrations used were 0.5, 2 and 1000 ng/ml however. The results are shown in Figure 3.17.

For the two lower INF- $\gamma$  concentrations the cC-Ab and BSA blocking seemed to allow little binding of INF- $\gamma$  or other proteins. The PEG-silane appeared to be less effective at preventing nonspecific adsorption than the PEG-thiol for the 0.5 and 2 ng/ml INF- $\gamma$  concentrations, though this is more evident in

the 2 ng/ml INF- $\gamma$  data. Interestingly, the percent difference between the normal ELISA and the four controls was the largest for 2 ng/ml INF- $\gamma$  regardless of the method used. The purpose of the 1  $\mu$ g/ml INF- $\gamma$  concentration was to more closely emulate the conditions used in the cantilever experiments. Unfortunately the linearity of the ELISA near this concentration is unknown and therefore it is not possible to directly compare these results to those at lower concentrations where the ELISA is linear.

The second examination of the blocking procedures was performed with Prolinker B. The chips were cleaned by sonicating in acetone, washing in IPA and water, sonicating in chloroform, and washing again in chloroform. The PEG-thiol gold chips were washed in water, 3x in PBS and incubated for 1 hour in 50  $\mu$ g/ml PEG-thiol. Due to the relatively poor performance of the PEG-silane in the previous experiment, a thermal silanization procedure was tested to improve the effectiveness of the blocker. In the thermal silanization procedure 2% PEG-Silane in ethanol solution was allowed to incubate for 5 minutes to initiate hydrolyzation. The chips were then placed in the solution for 2 minutes, dipped in 100% ethanol and baked at 110°C for 15 minutes. After cooling the chips were washed in 100% ethanol.

The plain silane chips were incubated in 2% PEG-silane in 100% ethanol for one hour and washed in 100% ethanol. All the PEG chips were then washed in water and chloroform. The remainder of the ELISA procedure was performed as described for Figure 3.14 starting at the Prolinker B incubation step. The exceptions are that the No BSA chips were not blocked with BSA, the cC-Ab control chips were incubated with cC-Ab instead of hC-Ab, and an additional set of chips was examined using 25  $\mu$ g/ml C-Ab and 1000 ng/ml INF- $\gamma$ . The results are shown in Figure 3.18.

The No BSA signals were equivalent or slightly greater than the Normal ELISA signals, which suggests that the BSA has a minimal effect on nonspecific adsorption. The cC-Ab results show that it does not bind INF- $\gamma$  or the other proteins in the ELISA. For the two lower INF- $\gamma$  concentrations the PEG-thiol was the most effective blocker, followed by the thermal silane and the plain silane. For

the 1000 ng/ml results the thermal silane appears to be more effective than the PEG-thiol or the ineffectual plain silane. In addition, the 25  $\mu\text{g/ml}$  C-Ab signals for the normal ELISA and No BSA control were slightly lower than for the 4  $\mu\text{g/ml}$  C-Ab, which suggests that there may be some nonspecific binding occurring at the lower C-Ab concentration. The greater signal from all but one of the PEG blocking procedures at the 25  $\mu\text{g/ml}$  C-Ab concentration compared to the 4  $\mu\text{g/ml}$  C-Ab concentration suggests that increasing the C-Ab concentration also increases the nonspecific adsorption of C-Ab to the blocked surface. Note that in this experiment, in contrast to the previous experiment, the PEG blocked chips were placed in the linker solution after the blocking step in order to better simulate the cantilever conditions.

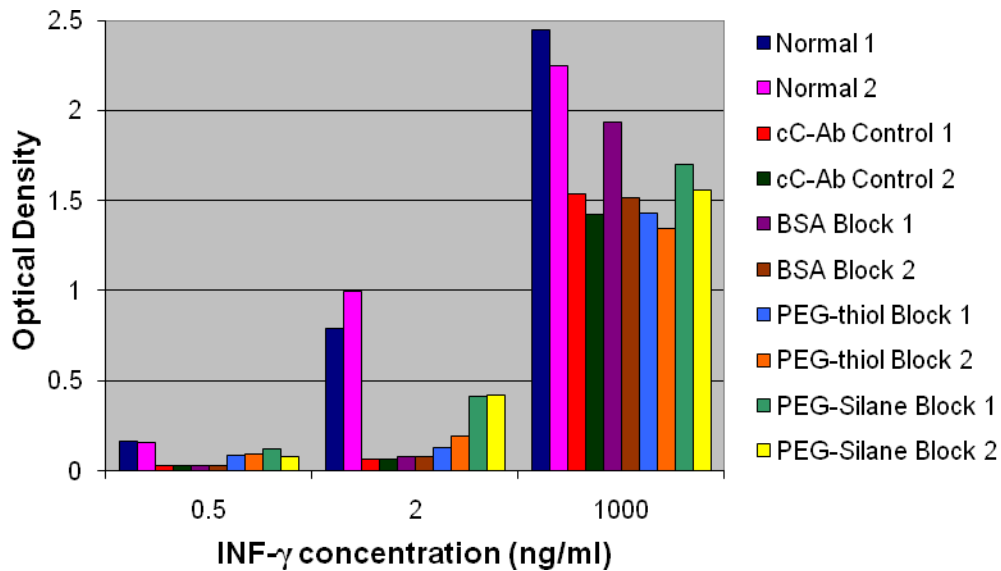


Figure 3.17: Comparison of blocking efficiency of cC-Ab, BSA, PEG-thiol and PEG-silane for different INF- $\gamma$  concentrations using DSP.

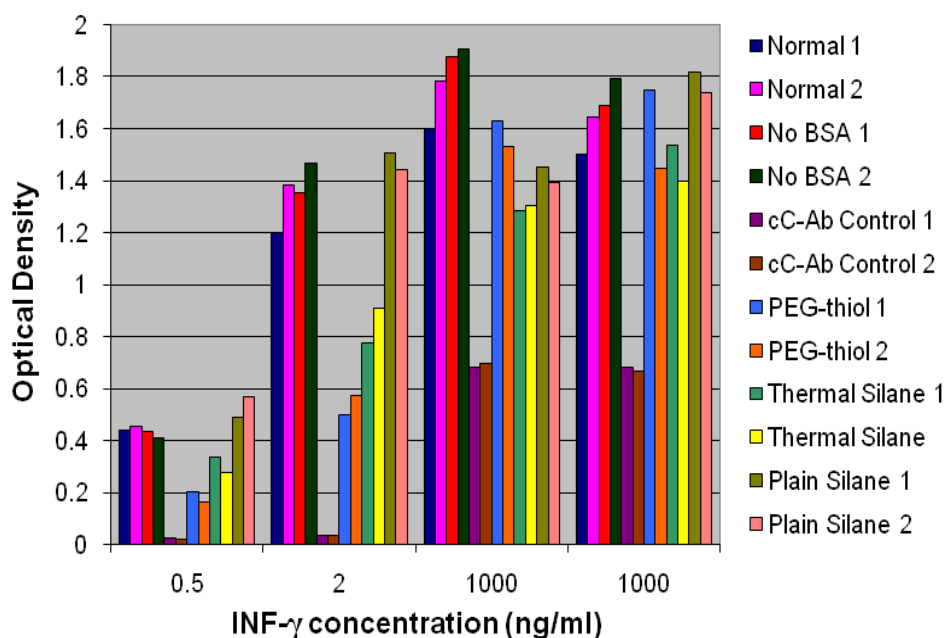


Figure 3.18: Comparison of blocking efficiency of cC-Ab, BSA, PEG-thiol and PEG-silane for different INF- $\gamma$  concentrations using Prolinker B. The right-most 1000 ng/ml INF- $\gamma$  concentration was measured with 25  $\mu$ g/ml C-Ab.

### 3.5.4 Discussion

In this section the ELISAs were performed in duplicate series of twofold dilutions of INF- $\gamma$  in order to determine which linkers were most reliable and effective. Also, the C-Ab through HRP-Streptavidin steps were performed in the same wells in the 96-well plate. The chips were then placed in a new set of wells for the colourimetric step. Both the previous (now empty) wells and the new wells were filled with colourimetric solution. The purpose of the empty well data was to provide a baseline to confirm that any variation observed in the linearity of the chip signals was caused by the linking procedure and not other variables in the ELISA procedure. Initially, all the linkers were tested separately to gain an impression of the linearity, reproducibility and rate of nonspecific binding of each linking procedure.

The DSP linker, aside from one aberrant point, resulted in good linearity when compared to the empty well data. The glutaraldehyde linking procedure

likewise resulted in good linearity, especially considering some nonlinearity in the first empty well data series (Figure 3.10 top). Even considering the nonlinearity observed in the empty wells series, the initial Protein A results were quite poor due to the very great rate of nonspecific binding at low INF- $\gamma$  concentrations. For the second experiment the C-Ab incubation time was increased, which led to a significant decrease in nonspecific binding, though there was still considerable nonlinearity due to nonspecific binding at the lower INF- $\gamma$  concentrations. This would likely be improved by increasing the C-Ab concentration but it was unfeasible given the cost of the reagents and because the C-Ab concentration was held constant at 4  $\mu\text{g/ml}$  for all the ELISA experiments to provide an accurate comparison of the linker's effectiveness. The DSP-PEG linker was only examined once and only one of the Gold Chip series was reasonably linear. In addition, it had the lowest rate of nonspecific binding, though it also produced the lowest overall signal. The EDC/Sulfo-NHS linking method had the same nonspecific binding issues as the Protein A linking method, but to a lesser degree. The best results, by a significant margin, were seen from the Prolinker B data. It had the second lowest nonspecific binding signal after the DSP-PEG, the greatest signal at 1 ng/ml INF- $\gamma$ , and the results for both experiments were nearly identical. It is also the only linker where the signal from the gold chips was larger than that of the empty wells.

In order to verify these results and given the difficulty of comparing ELISAs performed at different times, all the linkers were also tested simultaneously. Given the number of chips involved it was necessary to reduce the standard curve to three INF- $\gamma$  concentrations in addition to the 0 pg/ml INF- $\gamma$  control chips. The empty well series were very similar except for the DSP-PEG and EDC/Sulfo-NHS linking procedures, and they were all roughly linear. The Protein A linking procedure again showed considerable nonlinearity likely due to nonspecific binding at the two lower INF- $\gamma$  concentrations. The quantity of nonspecific binding for the 0 ng/ml INF- $\gamma$  control was considerably less than in the previous experiments, however. The cysteamine and glutaraldehyde linking procedure was reasonably linear as seen in section 3.5.1, and had the lowest signal

at 1 ng/ml INF- $\gamma$  aside from one of the DSP-PEG samples. Both DSP-PEG samples were reasonably linear, but had significantly different slopes, which is similar to the variability observed earlier. The DSP linker results were also linear, though with some variability between the two samples. It also resulted in the second largest signal at 1 ng/ml. The Prolinker B results, as before, were better than those for any of the other linkers. The results were nearly linear and effectively identical. Also, Prolinker B had the second lowest rate of nonspecific binding for the 0 ng/ml INF- $\gamma$  control (just behind the DSP-PEG), and the largest signal for every INF- $\gamma$  concentration aside from the nonspecific binding of the Protein A and EDC/Sulfo-NHS linkers at the 62.5 pg/ml INF- $\gamma$  concentration. The EDC/Sulfo-NHS linking procedure was also linear, but significant nonspecific binding occurred in the 0 ng/ml INF- $\gamma$  control, more than four times that of the Protein A linker. From this it is concluded that Prolinker B is the best linker, because it allows for the most sensitive and reproducible measurement of INF- $\gamma$ .

Following the linker investigation, two experiments were performed to test the blocking efficiency of PEG-thiol, PEG-silane, BSA and cC-Ab. In the first experiment (Figure 3.17) DSP was used as the linker, and the INF- $\gamma$  concentrations used were 0.5, 2.0 and 1000 ng/ml. It is important to note that the PEG-thiol and PEG-silane were deposited before being incubated with hC-Ab while the cC-Ab and BSA chips were not incubated with hC-Ab because they, unlike the PEG blockers, are not required to block the hC-Ab in the cantilever experiments. The 0.5 ng/ml INF- $\gamma$  data shows that cC-Ab and BSA are quite effective at blocking the INF- $\gamma$ . Neither PEG was very effective at blocking the surface at this INF- $\gamma$  concentration, though the thiol appeared to be more effective than the silane. For 2 ng/ml INF- $\gamma$  chips, the cC-Ab and BSA were again effective while both the PEG-thiol and PEG-silane were relatively more effective at blocking at this INF- $\gamma$  concentration. Again, the PEG-thiol performed better than the PEG-silane. At 1000 ng/ml all the blocking methods appear to be equally effective, though it is difficult to draw any definite conclusions since this concentration is not in the linear region of the ELISA.

The second blocking experiment (Figure 3.18) was performed with Prolinker B, the same INF- $\gamma$  concentrations, and a second set of 1000 ng/ml INF- $\gamma$  data using 25  $\mu$ g/ml C-Ab. In this case, in order to better determine the effect of BSA blocking, a series with no BSA was tested and the difference in signal between it and the normal ELISA was examined. At the 0.5 ng/ml INF- $\gamma$  concentration there was no apparent effect from omitting the BSA. There was, however, a slight increase in the signal in all three other data sets when the BSA blocking step was removed. This suggests that some nonspecific binding is occurring without BSA blocking. The effectiveness of the PEG-silane blocking layer was improved considerably by using a new thermal silanization procedure which was obtained from the manufacturer. In all but the 1000 ng/ml INF- $\gamma$  and 4  $\mu$ g/ml C-Ab samples the original silanization procedure was entirely ineffective with signals larger than for the normal ELISA procedure. Again the cC-Ab was effectively inert to human INF- $\gamma$  and was relatively more effective at the 1000 ng/ml INF- $\gamma$  concentrations than in the previous experiment. The PEG-thiol seems to be more effective than the PEG-silane for the two lower INF- $\gamma$  concentrations but less effective than the thermal PEG-silane for both the 1000 ng/ml INF- $\gamma$  cases and less effective than the original silanization procedure in the 1000 ng/ml INF- $\gamma$  and 4  $\mu$ g/ml C-Ab case. In addition, increasing the C-Ab concentration appeared to decrease the normal ELISA and No BSA signals while increasing all but one of the PEG signals. This suggests that the C-Ab is adsorbing to the PEG on the chip surfaces and that some nonspecific binding is occurring due to open Prolinker B binding locations on the chip surface despite the BSA blocking step in the normal ELISA. Given these results, the cC-Ab and thermal silanization procedure were used in the majority of the cantilever experiments.

### 3.6 Summary

Overall, the fluorescence and ELISA experiments provided useful results concerning the effectiveness of the linking and blocking procedures. From Figure 3.1 it is evident that the ELISA works as expected. The fluorescence experiments were performed on gold chips, and were used to verify that the linking procedures successfully bind the antibody to the gold surface, and that the INF- $\gamma$  can adhere to the bound antibodies. The experiments were hampered by fluorescence quenching due to the metal surface on which they were performed. This made it challenging to determine the difference in fluorescent intensity of the images by inspection. Instead, the summations of the numerical pixel values of the digital images were used to evaluate the effectiveness of the linking methods. In addition, in order to exclude nonspecific fluorescent signals, the signal from the control chips was subtracted from that of the sample chips. Since the difference for each of the linkers in both experiments was positive, it appears that the linkers successfully bind the antibodies to the surface, and that the INF- $\gamma$  can then adhere to the bound antibodies. Prolinker B produced the greatest difference between the active and control chip fluorescence in both experiments by a substantial margin. This suggests that it is the most effective linker.

The ELISA experiments were also performed on gold coated silicon chips. The examination of the effect of experimental conditions on the detection of INF- $\gamma$  led to a number of interesting results. Firstly, it was determined that the Prolinker A and B linking effectiveness is equivalent in chloroform solvent and 1:199 chloroform:methanol. Chloroform was used in subsequent experiments as it was recommended by the manufacturer and does not lead to the formation of a white precipitate. In addition, it was found that Prolinker B is either equally or more effective than Prolinker A, which is why Prolinker B was used in subsequent experiments. From the Protein A experiments, it was found that increasing C-Ab can substantially increase the quantity of INF- $\gamma$  bound to the surface. Also, high concentrations of Protein A and relatively low concentrations

of C-Ab lead to substantial nonspecific binding. As the concentration of C-Ab increases, however, this nonspecific binding decreases. Furthermore, results from the control chips in both the Prolinker and Protein A experiments show that there is substantial binding of proteins other than Protein A to bare gold and silicon surfaces. Since the chips for these experiments were only coated with gold on one surface, this led to considerable nonspecific signal from the silicon backside of the chips in each experiment. The signal from the silicon side was less than that from the gold side however, which means that the trends observed should remain true despite nonspecific signals from the silicon surfaces.

In the second ELISA section, substantial changes were made to the ELISA procedure in order to accurately compare the linking and blocking procedures. Each of the linking procedures was then examined individually. The DSP and glutaraldehyde linkers performed relatively well, with reasonable linearity in the standard curve, low nonspecific signals from the 0  $\mu\text{g/ml}$  INF- $\gamma$  control chips, and decent reproducibility. The DSP-PEG linking procedure produced the least nonspecific signal, but the reliability of the linker, as seen from the poor linearity in the standard curve, was less than that of the DSP and glutaraldehyde linkers. The Protein A and EDC/Sulfo-NHS linkers led to significant nonspecific binding at the lower INF- $\gamma$  concentrations. This was caused at least partially by the relatively low C-Ab concentration used in these experiments. In addition, these procedures were less reliable than the other linkers, as seen from the low degree of reproducibility and linearity in the standard curves. Prolinker B yet again led to the best results, with linear, nearly identical curves, the smallest nonspecific signals after the DSP-PEG, and the greatest specific signal of all the linkers.

In order to verify the results from the individual linker experiments, all the linking methods were compared concurrently. The results were comparable to those of the individual linker measurements. Both the DSP and glutaraldehyde performed relatively well with reasonably similar and linear standard curves. The linearity of the DSP-PEG curves was also fair, but the two curves had substantially different slopes. Both the Protein A and EDC/Sulfo-NHS linking procedures led to substantial nonspecific binding. The standard curves from the

Protein A linker showed poor linearity and reproducibility. Unlike previous experiments, however, the EDC/Sulfo-NHS standard curves were reasonably linear and similar in form. Prolinker B again led to the best results, with little nonspecific binding, the strongest specific binding signals, and reasonably linear and similar standard curves.

In the last subsection of the second ELISA section, the blocking procedures were examined. DSP was used as the linker in the first blocking experiments. The blockers tested were cC-Ab, BSA, PEG-thiol and PEG-silane. The signal from the all the blocked chips was less than that of the unblocked chips, which means that each blocking method was at least partially effective. The small signals from the cC-Ab and BSA blocked chips shows that they are relatively inert to INF- $\gamma$ , which makes them reasonable alternatives to block the active surface of the reference cantilevers. The PEG-thiol and PEG-silane blocking layers were shown to be reasonably inert to both C-Ab and INF- $\gamma$ , making them reasonable alternatives to prevent nonspecific binding on the backsides of the cantilevers. The cC-Ab and PEG-thiol performed better than the BSA and PEG-silane in this experiment.

In the second blocking experiment, Prolinker B was used instead of DSP. Also, the effect of the BSA blocking step in the normal ELISA was examined by removing the BSA blocking step from the procedure. Furthermore, in addition to the cC-Ab, PEG-thiol and PEG-silane procedures, a thermal PEG-silane procedure was tested. The removal of the BSA step had little, if any effect on the ELISA procedure, which indicates that the BSA blocking step has little effect on nonspecific binding. The cC-Ab blocking procedure was even more effective at preventing INF- $\gamma$  binding than in the DSP experiment. The PEG-thiol and PEG-silane blocking procedures were performed before the linking procedures in this experiment, while in the previous experiment the linking step was omitted for the PEG-thiol and PEG-silane blocked chips. The PEG-thiol blocking procedure was reasonably effective at reducing nonspecific binding of Prolinker B, C-Ab and INF- $\gamma$ , particularly for the two lower INF- $\gamma$  concentrations. The thermal PEG-silane procedure was also reasonably effective at reducing nonspecific binding of

Prolinker B, C-Ab and INF- $\gamma$ , and was more effective than the PEG-thiol at the 1  $\mu\text{g/ml}$  INF- $\gamma$  concentration. The original PEG-silane blocking procedure was ineffective, as it produced an equal or greater signal than the original ELISA procedure at every INF- $\gamma$  concentration.

Overall, Prolinker B appears to be the most effective linker, as seen in all the fluorescence and ELISA experiments. From the blocking experiments it is evident that, while none of the blocking procedures is perfect, the cC-Ab performed very well, and both the PEG-thiol and thermal PEG-silane procedures substantially reduce nonspecific binding. Therefore, these procedures were applied in the majority of the cantilever experiments discussed in Chapter 4. Given the difficulties that were encountered, however, other linking and blocking procedures were also tested in the search for a reliable method to measure proteins with deflection cantilever arrays.

## Chapter 4

# Deflection Cantilever Array-Based Detection of Interferon Gamma

The goal of the cantilever experiments was to determine a procedure to reliably and reproducibly measure INF- $\gamma$  concentrations using deflection cantilever arrays. It was to serve as a basis for the simultaneous measurement of multiple proteins in a liquid environment using a deflection cantilever array. Unfortunately, it proved challenging to reproduce the cantilever deflection results despite alterations to the linking and blocking procedures as well as other aspects of the functionalization process. Moreover, it was challenging to consistently achieve separation between the active cantilever signals and the reference cantilevers signals, especially when four active and four reference cantilevers were used. The unpredictable drift of the cantilevers in buffer solution was likely the major cause of this issue.

The nonspecific deflection of the cantilevers in solution was generally greater in magnitude than the deflection due to INF- $\gamma$ . Therefore several background subtraction procedures were attempted in order to extract the specific INF- $\gamma$  signal. In addition, in order to organize the data in a coherent fashion, the experiments were divided into three different categories depending on the degree of separation of the active and reference cantilevers. The materials and solutions that were used exclusively in the cantilever experiments are listed in section 4.1. The nature of the cantilever drift, classification of the data and drift corrections are discussed in section 4.2. Select experiments are described in section 4.3, and the effects of the various alterations to the experimental procedure are discussed in section 4.4. Lastly, there is a final discussion in section 4.5 along with a number of conclusions.

## 4.1 Materials and Solutions

Only new materials are listed in this section. Any materials that were used for the cantilever experiments which are not listed here were identical to those listed in section 3.1. This section also contains a brief description of the cantilever sensing platform and functionalization unit that were used.

### 4.1.1 Materials

**Concentris:** Cantisens measurement unit; functionalization unit; polymer-coated glass capillary tubes

**IBM (International Business Machines):** Silicon cantilever arrays, gold evaporated cantilever arrays

**Sigma-Aldrich:** (+)-BIOTIN-NHS, H1759; M6500; Sodium Hydroxide (KOH)

**Thermo Scientific:** EZ-Link Sulfo-NHS-LC-Biotin

### 4.1.2 Solutions

**Low concentration MES:** 10 mM 2-(N-morpholino)ethanesulfonic acid and 10 mM NaCl, pH 6.0

**Low NaCl content PBS:** Identical to normal PBS, but with 20 mM NaCl

**PB:** Identical to PBS but without any NaCl

### 4.1.3 Cantilever Sensing Platform and Functionalization Unit

It is useful to briefly discuss the cantilever arrays, measurement system and functionalization system used to perform the cantilever experiments. The deflection cantilever arrays used each had 8 silicon cantilevers, with dimensions

of  $500\ \mu\text{m} \times 100\ \mu\text{m} \times 1\ \mu\text{m}$  and were fabricated by IBM. The cantilever sensing system and the functionalization unit used were both supplied by Concentris. The Cantisens system was used to measure the cantilever deflection. It uses a PSD which records the reflected beam position of a laser diode as it scans across the tips of the cantilevers. The liquid handling system of the Cantisens platform allows a minimum uptake rate of  $0.417\ \mu\text{l/s}$  and a maximum of  $50\ \mu\text{l/s}$ . The volume of the measurement chamber was approximately  $5\ \mu\text{l}$  and the maximum volume of the syringe pump was  $500\ \mu\text{l}$ . A temperature controller enables specific control of the temperature in both the intake loop which channels the solution into the measurement chamber and the measurement chamber itself.

As mentioned earlier, reference cantilevers are used in order to separate nonspecific deflection from the specific deflection signal in the cantilever array experiments. The signal of the reference cantilever is subtracted from the active cantilever signal, leaving the specific deflection caused by the protein of interest. A functionalization unit supplied by Concentris was used to separately functionalize the cantilevers in the arrays. Capillary action filled glass capillaries  $150\ \mu\text{m}$  in diameter with functionalization solution and four non-adjacent cantilevers could be inserted into the glass capillaries at a time. This functionalization process was necessary to block the backsides of the cantilevers and separately coat the active and reference cantilevers.

## 4.2 Cantilever Drift and Potential Correction Methods

As was reported in section 2.3.2, many published cantilever deflection measurements of proteins were performed without reference cantilevers. In other cases, active and reference cantilevers were used, but the measurements were performed at separate times. In the cantilever array experiments up to two active cantilevers and multiple control cantilevers were used, but no simultaneous measurements were reported where four active and four control cantilevers were used. It is then perhaps unsurprising that it was such a challenge to achieve clear separation between the active and reference cantilevers. In fact, the only

simultaneous measurement of more than one protein with a cantilever array was performed by Arntz *et al.* in 2003.[28] While the difference in deflection caused by the proteins being detected was evident, the clarity of the signals was suboptimal, the experiment was not replicated, and the detection limit was relatively low. In fact, few experiments described in the review were performed with any reference to reproducibility, and those which were repeated showed some significant variation. [62] This lack of reproducibility was likewise a significant challenge for the INF- $\gamma$  experiments which are described below.

### 4.2.1 Cantilever Drift

All the cantilevers, whether reference cantilevers or active cantilevers, experienced significant drift unrelated to INF- $\gamma$  binding. Ordinarily this would not be a cause for concern since the subtraction of the reference signal from the active signal should be sufficient to cancel out any constant drift. Unfortunately, the drift experienced by the cantilevers often varied significantly from one cantilever to the next. Even bare silicon cantilevers in water experienced some deflection though the rate of deflection of the gold- and antibody- coated cantilevers in buffer solution was much greater.

Equilibration in buffer solution was performed in an attempt to eliminate the deflection. It was found that the deflection could be reduced, but not eliminated, by long equilibration periods and repeated cycling of the buffer solution. Representative deflection curves are shown in Figure 4.1. Long equilibration times led to a number of other problems however, including a greater signal to noise ratio and detrimental changes to the cantilever deflection behavior in the INF- $\gamma$  sample solution following the buffer equilibration.

The change in cantilever behavior following a long equilibration period may be related to the magnitude of the downward deflection of the cantilevers after a long period in buffer solution (Figure 4.2). In order to measure the cantilever deflection, the laser spot must be focused on the tips of the cantilevers

in the array. As a result of the downward deflection of the cantilevers, the visible surface area of the tips of the cantilevers where the laser spot must be focused is substantially decreased. This is observable in the difference between images A, B and C, D in Figure 4.2. The decreased surface area makes it difficult to focus the laser spot accurately. Also, the vertical location of the laser spot on the cantilever surface must be entered into the Cantisens to accurately measure the deflection of the cantilevers, and this becomes more difficult to determine as the cantilever deflects downwards. Furthermore, the substantial downward deflection decreases the reflected intensity from the cantilever surface, decreasing the reliability of the deflection measurements. For these reasons, long equilibration times were not found to be a suitable solution to the buffer deflection problem.

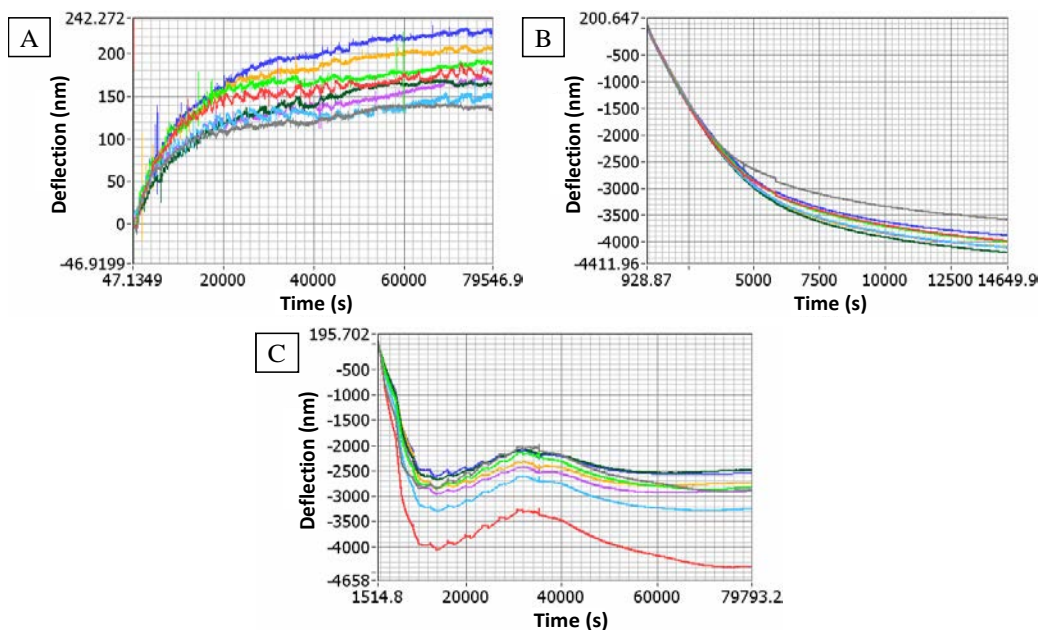


Figure 4.1: Examples of the deflection of cantilevers in water and buffer solution. A - Deflection of a bare silicon cantilever array removed directly from the package and placed in water. B – The deflection of a gold-coated C-Ab functionalized cantilever array in still PBS. C - The deflection of a gold-coated C-Ab functionalized cantilever in PBS. Buffer was repeatedly pumped through the measurement chamber during the first 38k seconds, after which the cantilevers were left to deflect in the still buffer.

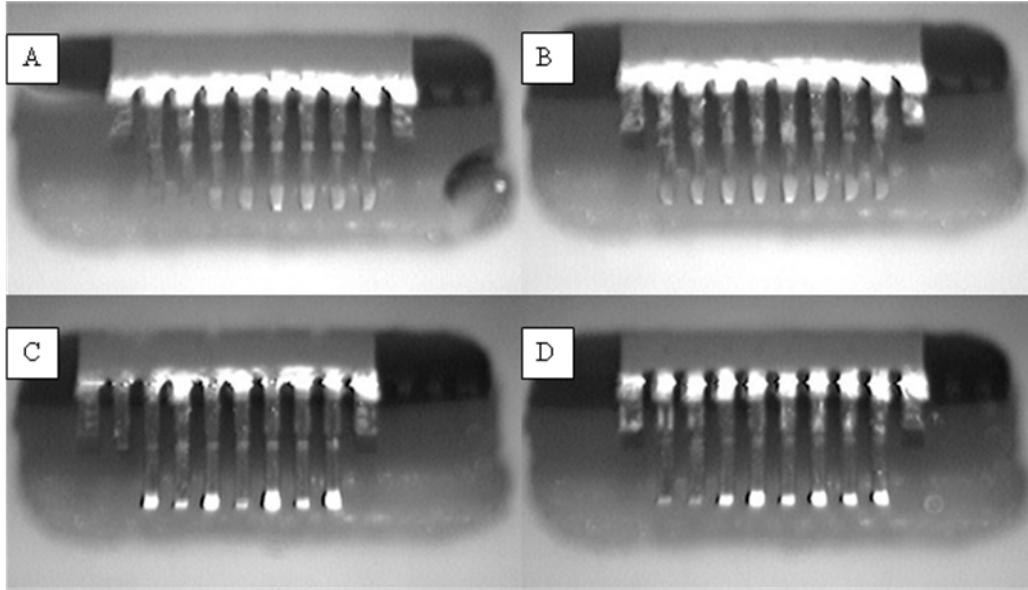


Figure 4.2: Comparison of cantilever deflection based on the period in solution. In A the cantilever was left in PBS to equilibrate for 80,000 seconds. The deflection data corresponding to the image is shown in Figure 3.1C. In B the cantilevers were immersed in INF- $\gamma$  for 2 days after they were functionalized with the linker and antibody. The images C and D were taken shortly after the cantilevers were submerged in buffer solution.

Backmann *et al.* used a different method to avoid the differential cantilever deflection. A heat test was performed to isolate the cantilevers with identical or near identical deflection, and only these cantilevers were used for the protein measurements.[74] This test primarily serves to isolate differential deflection due to disparity in the mechanical manufacture of the cantilevers. Heat tests were performed in a number of experiments in order to determine whether the differential deflection observed was caused by physical differences in the cantilever construction. Generally, little differential deflection was observed during the heat tests, aside from constant downward deflection experienced by all cantilevers in buffer solution. A representative heat test is shown in Figure 4.3. The buffer deflection is evident from the decreasing starting deflection for each successive cycle in the heat test.

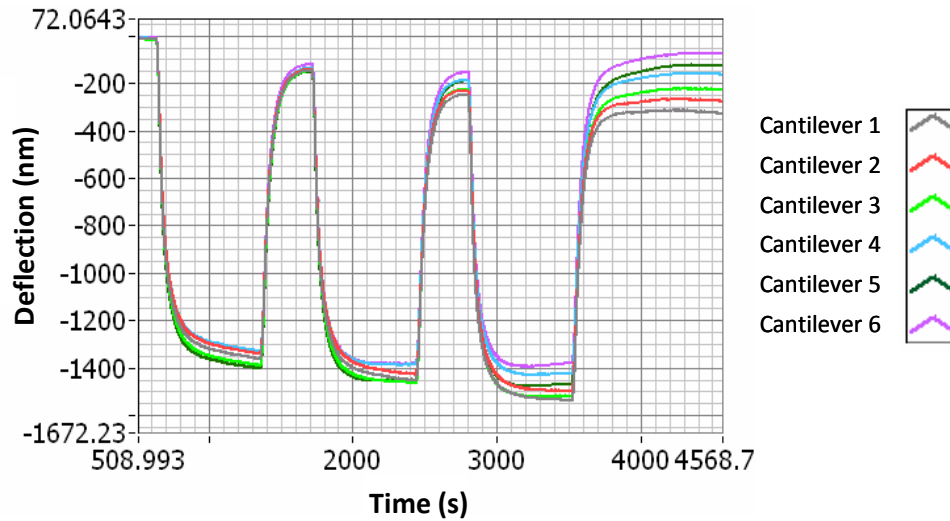


Figure 4.3: A representative heat test. The heat test began at 20°C, and at 630 seconds the temperature was raised to 30°C for 720 seconds then lowered to 20°C for 360 seconds. This cycle was repeated twice more as seen in the deflection pattern of the cantilevers.

#### 4.2.2 Classification of Cantilever Deflection Results

The results of the cantilever experiments were organized into three categories based on the degree of separation between the active and reference cantilevers. Clear separation between all the active and reference cantilever deflection signals over the majority of the time period examined were designated group I data. Similarly, group II data show a clear separation between the majority of the active and reference cantilever deflection signals over the majority of the time period examined. The remaining data sets with less separation between the active and reference cantilever signals were classified as group III results.

#### 4.2.3 Drift Corrections

If not for the variability of the drift from one cantilever to the next in every array, it would be a simple process to eliminate the drift by subtracting the reference cantilever signals from the active cantilever signals. Instead, three

background subtractions were evaluated to determine which would be most effective at reducing or eliminating the drift from the individual cantilever signals. In order to perform an accurate background subtraction it is necessary to find a period in the data which accurately reflects the background signal present in the remainder of the experiment. By fitting an equation to this set of data, and subtracting the equation from the experimental data it is then possible to eliminate the background signal.

There are two periods in the experimental data where a background subtraction can reasonably be performed. In order to better describe the process it is necessary to describe the measurement process. Once placed in the Cantisens machine the cantilever arrays underwent an washing step and sometimes a heat test. Next the array was allowed to equilibrate in the still buffer solution. This is the first period which was used for background subtractions. The next step in the measurement process was to flow buffer solution past the cantilever array. This was the second period where a background subtraction was performed. Once the disturbance caused by the pump activation and flowing buffer had dissipated, the sample intake was initiated. This step generally lasted approximately 10 minutes. Next, the liquid intake was halted and the INF- $\gamma$  solution was permitted to react with the cantilevers for several hours. The deflection of the cantilevers in the buffer solution differed considerably depending on whether the buffer solution was still or flowing. Therefore, the background subtractions performed on the still buffer deflection was only valid for the still sample solution period, and the background subtraction fitted through the flowing buffer data was only valid for the INF- $\gamma$  intake period.

Two separate linear background subtractions were performed. The first subtraction was performed during the first period discussed above, and is referred to as the linear flowing buffer background subtraction. The second was performed during the second period discussed above, and is referred to as the linear still buffer background subtraction. Upon examination, it became apparent that the linear background subtractions did not accurately reflect the data, especially during the still sample measurements. Though the rate of deflection of the

cantilevers in the still buffer solution varied from one experiment to the next, the deflection curve was nearly always concave up. A logarithmic curve was selected to fit the first period as it better approximates the deflection of the cantilevers in the still buffer solution (Figure 4.1B).

The three background subtractions, where applicable, were performed on 52 different data sets, with mixed results. Some of the data sets only included sample intake data and little still sample data, so only the flowing linear background subtraction was performed. In other cases a background subtraction was not performed because there was insufficient still buffer data, the data was too rough to accurately plot a background subtraction, or the still buffer data was concave down making a logarithmic subtraction infeasible. In the majority of the cases, the background subtractions did not improve the results sufficiently to upgrade the classification. In some cases the background subtractions were detrimental rather than beneficial to the results. In a greater number of cases however, the background subtractions did provide an improvement of the data classification. A summary of the results is provided in Table 4.1.

Table 4.1: Summary of the classification of the cantilever deflection experiments and background subtractions. Of the 52 experiments, 49 were designed to detect INF- $\gamma$ , while 3 were designed to detect streptavidin. Whether a background subtraction left the data worsened, improved or unchanged was determined by whether it decreased, increased or maintained the group classification respectively. The no background categorization indicates that the background subtraction was infeasible for that particular data set.

	Original Data		Background Subtraction		
	Flowing	Still	Still Linear	Flowing Linear	Still Logarithmic
Group I	6	6	9	9	8
Group II	11	10	19	20	5
Group III	35	32	15	22	11
No Background	-	-	9	1	28
Detrimental	-	-	5	3	2
Equivalent	-	-	19	30	15
Improvement	-	-	19	18	7

## 4.3 Cantilever Deflection Results

Out of the 52 experiments that were performed, 16 yielded one or more group I results either in the original data or from one of the background subtractions. The successful group I results were produced using a variety of conditions, linkers and blockers. This is because when one linking procedure, blocking procedure and set of conditions did not produce reproducible separation between the active and reference cantilevers, the methodology was altered in an attempt to reach this goal. The majority of the experiments that led to a group I result are described and listed by linker below. The experiments were performed at 20°C unless otherwise indicated. Also, the length of the tubing between the sample holder and the measurement chamber was 35  $\mu\text{l}$  in volume, so with the intake rate of 0.417  $\mu\text{l/s}$  there was a delay of 84 seconds between the initiation of the sample intake and the time the sample entered the measurement chamber.

### 4.3.1 Detection of INF- $\gamma$ Using Prolinker B as the Linker

A substantial number of the group I classified results came from the Prolinker B experiments. The first set of experiments was performed with BSA blocking after the C-Ab incubation step, which allowed adhesion of the C-Ab to the silicon backside of the arrays. Also, the arrays used were pre-evaporated with 40 nm of gold, which made proper blocking of the backside without contaminating the gold surface difficult. Thirdly, the INF- $\gamma$  concentrations used in these experiments was relatively low, in the tens of ng/ml. Therefore these experiments yielded few positive results. (Data not shown).

In order to improve the results the whole procedure was substantially altered. In the following experiment a bare silicon array was cleaned in piranha for 20 minutes, washed in water and IPA and dried with nitrogen to improved the cleanliness of the cantilevers. The array was then passivated with PEG-silane using the thermal silanization procedure from section 3.5.3, washed in ethanol and

dried in nitrogen. A 3 nm titanium adhesion layer and a 40 nm layer of gold were evaporated onto the surface of the cantilever array. The array was then incubated in 3 mM Prolinker B for 1 hour, was washed in chloroform, acetone, IPA, water and ethanol, and dried with nitrogen. Each of the following three steps was succeeded by a 3x wash in wash buffer. Cantilevers 1 and 3 were incubated in 100  $\mu\text{g/ml}$  cC-Ab while 5 and 7 were incubated in 100  $\mu\text{g/ml}$  hC-Ab for 4 hours. The array was then blocked with 7% ethanolamine in PBS for 1 hour and further blocked with 100  $\mu\text{g/ml}$  hPEG-thiol in ethanol for 30 minutes. The array was then inserted into the Cantisens and the PBS buffer intake was initiated at 568 s, the sample intake began at 698 s, the 10  $\mu\text{g/ml}$  INF- $\gamma$  sample in PBS entered the chamber at 782 s and intake was halted at 1298 s. The results are shown in Figure 4.4.

There appeared to be some separation between the cC-Ab and hC-Ab signals in the buffer deflection, though for the flowing buffer data the separation was likely due to the location of the cantilevers on the array. The automated liquid intake function of the Cantisens system causes the cantilever signals to fan out, separating the cantilever signals according to their position on the array. Both the original sample intake and the flowing buffer subtraction data show clear separation between the two active hC-Ab cantilevers and all the reference cantilevers. This classifies them as group I data. The linear still buffer background subtraction shows no separation between the active and reference cantilevers, and was thus classified as group III data.

The original data in the still sample solution was also classified as group I data despite the one ethanolamine and thiol blocked cantilever curve which passed through the hC-Ab signal. This is because a number of experiments (data not shown) similar to the buffer equilibration in Figures 4.5A showed a distinct separation between deflection of the C-Ab coated cantilevers and the ethanolamine, PEG-thiol and/or BSA blocked cantilevers during the buffer deflection. For this reason the group classification was limited to the separation between the cC-Ab or INF- $\gamma$  (when used) blocked cantilevers and the hC-Ab cantilever data.

The next data set of interest was produced using a sputtered cantilever array which, though generally less commonly used for cantilever deflection experiments, was tested as an alternative to improve the reproducibility of the cantilever deflection. The array was cleaned and silanized as in the previous experiment, but it was sputtered with a 5 nm adhesion layer of chromium and 40 nm of gold. Titanium was not used because it was not permitted in the sputter system. The array was then placed in 1 mM Prolinker B for one hour, was washed in chloroform, acetone, IPA, water and ethanol, and was dried with nitrogen. In all the solutions a 1/10 dilution of normal PBS in water was used. This reduced concentration buffer was tested because salt buildup on the cantilevers was significantly affecting their deflection. Further information concerning this issue can be found in section 4.4.2. Cantilevers 2 and 4 were placed in 50  $\mu\text{g/ml}$  hC-Ab, cantilevers 6 and 8 were placed in 50  $\mu\text{g/ml}$  cC-Ab, and they were left to incubate for 2 hours. The array was washed 3x in wash buffer and blocked with 3% BSA in the dilute PBS for 40 minutes. It was washed again 3x in wash buffer and placed in the Cantisens. A long buffer equilibration was performed, with repeated intake of buffer solution from 165 s to 12371 s. The PBS buffer intake for the sample test began at 61493 s, and the sample intake began at 61624 s. The 10  $\mu\text{g/ml}$  INF- $\gamma$  in PBS sample entered the measurement chamber at 61577 s, and the intake was stopped at 62333 s. The results are shown in Figure 4.5.

From the buffer equilibration it is evident that the buffer deflection continues even after a 16 hour equilibration period. Also, as mentioned before, there is a clear separation between the C-Ab cantilever deflection and the ethanolamine/PEG-thiol cantilever signals. The separation of the cC-Ab and hC-Ab coated cantilever deflection signals were again a result of the liquid handling system. There does not appear to be any pattern in either buffer deflection data set. Also, although the cantilever deflection in the still buffer after the buffer equilibration was less than in similar experiments without a long equilibration time, the magnitude of the deflection and separation between the cantilevers in the flowing buffer period was not significantly altered. Neither the sample intake nor the still sample data showed separation between the active and reference

cantilevers and were therefore classified as group III data. The three background subtractions, however, led to clear separation between the active and reference cantilevers and were all classified as group I data.

Due to the buildup seen visually on the cantilever surfaces, and the effect of this buildup on cantilever deflection seen in one sputtering experiment, low NaCl PBS was substituted for normal PBS in the following three Prolinker B experiments. The array was prepared using the same cleaning, silanization and evaporation procedure which led the results in Figure 4.4. The even numbered cantilevers were blocked with 100  $\mu\text{g/ml}$  hPEG-thiol for one hour, and the array was washed 3x in PBS. The array was then incubated in 3 mM Prolinker B for 1 hour, was washed in chloroform, IPA, water was ethanol, and was dried with nitrogen. Cantilevers 1 and 3 were placed in 50  $\mu\text{g/ml}$  cC-Ab, cantilevers 5 and 7 were placed in 50  $\mu\text{g/ml}$  hC-Ab, and the incubation time was 3 hours. The array was then washed 3x in wash buffer, dried with nitrogen, blocked with 7% ethanolamine in PBS for 1 hour, and washed 3x in wash buffer. In the Cantisens the PBS buffer intake was initiated at 422 s, the sample intake began at 552 s and the 10  $\mu\text{g/ml}$  INF- $\gamma$  sample in PBS entered the chamber at 636 s. The results are shown in Figure 4.6. There was no pattern to the buffer deflection, aside from the usual spreading at the start of the buffer intake. Both original data sets were classified as group III data, while all three background subtractions produced group I data.

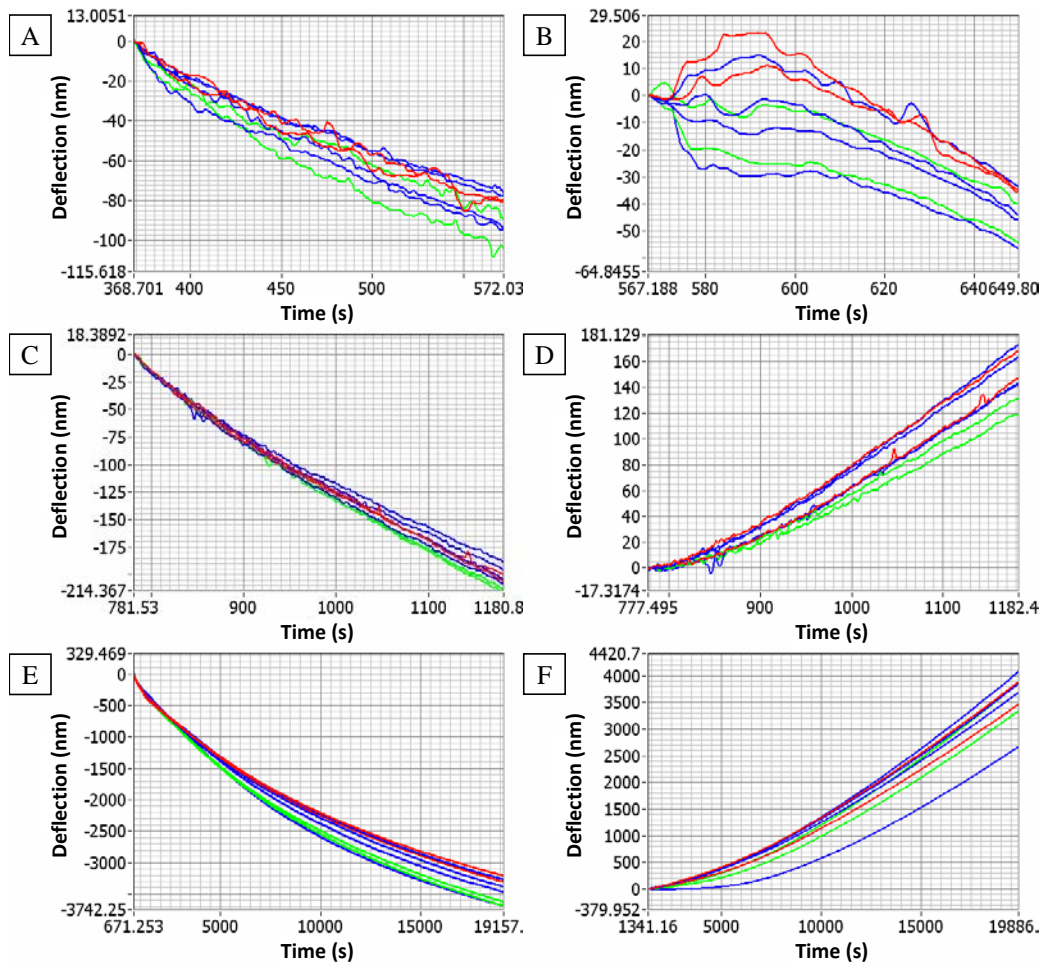


Figure 4.4: Cantilever deflection results with Prolinker B as the linker and including data classified as group I. A - The still buffer deflection. B - The flowing buffer deflection. C - The deflection during the sample intake. D - The linear flowing buffer background subtraction. E - The deflection in the still sample solution. F - The linear still buffer background subtraction. The green series, red series and blue series represent the active cantilevers functionalized with hC-Ab, the reference cantilevers which were coated cC-Ab and the other reference cantilevers which were blocked with ethanolamine and PEG-thiol respectively.

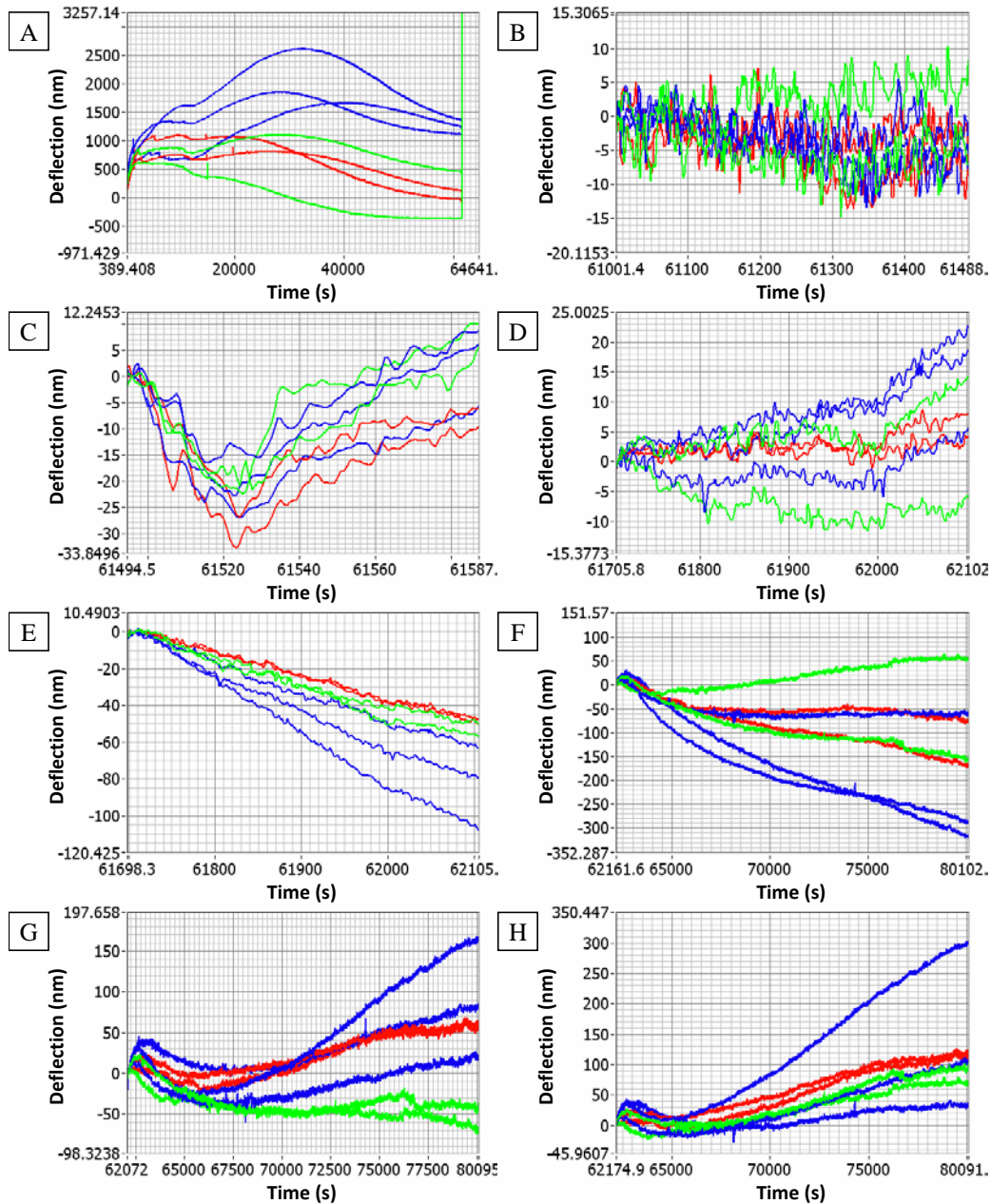


Figure 4.5: Cantilever deflection results with Prolinker B as the linker and including data classified as group I. A - The deflection during the buffer equilibration. B - The still buffer deflection. C - The flowing buffer deflection. D - The deflection during the sample intake. E - The linear flowing buffer background subtraction. F - The deflection in the still sample solution. G - The linear still buffer background subtraction. H - The logarithmic still buffer background subtraction. The green, red and blue series represent the active cantilevers functionalized with hC-Ab, the reference cantilevers which were coated with cC-Ab and the other reference cantilevers which were blocked with 3% BSA respectively.

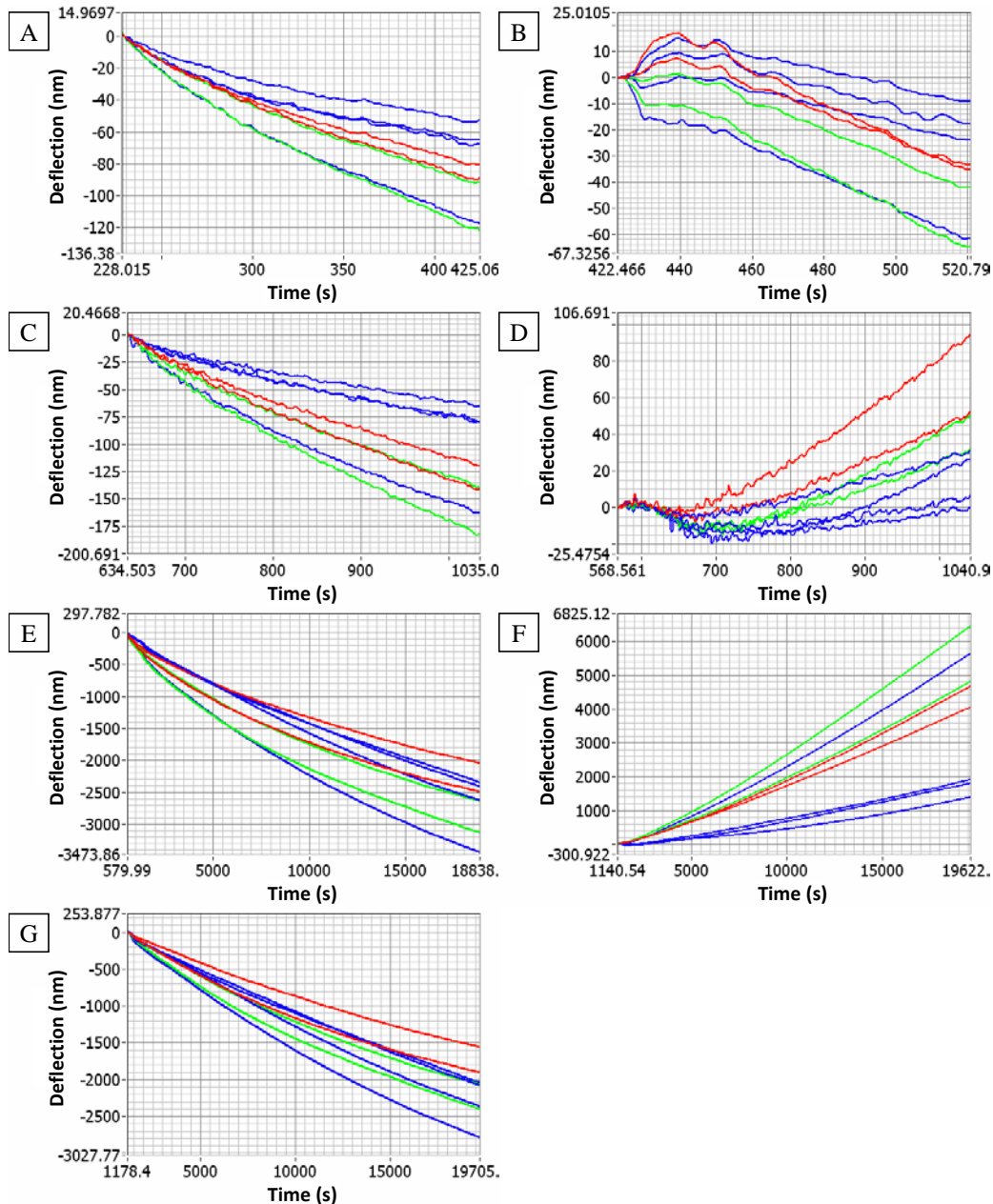


Figure 4.6: Cantilever deflection results with Prolinker B as the linker and including data classified as group I. A - The still buffer deflection. B - The flowing buffer deflection. C - The deflection during the sample intake. D - The linear flowing buffer background subtraction. E - The deflection in the still sample solution. F - The linear still buffer background subtraction. G - The logarithmic still buffer background subtraction. The green series represent the active cantilevers functionalized with hC-Ab, the red series represent the reference cantilevers which were coated with cC-Ab and the blue series represent the other reference cantilevers which were blocked with PEG-thiol.

The next cantilever array was silanized and evaporated identically to the previous experiments presented in Figures 4.4 and 4.6. Low NaCl PBS was used again in this experiment. Cantilevers 2, 6, and 8 were blocked with 100  $\mu\text{g/ml}$  PEG-thiol in PBS for 2 hours while an air bubble in the capillary left cantilever 4 unblocked. The array was then washed 3x in PBS and once in chloroform. Next it was submerged in 3 mM Prolinker B for 1.5 hours and was washed in chloroform, IPA, water and ethanol. Subsequently it was dried with nitrogen and four cantilevers were incubated in 50  $\mu\text{g/ml}$  C-Ab overnight with 1 and 3 in cC-Ab, and 5 and 7 in hC-Ab. The array was again washed 3x in PBS and submerged in 7% ethanolamine for 2 hours. The array was then immersed in wash solution overnight to equilibrate the cantilevers. Finally the array was washed twice in wash solution and once in mQ water before it was inserted into the Cantisens reader. In the Cantisens the PBS buffer intake was initiated at 641 s, the sample intake began at 771 s, the 10  $\mu\text{g/ml}$  INF- $\gamma$  in PBS entered the chamber at 855 s and the sample flow was stopped at 1265 s. The results are shown in Figure 4.7. There was a distinct separation in the still buffer deflection between the cC-Ab and hC-Ab signals. There was no separation in the sample intake data between the cC-Ab and hC-Ab signals thus it was classified as group III data. All the other data sets were classified as group I data, though the logarithmic subtraction did not show as clear a separation between the active and reference cantilevers as the other data sets.

The final Prolinker B array was prepared identically to the previous array (Figure 4.7) up to the Prolinker B step. Low NaCl PBS was again used in this experiment, but the linker incubation time was 3 hours and the Prolinker B concentration was 1.5 mM. The array was washed in chloroform, IPA, water and IPA, and was dried with nitrogen. All eight cantilevers were functionalized with C-Ab. The odd cantilevers were incubated in 50  $\mu\text{g/ml}$  hC-Ab overnight, and the array was washed in wash buffer, PBS and twice in water. All the even cantilevers except cantilever 4 were then incubated in 50  $\mu\text{g/ml}$  cC-Ab overnight and were washed as before. Cantilever 4 was not coated in cC-Ab because there was an air bubble in the capillary again. No additional blocking buffer was used and the

results are shown in Figure 4.8. In the Cantisens the buffer intake was initiated at 1070 s, the 10  $\mu\text{g/ml}$  INF- $\gamma$  in PBS sample intake began at 1201 s, the sample entered the chamber at 1285 s and the sample flow was stopped at 1692 s. Again there was a very clear separation between the cC-Ab and hC-Ab signals in the still buffer deflection, possibly due to the overnight incubation steps occurring separately for the active and reference cantilevers. This separation was also evident in the buffer intake data and should be eliminated by the background subtractions. Both the sample intake and linear flowing background subtraction were classified as group I data, as were both background subtractions for the still sample data. The original still sample data had an interesting pattern where the hC-Ab signals cross over the cC-Ab signals, and was classified as group II data.

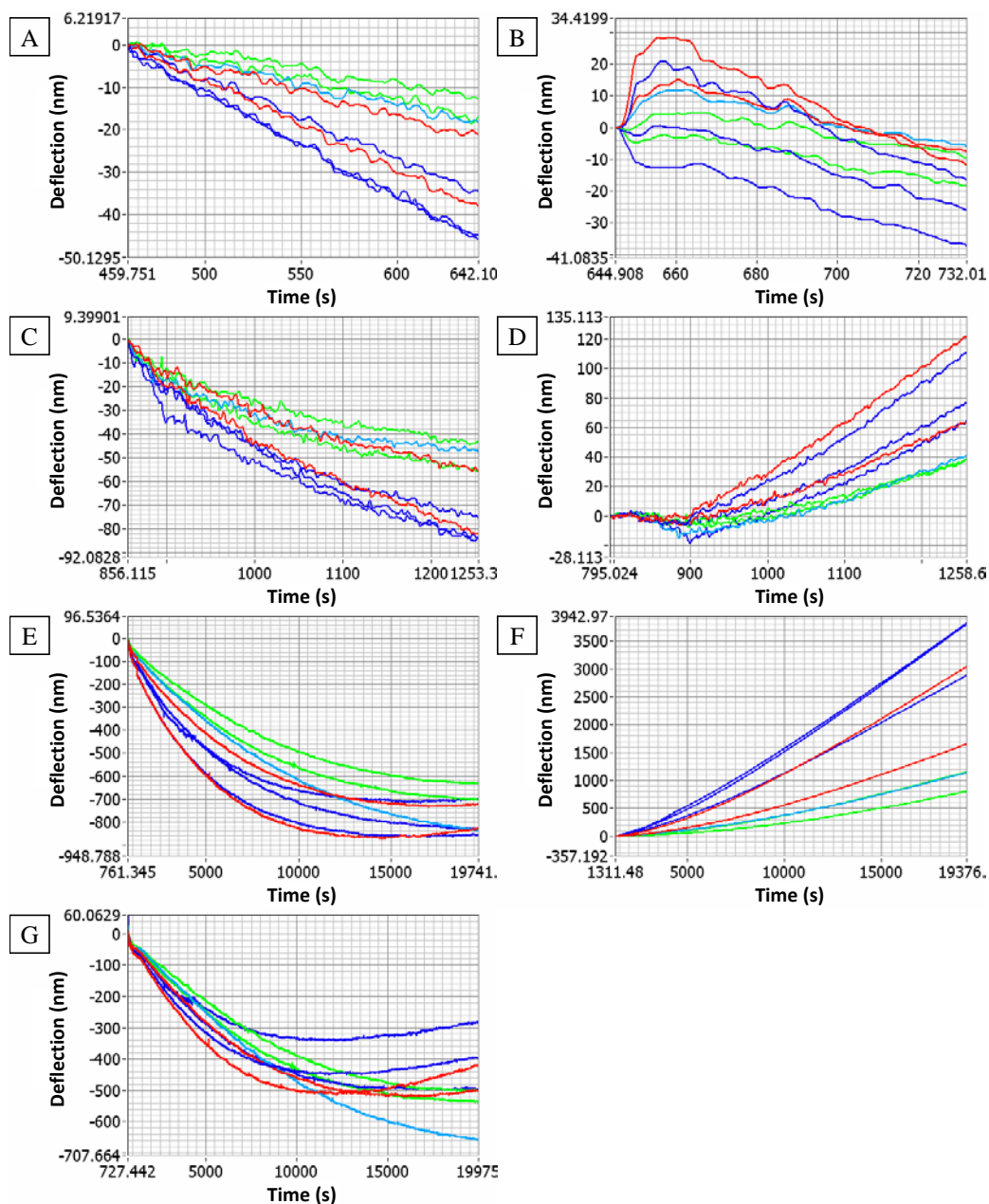


Figure 4.7: Cantilever deflection results with Prolinker B as the linker and including data classified as group I. A - The still buffer deflection. B - The flowing buffer deflection. C - The deflection during the sample intake. D - The linear flowing buffer background subtraction. E - The deflection in the still sample solution. F - The linear still buffer background subtraction. G - The logarithmic still buffer background subtraction. The green, red, dark blue and light blue series represent the active cantilevers functionalized with hC-Ab, the reference cantilevers coated with cC-Ab, the other reference cantilevers blocked with PEG-thiol, and the cantilever which was only coated with Prolinker B before it was placed into the measurement chamber.

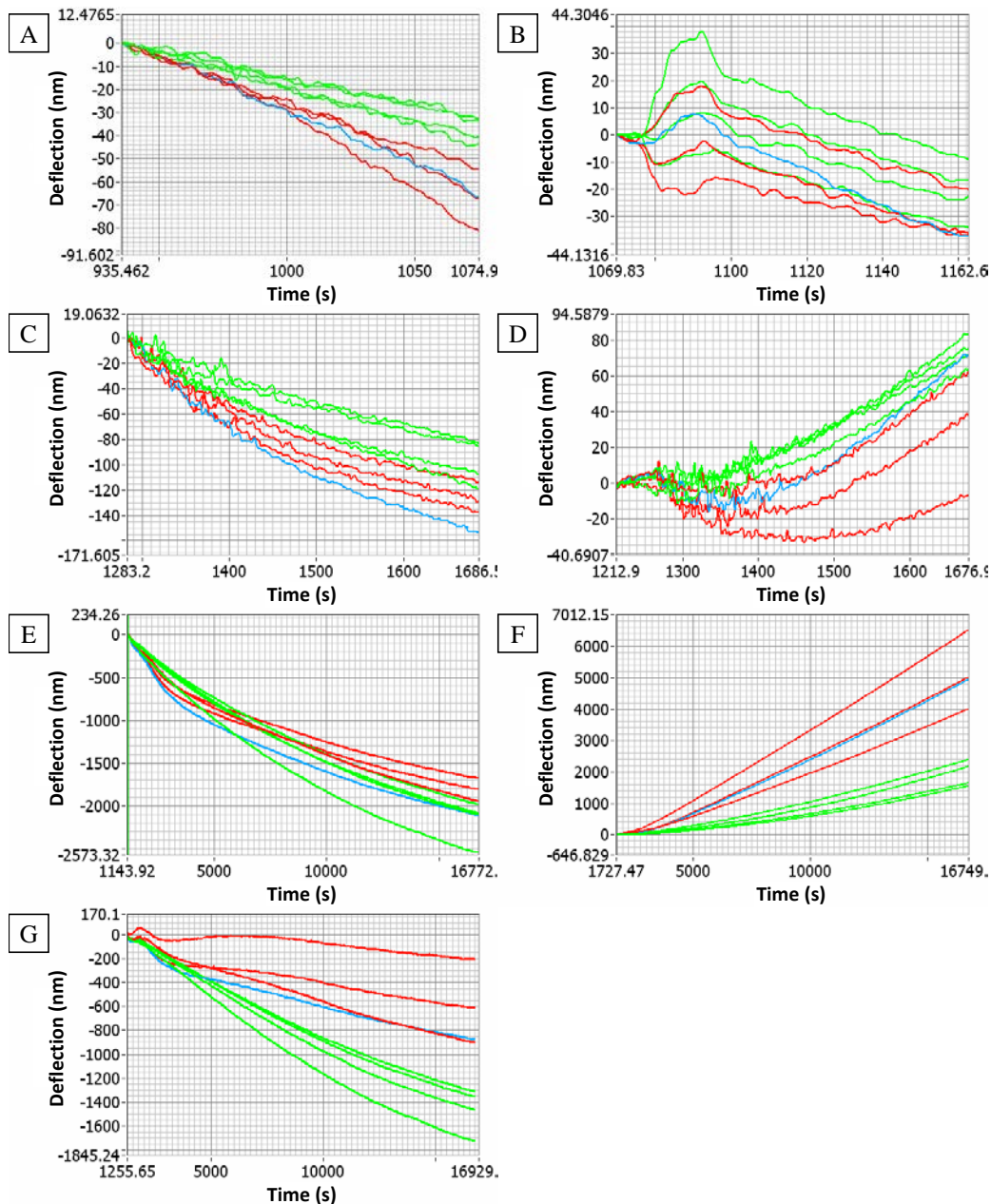


Figure 4.8: Cantilever deflection results with Prolinker B as the linker and including data classified as group I. A - The still buffer deflection. B - The flowing buffer deflection. C - The deflection during the sample intake. D - The linear flowing buffer background subtraction. E - The deflection in the still sample solution. F - The linear still buffer background subtraction. G - The logarithmic still buffer background subtraction. The green series represent the active cantilevers functionalized with hC-Ab, the red series represent the reference cantilevers which were coated with cC-Ab and the blue series represents the cantilever which was only coated with Prolinker B before it was placed into the measurement chamber.

### 4.3.2 Detection of INF- $\gamma$ Using Glutaraldehyde as the Linker

Glutaraldehyde exclusively links to free amine groups so it is necessary to aminate the cantilever surface. The array was incubated in APTES instead of PEG-silane, and 3 nm titanium and 40 nm gold were evaporated on the backside of the array. Again low NaCl concentration PBS was used in this experiment. The array was submerged in 100  $\mu\text{g/ml}$  PEG-thiol in PBS for 1 hour to block the backside, washed 3x in PBS and placed in 2% glutaraldehyde in PBS for 2 hours. It was then washed in wash buffer, PBS and water, and was dried with nitrogen. The next two steps were similarly followed by washes in wash buffer, PBS and water. Cantilevers 1 and 3 were functionalized with 50  $\mu\text{g/ml}$  cC-Ab and cantilevers 5 and 7 were functionalized with 50  $\mu\text{g/ml}$  hC-Ab for 3 hours. The array was then blocked with 7% ethanolamine in PBS for 2 hours. Subsequently it was placed in the Cantisens and the buffer intake was initiated at 788 s, the 10  $\mu\text{g/ml}$  INF- $\gamma$  in PBS sample intake began at 918 s, the sample entered the chamber at 1002 s and the sample flow was stopped at 1411 s. The results are shown in Figure 4.9. There was no important separation of the signals in the still buffer deflection, but the flowing buffer deflection shows some separation between the cC-Ab and hC-Ab signals. The original sample intake data and the linear flowing buffer background subtraction both qualify as group I data as do the still sample deflection and logarithmic background subtraction. The linear still buffer background subtraction was classified as group III data.

The previous glutaraldehyde experiment was repeated with a few modifications. Firstly, all the even cantilevers were coated with cC-Ab and all the odd cantilevers were coated with hC-Ab each with an incubation time of 3 hours. No ethanolamine was used to block the cantilevers and 5  $\mu\text{g/ml}$  INF- $\gamma$  was used instead of 10  $\mu\text{g/ml}$  INF- $\gamma$ . In addition, the blocked gold layer was the top side of the cantilever array as opposed to the bottom side to allow for better reflection in the Cantisens. The results are shown in Figure 4.10. There was no significant

separation in the buffer deflection signals. The sample intake data and the linear flowing buffer background subtraction were both classified as group II data, as was the logarithmic background subtraction. The still sample data and the linear still buffer background subtraction were classified as group III and group I data respectively.

Due to financial considerations, the third experiment that used glutaraldehyde as the linker and lead to group I results was performed with a reused cantilever array. The buffer used was PB which does not contain any NaCl. The array was washed twice sequentially in gold etch, water, 30%:10% KOH:H<sub>2</sub>O<sub>2</sub> and again in water. It was dried with nitrogen, piranha cleaned for 20 minutes, washed in water and IPA, and dried with nitrogen. The top surface of the array was evaporated with 5 nm titanium and 40 nm gold, and it was then incubated in 10 mM cysteamine-HCl in PBS overnight. The array was washed 3x in PB and was submerged in 2% PEG-silane in 100% ethanol for 40 minutes, and was washed 3x in ethanol and 2x in water. It was then placed in 2% glutaraldehyde in PB with pH 7.5 for 2 hours and washed 3x in water. The whole array was incubated in 100 µg/ml hC-Ab in PB for 2 hours, and washed 3x in PB. The even cantilevers were blocked with 10 µg/ml INF-γ for 1 hour and 35 minutes. The array was then placed into the Cantisens and washed 5x with PB using 500 µl for each uptake and a 10 µl/s flow rate. The INF-γ sample concentration was 10 µg/ml in PB, and the results are shown in Figure 4.11. The PB buffer intake began at 2196 s and the sample intake began at 2328 s, so the INF-γ entered the chamber at 2412 s and intake was halted at 2819 s. There was no significant separation in the buffer deflection signals. Both original data sets were classified as group I data though the still sample deflection series took a long time to separate because the four hC-Ab signals crossover the four cC-Ab signals. The linear flowing buffer background subtraction belongs to the some of the worst data in the group III classification, as the active and reference cantilever signals are overlapping. The other two background subtractions were classified as group I data, though the still linear subtraction only just fits the criteria as there is some deviation from one of the reference cantilevers near the 16000s mark.

The procedure for the fourth experiment was identical to that of the previous experiment. After a heat test, the buffer intake was initiated at 1422 s and the sample intake began at 1552 s, so the INF- $\gamma$  entered the chamber at 1636 s and the sample flow was halted at 2045 s. The results are shown in Figure 4.12. The results demonstrate how one or two deviant cantilevers can alter the group classification. In the Figure 4.12 sample intake data one reference cantilever is off from the rest while in the two linear background subtractions one cC-Ab and one hC-Ab coated cantilever are off from the rest. The still sample data is very similar in pattern to the data set presented in Figure 4.11, but the crossing of the active and reference series was sufficiently different that it was classified as group III data. The still buffer logarithmic background subtraction produced the group I result in this experiment. There was a pattern to the buffer deflection as the active cantilevers on average deflected more than the reference cantilevers.

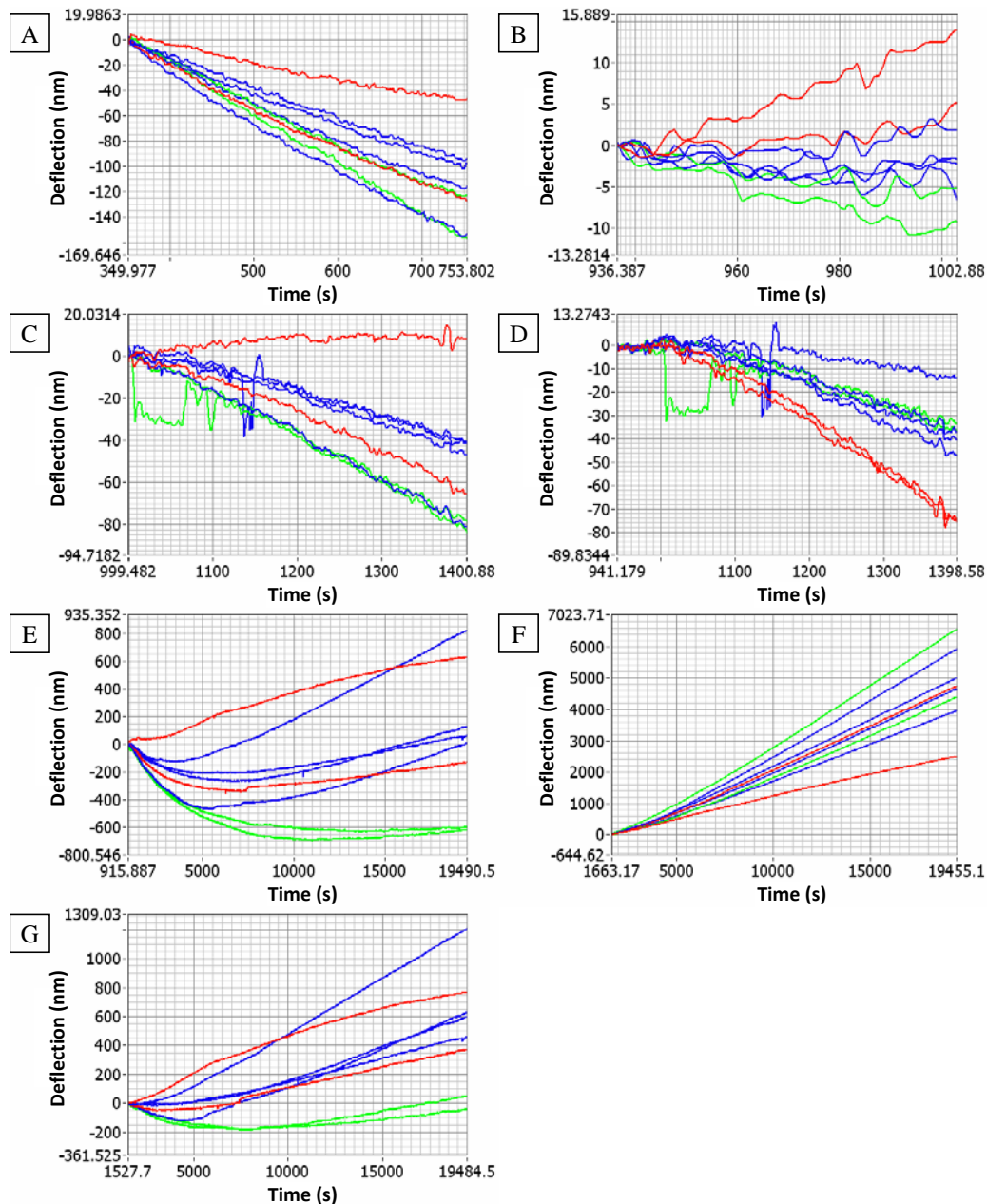


Figure 4.9: Cantilever deflection results with glutaraldehyde as the linker and including data classified as group I. A - The still buffer deflection. B - The flowing buffer deflection. C - The deflection during the sample intake. D - The linear flowing buffer background subtraction. E - The deflection in the still sample solution. F - The linear still buffer background subtraction. G - The logarithmic still buffer background subtraction. The green series represent the active cantilevers functionalized with hC-Ab, the red series represent the reference cantilevers coated with cC-Ab and the blue series represent the other reference cantilevers which were blocked with ethanolamine.

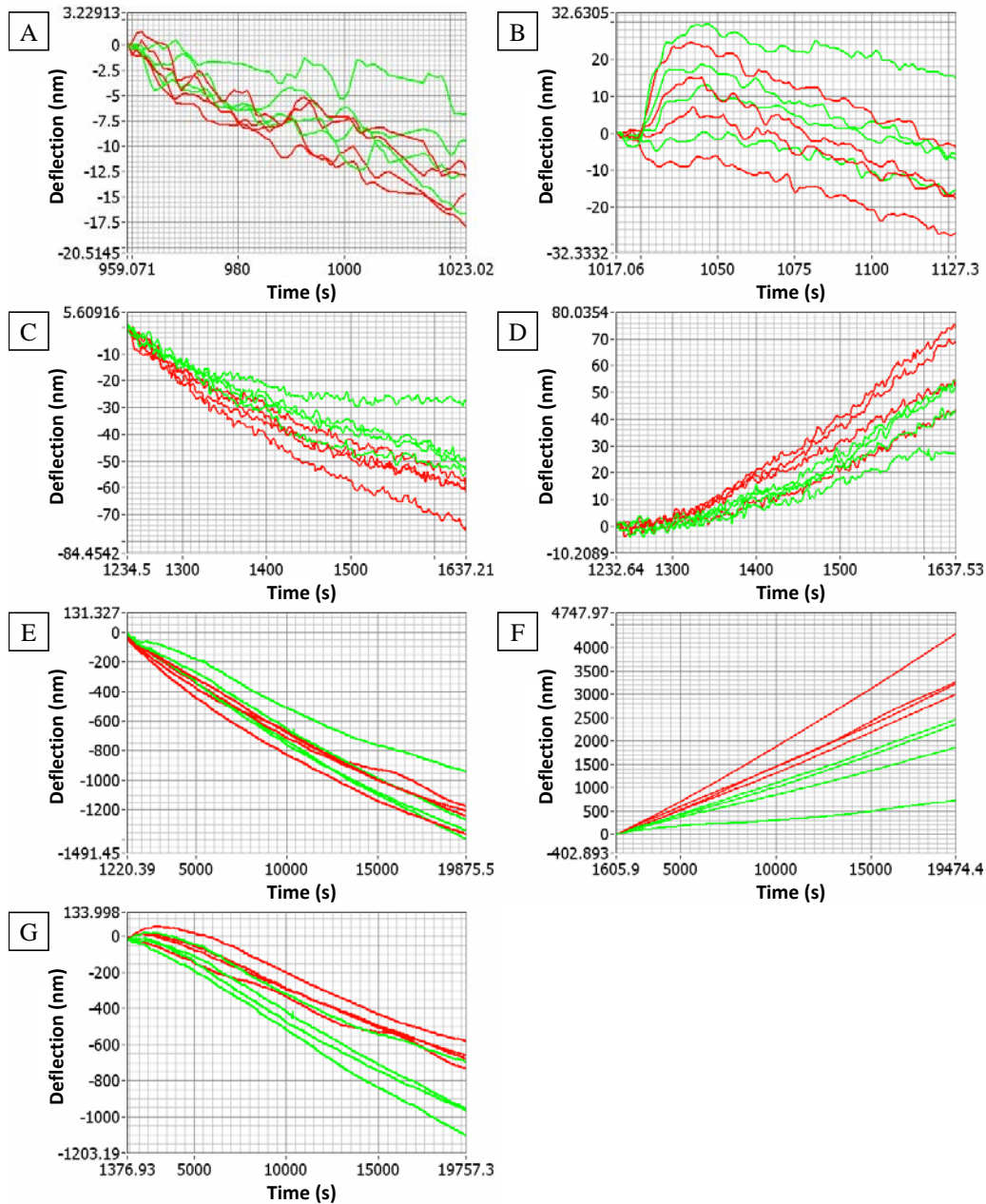


Figure 4.10: Cantilever deflection results with glutaraldehyde as the linker and including data classified as group I. A - The still buffer deflection. B - The flowing buffer deflection. C - The deflection during the sample intake. D - The linear flowing buffer background subtraction. E - The deflection in the still sample solution. F - The linear still buffer background subtraction. G - The logarithmic still buffer background subtraction. The green series represent the active cantilevers functionalized with hC-Ab and the red series represent the reference cantilevers coated with cC-Ab.

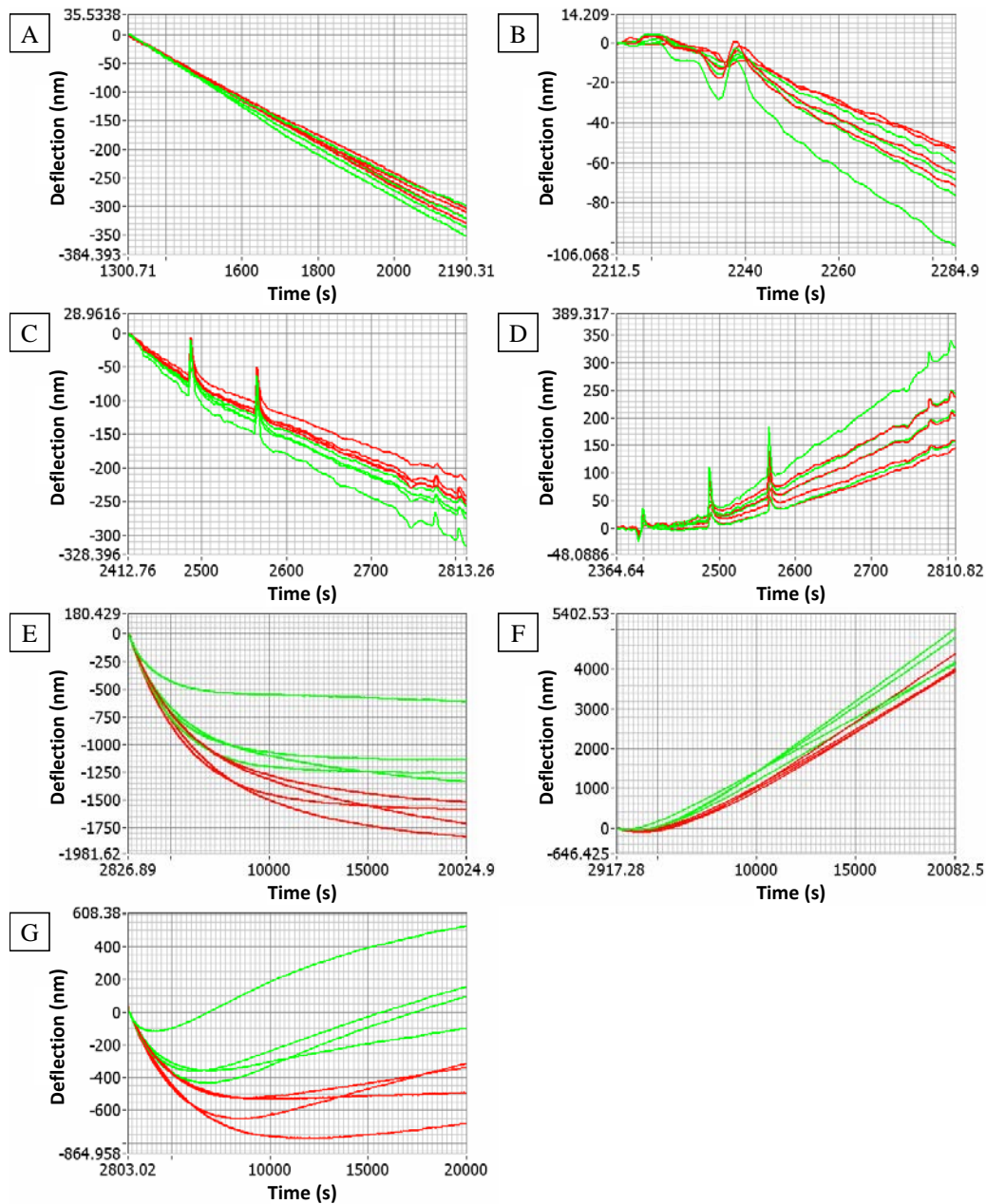


Figure 4.11: Cantilever deflection results with glutaraldehyde as the linker and including data classified as group I. A - The still buffer deflection. B - The flowing buffer deflection. C - The deflection during the sample intake. D - The linear flowing buffer background subtraction. E - The deflection in the still sample solution. F - The linear still buffer background subtraction. G - The logarithmic still buffer background subtraction. The green series represent the active cantilevers functionalized with hC-Ab and the red series represent the references cantilevers which were blocked with INF- $\gamma$ .

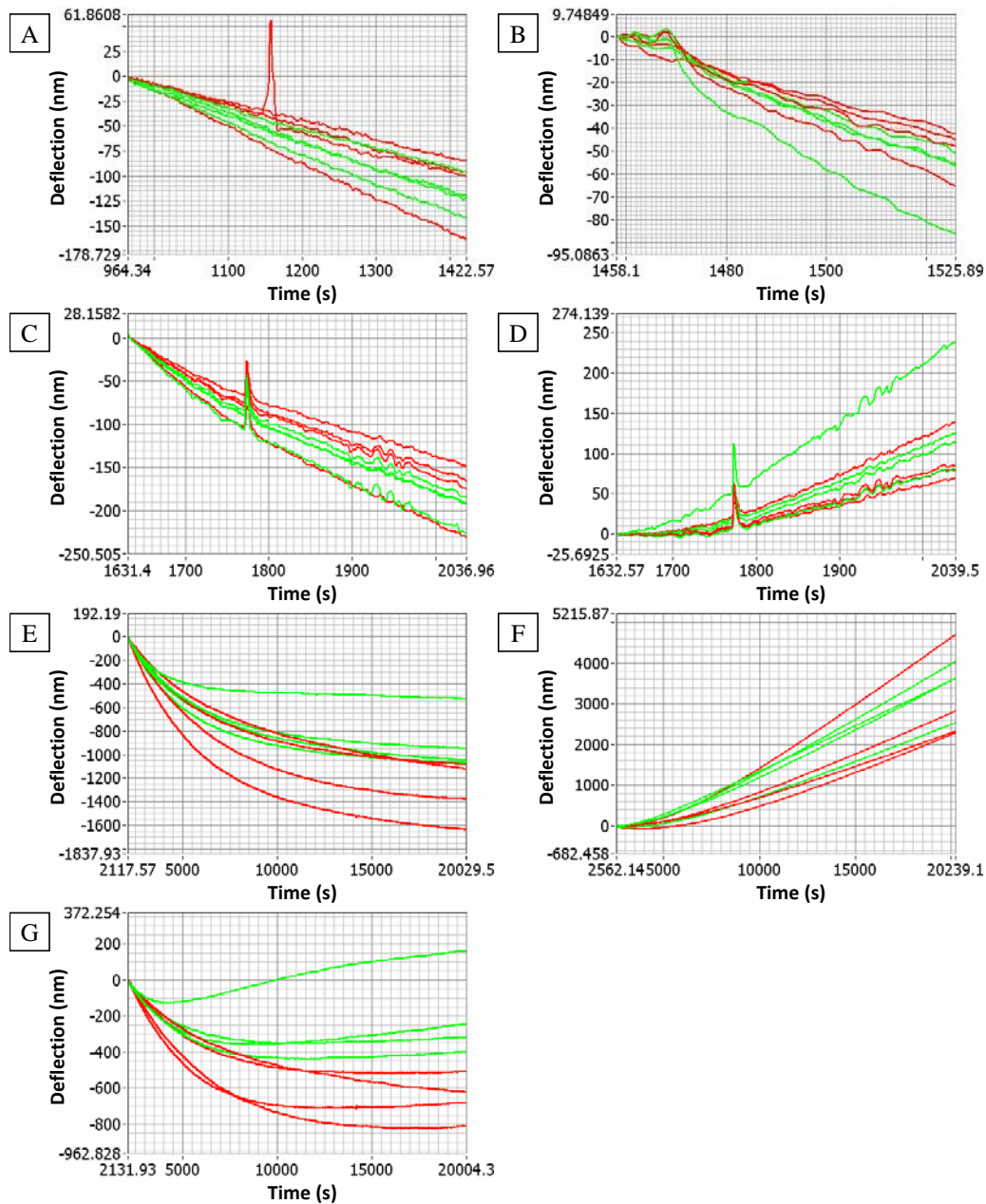


Figure 4.12: Cantilever deflection results with glutaraldehyde as the linker and including data classified as group I. A - The still buffer deflection. B - The flowing buffer deflection. C - The deflection during the sample intake. D - The linear flowing buffer background subtraction. E - The deflection in the still sample solution. F - The linear still buffer background subtraction. G - The logarithmic still buffer background subtraction. The green series represent the active cantilevers functionalized with hC-Ab and the red cantilever signals represent the reference cantilevers which were blocked with INF- $\gamma$ .

### 4.3.3 Detection of INF- $\gamma$ Using 1-Ethyl-3-[3-dimethylaminopropyl] carbodiimide/N-hydroxysulfosuccinimide as the Linkers

The best deflection cantilever array measurement of INF- $\gamma$  was produced using EDC and Sulfo-NHS to link the C-Abs to cysteamine on the gold cantilever surface. Again, low NaCl concentration PBS was used in this experiment. The array was PEG-silanized and evaporated using the same experimental procedure as in the first Prolinker B experiment (Figure 4.4). It was then placed in 10 mM cysteamine in water overnight and washed 2x in water. A solution of 50  $\mu\text{g/ml}$  cC-Ab, 55 mM Sulfo-NHS and 50 mM EDC in 10 mM 2-(N-morpholino)ethanesulfonic acid and 38 mM NaCl MES buffer with pH 5.5 was prepared and allowed to react for 15 minutes. Next, 47 mM 2-mercaptoethanol was added to the solution to halt the EDC reaction, and the solution volume was doubled with PB. The addition of PB increases the pH to above 7, which activates the Sulfo-NHS. The solution was used to functionalize the even cantilevers for 1.75 hours. The array was then washed 2x in water and the process was repeated using hC-Ab to functionalize the odd cantilevers. The array was then incubated for 15 minutes in 7% ethanolamine, was washed 2x in water and was placed in the Cantisens. The buffer intake was initiated at 254 s, the 5  $\mu\text{g/ml}$  INF- $\gamma$  in PBS sample intake began at 385 s, the sample entered the chamber at 469 s and the sample flow was stopped at 878 s. The results are shown in Figure 4.13. There was no pattern to either buffer deflection. The sample intake data was classified as group II data while the still sample data was the best group I data that was produced. There was a clear separation between the active and reference cantilevers and none of the signals crossed during period of interest. The fluctuations and short length of the buffer deflection data made the background subtractions unfeasible.

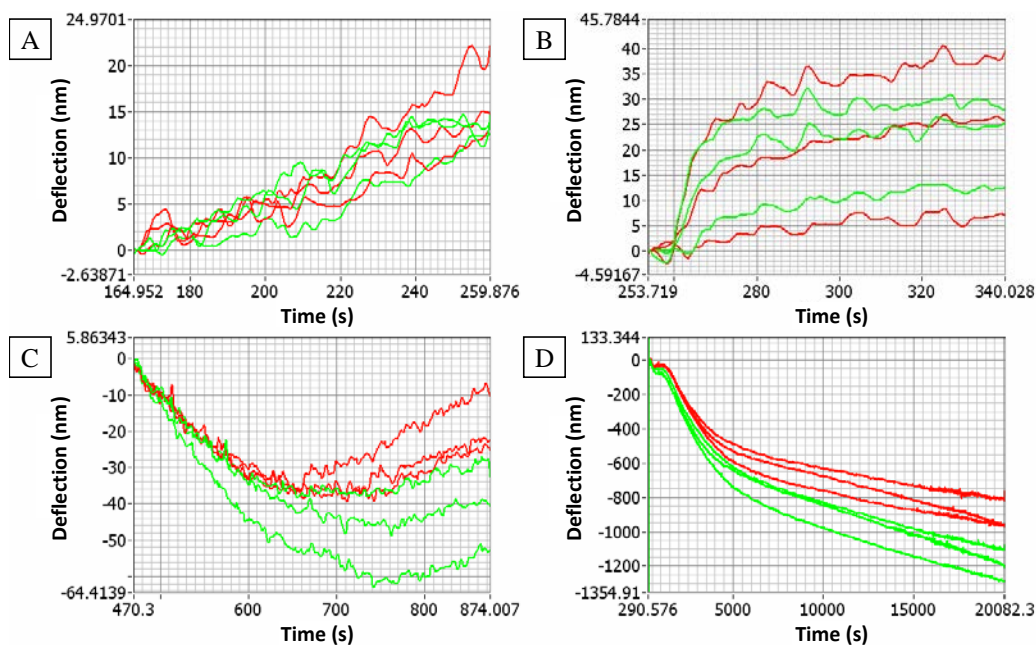


Figure 4.13: Cantilever deflection results with EDC/Sulfo-NHS as the linker and including data classified as group I. A - The still buffer deflection. B - The flowing buffer deflection. C - The deflection during the sample intake. D - The deflection in the still sample solution. The green series represent the active cantilevers which were functionalized with hC-Ab while the red series represent the reference cantilevers which were coated with cC-Ab.

#### 4.3.4 Detection of Biotin with Streptavidin and Hydrocarbon-thiols with Gold

Given the difficulties in producing reliable measurements of INF- $\gamma$  in the previous experiments and in the other experiments which were not shown, the cantilever arrays were tested using two more simplistic systems. The two systems tested were hydrocarbon-thiol binding to gold and the measurement of streptavidin using biotin. Obtaining results for the hydrocarbon-thiol binding was challenging due to frequent air bubble formation in the measurement chamber. One of the biotin-streptavidin experiments produced positive results however. The array was used previously and was cleaned sequentially in gold etchant, 3x in water, once in 15% NaOH and 5% H<sub>2</sub>O<sub>2</sub> in water by volume, 3x in water, again in gold etchant and 3x in water. The array was then dried with nitrogen. It was then piranha cleaned for 20 minutes, washed in water, washed in IPA, and dried with

nitrogen. Next, 5 nm of titanium and 40 nm of gold were evaporated onto the top surface, and the array was incubated in 10 mM cysteamine-HCl in water overnight. The array was washed 3x in water and incubated in 4 mg/ml EZ-link in water for 1 hour. It was then washed again 3x in water and the odd numbered cantilevers were blocked with 0.5 mg/ml streptavidin for 35 minutes in PB. The array was washed in PB in the Cantisens and streptavidin binding was measured using a 0.5 mg/ml streptavidin sample in PB. The buffer intake began at 2321 s and the sample intake began at 2452 s, entered the chamber at 2536 s and ended at 2943 s. The results are shown in Figure 4.14. There is a definite separation between the active and reference cantilevers in the buffer deflection, which is not surprising since there is a considerable difference between the biotin on the active cantilevers and the linked biotin-streptavidin on the reference cantilevers. All the data sets except the still linear background subtraction show clear separation between all the active and reference cantilevers, and the cantilever signals do not cross. Therefore all but the still linear background subtraction were classified as group I data while it was classified as group II data. The successful background subtractions are particularly important in this case because they show that the separation between the active and reference cantilevers is not caused solely by the difference in the rate of buffer deflection between the active and reference cantilevers.

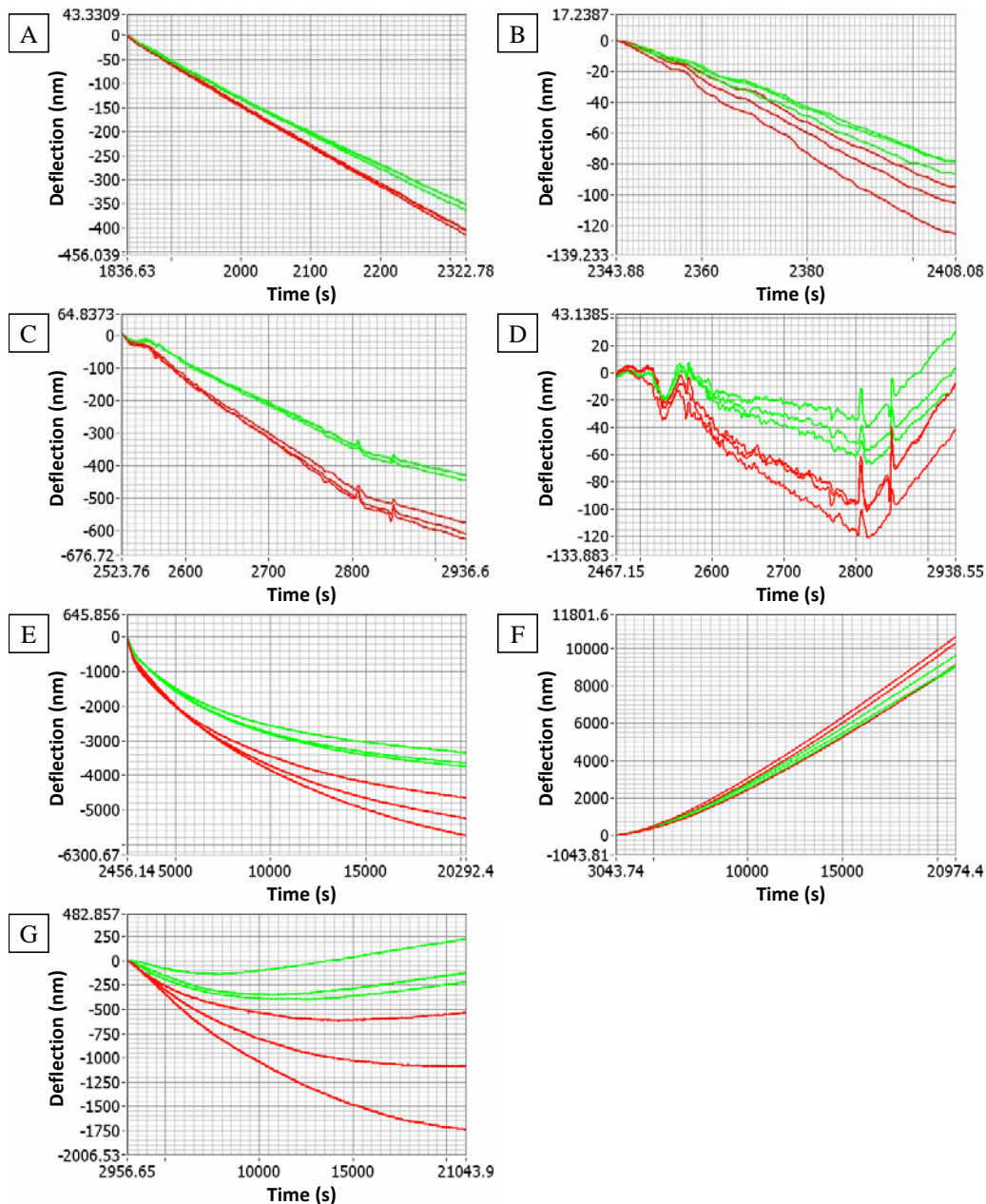


Figure 4.14: Cantilever deflection caused by streptavidin binding to biotin linked to the surface with EZ-link and including data classified as group I. A - The still buffer deflection. B - The flowing buffer deflection. C - The deflection during the sample intake. D - The linear flowing buffer background subtraction. E - The deflection in the still sample solution. F - The linear still buffer background subtraction. G - The logarithmic still buffer background subtraction. The green series represent the active cantilevers functionalized with biotin and the red series represent the reference cantilevers which were blocked with streptavidin.

## 4.4 A Discussion of the Experimental Conditions and their Effects on the Cantilever Measurements

As is evident from the cantilever measurements, a variety of different procedures were evaluated over the course of this project, the purpose of which was to find a reliable procedure that results in consistent clean measurements of INF- $\gamma$ . The major factors that were altered include: the method of gold coating, the buffer solutions and concentrations, the blocking methods, the linking methods, and the INF- $\gamma$  concentrations. In addition, this section covers other issues which were encountered including the effectiveness of the reference cantilever coatings and the sequential deflection of the cantilevers.

### 4.4.1 Gold Coating

The cantilever arrays were coated with gold using several different methodologies. The first experiments were performed using cantilevers which were coated with gold by IBM during the fabrication process, with few positive results. In subsequent experiments bare silicon cantilevers were used, which were later evaporated or sputtered with gold. The bare silicon arrays allowed for better cleaning using piranha. In addition, the application of a silane layer for linking or blocking could be performed before the deposition of the gold layer. It was also anticipated that the improved cleaning and blocking procedures would help to reduce the buffer deflection, but unfortunately this was not the case. In addition to the single layer gold deposition methods, several arrays were evaporated with gold on both sides to reduce the rate of buffer deflection as will be discussed further in section 4.4.3.

Sputtering with chromium and gold was attempted as an alternative to evaporation to reduce the buffer deflection. There were multiple advantages to the sputtering machine over the evaporator including the ease of operation, increased accuracy of the coating thickness and speed of operation. One of the sputtered

arrays produced positive results (Figure 4.5), though the rate of deflection was less smooth and consistent than those of the evaporated cantilevers. The sputtered gold cantilevers also deflect in the opposite direction from the evaporated gold cantilevers during the buffer deflection. In addition, one of the experiments led to some interesting results concerning salt deposition on the cantilever surfaces and cantilever deflection. These results are discussed in section 4.4.2. Due to the decreased smoothness of the rate of cantilever deflection, lack of improvement concerning the buffer deflection of sputtered cantilevers and the better stress conduction inherent to evaporated surfaces, the majority of the experiments were performed with evaporated gold instead of sputtered gold.

#### 4.4.2 Buffers

Salt buildup on the cantilever surfaces was a major issue especially for longer incubation periods in the functionalization unit. This problem was only partially eliminated by sealing the functionalization unit and increasing the humidity during functionalization. The potential impact of the salt buildup on the cantilever deflection became evident from one of the sputtered cantilever experiments. Normal concentration PBS was used for this experiment. During the incubation in the functionalization unit salt deposits formed patterns on the gold surface of the cantilevers which were visible after the cantilevers were removed from the functionalization unit. The gold surfaces of cantilevers 2, 4, and 6 were covered in salt apart from a bare oval spot in the centre of each cantilever. The surfaces of cantilevers 3 and 5 had the greatest buildup of salt while 7 had less than 3 and 5 but more than 2, 4, and 6. The array was left in 10  $\mu\text{g/ml}$  INF- $\gamma$  in PBS overnight. When the array was removed from the Cantisens the bare oval spots on cantilevers 2, 4, and 6 were filled in with salt, while the salt concentration on cantilevers 1, 7, and 8 were mostly unchanged. This is interesting because the deflection of cantilevers 2, 4 and 6 were larger than those of the other cantilevers, as can be seen in Figure 4.15. It is important to note that the even cantilevers were blocked with ethanolamine and PEG-thiol while

cantilevers 1 and 3 were coated with cC-Ab and 5 and 7 were coated with hC-Ab. This means that the difference in deflection is not related to cantilever functionalization. This all indicates that salt buildup can significantly affect cantilever deflection.

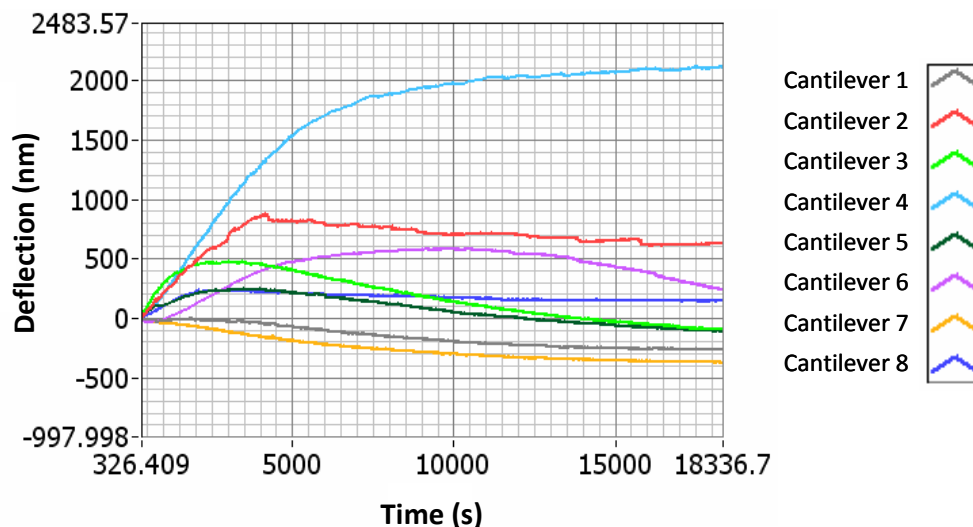


Figure 4.15: Effect of salt formation on cantilever deflection. The units of deflection and time were nanometers and seconds respectively. Open areas on cantilevers 2, 4 and 6 filled in with salt crystals overnight. Cantilevers 1 and 3 were coated with cC-Ab while cantilevers 5 and 7 were coated with hC-Ab. The remaining cantilevers were blocked with ethanolamine and PEG-thiol.

In order to reduce the deposition of salt on the cantilevers the NaCl concentration of all buffer solutions and the 2-(N-morpholino)ethanesulfonic acid concentration in the MES buffer were significantly reduced in the majority of the group I cantilever experiments. Unfortunately, decreased salt concentration also significantly increases the probability of non-specific protein interactions. Despite this, the best results were obtained with the lower NaCl concentration buffers.

Aside from the changes in buffer concentration, the only major change to the buffers was the use of reagent diluent for some of the INF- $\gamma$  samples. The vast majority of the INF- $\gamma$  tests were performed with INF- $\gamma$  in PBS instead of reagent diluent due to possible difficulties concerning BSA binding. [62] Despite these issues, several later arrays were tested with INF- $\gamma$  in reagent diluent in an effort to improve the results, but without success.

## 4.4.3 Cantilever Blocking

### 4.4.3.1 Backside Blocking

As mentioned earlier, preventing the proteins from binding nonspecifically to the cantilevers (also known as blocking the cantilevers) is critical for effective cantilever deflection measurements. For some deflection experiments, such as the adsorption of hydrocarbon-thiols on gold, blocking is less critical because thiols bind specifically to gold and not to silicon. Also, the reaction occurs relatively quickly over several minutes. Since the rate of deflection due to a nonspecific signal is relatively small, it has much less impact on a short measurement period. Proteins do not bind exclusively to the C-Ab or linker of interest, however, but often bind to a variety of surfaces like the silicon backside of cantilevers if they are left bare (section 3.4.3). Furthermore, if the capture protein does not adequately cover the active surface then the protein of interest can bind to any open spaces as well. This non-specific binding can significantly affect the deflection caused by the specific antibody antigen reaction.

Initially BSA was used to block the pre-evaporated gold cantilevers as was used in [28]. Unfortunately, since the BSA blocking step took place after the C-Ab step, C-Ab was left bound to the silicon backside of the cantilevers. While the results from the thermal PEG-silane tests were poorer than expected, it was preferable to BSA for blocking the cantilevers because it is resistant to the vacuum and increased temperature. This is important because to block the silicon backside of the cantilevers without contaminating the gold side the blocking procedure had to be completed before the evaporation procedure. The thermal PEG-silane procedure was used to block the silicon backside of the majority of the cantilever arrays used, including 9 of the experiments which led to group I results. The active surface was then evaporated with gold as seen in [74]. In the two glutaraldehyde experiments shown in Figures 4.11 and 4.12 the silanization process was performed after the gold was deposited on the cantilever surface and

a cysteamine monolayer was formed on the gold surface. The silanization process was performed after the evaporation procedure because the gold was peeling away from the cantilever surface when the silanization was performed first. The source of this problem was the deterioration of the PEG-silane over time and was solved when new PEG-silane was used.

PEG-thiol was the third method of blocking the cantilever backsides which was examined. The particular PEG-thiol used was shown to be effective for preventing protein adsorption in [82]. The PEG-thiol blocked arrays were first silanized with APTES to provide free amines on the silicon surfaces. Subsequently, one side was evaporated with gold and this gold surface was then blocked with PEG-thiol. This procedure was used in conjunction with glutaraldehyde to link the C-Abs to the surface to produce the data in Figures 4.9 and 4.10.

The other PEG-thiol blocking methodology used was demonstrated by Shu *et al.* [70] The backsides of the cantilevers were evaporated with gold and blocked with PEG-thiol. The other silicon surface was also evaporated with gold and the C-Abs were then linked to this surface. The advantage of this approach was that with both sides evaporated with gold, the cantilever deflection due to temperature and ionic conditions should be significantly reduced as compared to the single-side gold coated cantilevers. While the deflection due to temperature change decreased, the new maximum deflection was approximately 50% of the original deflection whereas in the published paper the deflection was roughly 1% of the original deflection. [70] Whether there was a decrease in the buffer deflection of the cantilevers was difficult to evaluate given the variation in buffer deflection in both the dual and single gold-coated array experiments. In addition, some very unusual behavior was observed during the cantilever deflection in the sample solution including sudden changes in the rate of deflection without any external cause and in some cases greater variation in buffer deflection than any of the single-side gold-coated arrays. Therefore, while PEG-thiol blocking was effective in Figures 4.9 and 4.10, the dual-side gold blocking method was ineffective as it resulted in undesirable cantilever deflection behavior.

#### 4.4.3.2 Reference Cantilever Blocking

The early reference cantilevers were blocked with 1% BSA and 0.05%  $\text{NaN}_3$  in PBS as was used in the ELISA kit. The active cantilevers were functionalized with hC-Ab and the entire array was then placed in the blocking solution. The  $\text{NaN}_3$  was soon removed from the blocking buffer because it can react strongly with gold. The use of BSA for blocking was discontinued because it may desorb from the cantilever surfaces, thus causing non-specific deflection leading to poor results as were seen in [62].

Later reference cantilevers were blocked with PEG-thiol and ethanolamine. Ethanolamine was used to block any remaining active linker sites after the C-Ab step while the PEG-thiol was used to fill in any remaining bare gold. These reference cantilevers showed few positive results and were discontinued in favour of cC-Ab. The best results were obtained from the reference cantilevers coated in cC-Ab, likely because it closely resembles hC-Ab in form. The similarity of the cC-Ab and hC-Ab deflection as opposed to that of the otherwise coated reference cantilevers was obvious in Figure 4.5A and similar experiments (data not shown). Successful results were also obtained by using  $\text{INF-}\gamma$  to block the reference cantilevers as shown in Figures 4.11 and 4.12.

#### 4.4.4 Linking Methods

In the ELISA and fluorescence sections, seven different linkers were examined for use in the cantilever experiments. Out of these seven linkers, five were tested in the search for methodology that would allow reproducible measurement of  $\text{INF-}\gamma$ . DSP was not tested after lack of positive results from the DSP-PEG experiments. In addition, biotin-streptavidin binding was tested using EZ-Link (Sulfo-NHS-LC-Biotin) to link the biotin to cysteamine on the gold surface.

The first cantilever experiments were performed using Protein A and Prolinker B. Prolinker B was selected because throughout the ELISA and fluorescence experiments it outperformed all the other linkers by a significant margin. Protein A was selected because it vertically orients the C-Abs, which should increase the number of active C-Abs on the cantilever surface and bring the bound INF- $\gamma$  molecules into closer proximity. This in turn should increase the stress caused by INF- $\gamma$  binding, thus increasing the sensitivity of the measurement. After a number of Protein A experiments, with one group I result (data not shown), the use of Protein A was discontinued. This was due to concerns about the linker building up in layers on the cantilever surface, the tendency to adsorb to silicon and the decrease in deflection seen in [75] for longer linkers. [87] The experiments with Protein A may also have been hampered, however, due to the relatively low INF- $\gamma$  concentrations which were used (in the range of 10 ng/ml to 500 ng/ml).

The experiments with Prolinker B produced more successful results. The majority of the Prolinker B experiments were performed with two hC-Ab coated active cantilevers, two cC-Ab coated reference cantilevers, and four other reference cantilevers. The other reference cantilevers were blocked with BSA, ethanolamine and/or PEG-thiol, and did not perform very well. While the majority of the group I classified results were produced using Prolinker B, it is likely that the group I classification was achieved more readily in most cases because only two active and two reference cantilevers were used. An advantage of simultaneously incubating the active and reference cantilevers is that it ensures that the active and reference cantilevers are functionalized under the same ambient conditions including humidity, temperature and airflow. The separate functionalization of the active and reference cantilevers in experiments with more than two active and two reference cantilevers was necessitated by the construction of the functionalization unit. Only four non-adjacent cantilevers could be functionalized at one time, which meant that in order to have adjacent active and reference cantilevers it was necessary to functionalize the active and reference cantilevers separately. The advantage of adjacent active and reference cantilevers

is that they should again experience similar ambient conditions, like temperature change and turbulence in the solution. This allows for a more accurate background subtraction when the reference cantilever deflection is subtracted from the cantilever deflection of the a neighboring active cantilever. Some of the experiments were performed with simultaneous functionalization of cC-Ab and hC-Ab cantilevers, but unfortunately, as only 4 cantilevers could be functionalized at a time there was still the possibility of discrepancy between the two sets of cantilevers which were functionalized at different times.

Despite the large number of group I classified Prolinker B results, the single best result was obtained using EDC and Sulfo-NHS to link the C-Abs to the aminated gold surface as shown in Figure 4.13. The reference and active cantilever signals separated immediately, and remained separate throughout the measurement period. Unfortunately, shortly after this experiment the occasional occurrence of gold peeling off the cantilever arrays became a perpetual issue. Initially it was believed that cleanliness was the cause of this issue but it was later determined that the aging PEG-silane was the cause of this problem as using new PEG-silane solved the issue. A consequence of the peeling problem was that a number of arrays needed to be reused. The result in Figure 4.13 therefore proved difficult to repeat precisely though an identically performed group II result favorably resembles it as seen in the side by side comparison in Figure 4.16. The similarity becomes particularly evident if the two outlying cantilever series from Figure 4.16B are excluded.

The third linker which led to a number of group I results was glutaraldehyde. This linker was tested using two different methods, firstly by linking to APTES on silicon while the gold backside was blocked with PEG-thiol (Figures 4.9 and 4.10) and secondly by linking to cysteamine on the gold side while the silicon backside was blocked with PEG-silane (Figures 4.11 and 4.12). The separation between the active and reference signals was inferior to that seen in Figure 4.13. Despite this, glutaraldehyde was the only linker which produced at least one group I result in each experiment. The procedure was still imperfect however, as the difference between the Figures 4.11 and 4.12 results demonstrates.

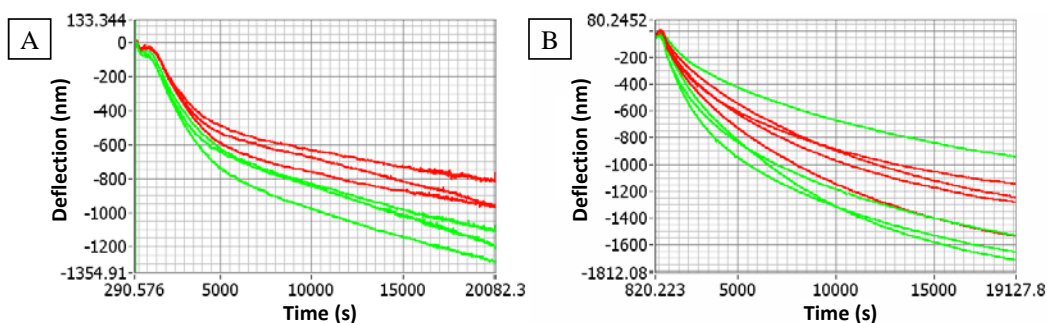


Figure 4.16: Comparison of two identical EDC/Sulfo-NHS linking experiments. The only EDC/Sulfo-NHS group I result is shown on the left while the best reproduction using the same procedure is shown on the right. The red series represent the reference cantilevers coated with cC-Ab and the series represent the active cantilevers coated in hC-Ab.

The last linker, DSP-PEG yielded quite poor results, which may have been caused by the dual-sided gold evaporation of the arrays with which it was tested. Due to these poor results DSP was not tested, as it is very similar to DSP-PEG.

#### 4.4.5 Temperature and Sequential Deflection

Single-side gold-coated cantilevers are sensitive to temperature change because of the difference in thermal expansion coefficient between the gold and silicon sides. Fortunately, the Cantisens temperature controller can regulate the temperature to within 0.01°C which means that the deflection due to temperature variation was effectively negligible. The temperature controller also proved valuable as a diagnostic tool to determine whether the array was diagonal in the measurement chamber. This was critical because improper positioning of the array can overshadow any other stress effects (Figure 4.17). A heat test of 10°C over 10 minutes was found to be sufficient to determine whether the cantilever signals fan out in the characteristic pattern in Figure 4.17, denoting that the array needs to be repositioned.

Nearly all the experiments, including those shown earlier, were performed at 20°C. It should be noted that the difficulties encountered regarding buffer deflection would be much less significant if the experiment took place over a

much shorter period of time. For this reason several experiments were performed at 37°C in an attempt to accelerate the antigen-antibody binding process, but without success.

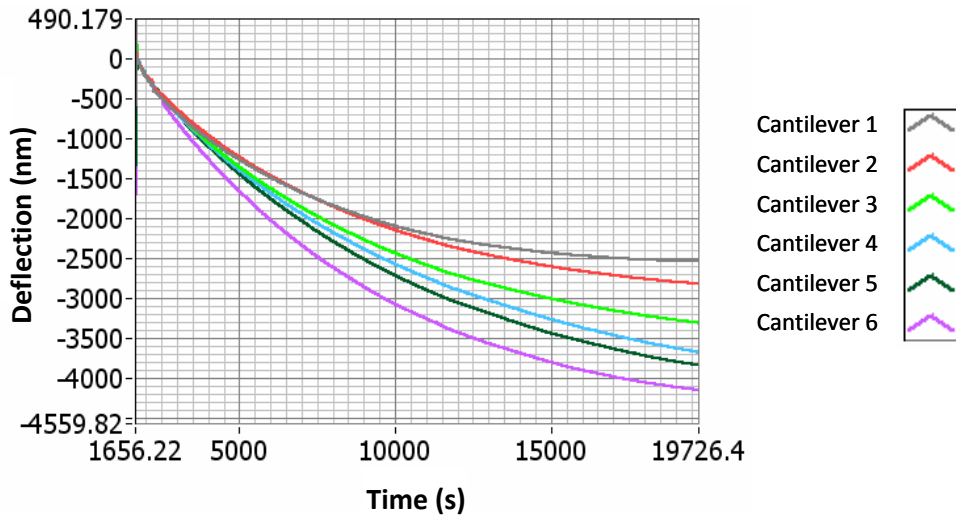


Figure 4.17: Cantilever signals depicting the sequential order of deflection which is caused by crookedness of the cantilever array in the cartridge or holder.

#### 4.4.6 INF- $\gamma$ Concentration

As mentioned above, the concentrations of INF- $\gamma$  used for the early experiments were relatively low, in the range of 1-100 ng/ml. This was mainly because the concentration of INF- $\gamma$  supplied with the ELISA kit was only 50 ng/ml and the review of cantilever detection indicated that detection at these levels should be possible. Few positive results were obtained at these concentrations, however, so the concentration was successively raised to 50 ng/ml, 500 ng/ml, and finally to 5 or 10  $\mu$ g/ml INF- $\gamma$ , which were the concentrations used in the majority of the experiments. Higher concentrations were determined to be unfeasible due to the high cost of the purified INF- $\gamma$ .

## 4.5 Summary

The major difficulty encountered in the cantilever experiments was the varying deflection of the cantilevers in buffer solution. Since the deflection in buffer solution was comparable to that in INF- $\gamma$  sample solution, it was challenging to extract useful information from the data. Also, in some of the data sets there was a distinct separation between the active and reference cantilever deflection in the buffer solution. Therefore simple background subtractions were tested to remove the buffer deflection from the cantilever signals. Simple background subtractions were selected mainly due to the lack of mathematical theory available for cantilever deflection, especially where proteins are concerned.

The cause of the varying deflection of the cantilevers in buffer solution was difficult to determine. Upon reflection, it is possible that the salt buildup seen on the cantilevers may be indicative of other patterns forming on the cantilever surface, including patterns of the C-Abs. During the fluorescence measurements some of the gold chips had larger particulates on the surface, but not to the same degree as was seen on the cantilevers after they were placed in the functionalization unit. It is possible that the random patterns formed by salt and C-Ab on the cantilever surfaces were responsible for the varying buffer deflection which was observed.

The varying deflection of cantilevers in buffer solutions has also been observed by other researchers. Yue *et al.* discussed this phenomenon in some detail, and refer to the cantilevers in the array as either tracking or non-tracking depending on whether there is any correlation between the deflections of the cantilevers in the array. [88] This paper was not discussed earlier because it deals primarily with the measurement of DNA strands as opposed to proteins. Also, the relative magnitude of the cantilever deflection of the non-tracking cantilevers reported here was greater than those seen in the paper. As mentioned earlier, Backmann *et al.* also discussed non-tracking cantilevers, and eliminated them using a heat test.[74]

On the whole, the background subtractions appear to be beneficial rather than detrimental as they improved a greater number of data sets. Percentage wise, the still linear background subtraction improved the greatest number of data sets followed by the flowing linear background subtraction and the logarithmic background subtraction. The ratio of improved data sets to detrimental data sets was the greatest for the flowing linear background subtraction, followed by the still linear background subtraction and logarithmic background subtraction. These results are somewhat skewed, however, as the logarithmic background subtraction was inapplicable in a large number of cases either due to insufficient data or poor data for fitting. Regardless, all three methods proved to be more advantageous than detrimental, which suggests that background subtractions are worth pursuing.

It is difficult to make any conclusive determination of linker and blocker reliability based purely on the magnitude of deflection. This is due to a number of factors. Firstly, despite the improvements made by the background subtractions, the buffer deflection was not removed perfectly. This is particularly evident in the linear still buffer background subtractions which substantially skew the deflection results. Two more serious issues concerning the magnitude of deflection are related to the Cantisens system itself. Firstly, the crookedness of the array can greatly impact the deflection results, to the point where it overshadows all other effects. Secondly, the system requires the laser spot to be manually centered on exactly the same location on the cantilever tip for each experiment. It is unreasonable to expect that this can be accomplished with sufficient precision to allow reproducible magnitude measurements from one experiment to the next. For these reasons the categorization system was used to evaluate the effectiveness of the linking and blocking procedures.

With respect to the blocking methodologies, the PEG-silane and single-sided gold PEG-thiol blocked cantilevers performed well, while the BSA and dual-side gold PEG-thiol blocking procedures produced poor results. In addition, the cC-Ab coated reference cantilevers were more effective than the other reference cantilever coating methods examined, including ethanolamine, PEG-thiol, and/or BSA.

Evaluating the efficacy of the different linking methods used is a more challenging task. The least successful linker results were produced with PEG-DSP, though the dual-sided gold PEG-thiol blocking may also have been the cause of these poor results. The Protein A linker led to few positive results, and it was discontinued because multiple layers of Protein A may form on surfaces, and because longer linkers likely lead to reduced stress conduction. It is possible that blocking the backsides of the cantilevers with PEG-silane and increasing the concentration of the INF- $\gamma$  sample would lead to better results.

The other three linkers that were tested were all relatively successful. Ten out of sixteen experiments with group I results were produced with Prolinker B including those shown in Figures 4.4 – 4.8. Unfortunately, the majority of the array only had two active and two reference cantilevers which skews the data because two pairs more readily show distinct separation than three or four pairs. All the glutaraldehyde-coated cantilever arrays resulted in at least one group I result. This was true for both the PEG-thiol blocked APTES silanized arrays in Figures 4.9 and 4.10 and the PEG-silane blocked cysteamine arrays in Figures 4.11 and 4.12. The experiment where the EDC/Sulfo-NHS linking method was first used produced the best result out of any of the cantilever experiments that were performed aside from the biotin-steptavidin experiment shown in Figure 4.13. This linking method did not lead to any further group I results however, even after a number of repetitions. The closest reproduction of this data is shown in Figure 4.16B and was classified as group II data. Despite this, the linking procedure shows promise due to the excellent initial results and the possibility of reproducing them relatively accurately. In summary, the most group I results were produced using Prolinker B, the most reliable linker was gluteraldehyde, as it consistently produced group I results, and the best results were produced using the EDC/Sulfo-NHS linking method.

## Chapter 5

### Summary and Recommendations

The goal of this project was to develop a methodology that would allow for reliable and accurate measurement of multiple proteins using individual cantilever arrays. In the interest of developing a methodology which is applicable to a wide range of proteins, antibodies were selected to bind the proteins to the surface. INF- $\gamma$  was selected as a test protein, and to ensure a good match between the INF- $\gamma$  and the anti INF- $\gamma$  antibodies an ELISA kit was used. The developmental approach was twofold. Firstly the functionalization materials and conditions were investigated through fluorescent antibodies and ELISA. This included various linking and blocking procedures, incubation solutions and antibody concentrations. Secondly, the best procedures were implemented on the cantilever arrays to measure INF- $\gamma$ .

The fluorescence and ELISA experiments were all performed with 5x7 mm silicon chips, most of which were coated with gold. Initial fluorescence experiments were performed with the ELISA reagents and fluorescently labeled streptavidin. The resultant fluorescence was very weak so it was difficult to see the separation between the active and control chips. Alexa fluor labeled antibodies were purchased in order to increase the fluorescence intensity. Two antibodies, specific to rabbit C-Ab and human INF- $\gamma$  respectively, were selected in order to separately image the C-Ab and INF- $\gamma$  on the surface of the chips. Unfortunately the fluorescence intensity was still very low, and visually there was little difference between the active and control signals. This was likely due to the quenching that metal surfaces have on fluorophores. In order to extract useful information from the images the numerical pixel values of the representative images were compared. This is a valid approach since the pixel values were linearly related to the fluorescent intensity. The difference between the active and

control chip pixel summations was used to determine the effectiveness of the linkers at linking the C-Ab to the surface and the efficiency of INF- $\gamma$  capture by the C-Ab linked to the surface.

The effectiveness of the six linkers Prolinker B, Protein A, EDC/Sulfo-NHS, DSP, DSP-PEG, and glutaraldehyde was examined with each antibody. In each case the difference between the active and control chips was positive, which means that each linker can successfully link the C-Ab to the surface, and the linked C-Ab can bind the INF- $\gamma$ . In the examination of C-Ab density the Prolinker B and Protein A performed substantially better than the other linkers. In the examination of the captured INF- $\gamma$  density the Prolinker B again outperformed all the other linkers, followed by the DSP-PEG and Protein A. It was also deduced that increased C-Ab substantially increases INF- $\gamma$  capture, as was expected.

As mentioned earlier, the intensity of the fluorescent antibodies was substantially reduced by fluorescent quenching. In order to amplify the signal, the fluorescent antibodies could be replaced by ELISAs with a precipitating fluorescent substrate. The HRP-streptavidin in the INF- $\gamma$  measurements could be replaced by alkaline phosphatase-streptavidin, and the colorimetric solution could be replaced by the alkaline phosphatase substrate in the ELF 97 Immunohistochemistry Kit from Invitrogen. Similarly, the C-Ab measurements could be performed with an alkaline phosphatase linked anti-rabbit antibody and the same alkaline phosphatase substrate from the ELF 97 Immunohistochemistry Kit. These changes should sufficiently amplify the fluorescent intensity to allow visual inspection of the C-Ab and INF- $\gamma$  on the surface and should improve the fluorescent intensity difference between the active and control chips.

The first set of ELISA experiments were performed with Protein A and Prolinker B, as they were determined to be the best options for the cantilever measurements. A number of different conditions were examined. It was found that the solvent used for the Prolinker linking step did not substantially affect the effectiveness of the linkers. Also, the quantity of INF- $\gamma$  captured with Prolinker B was found to be equal or greater than that of Prolinker A. Therefore Prolinker B in chloroform was used in further experiments.

The effects of the Protein A and C-Ab concentrations on the quantity of INF- $\gamma$  capture were examined. The results showed that between 25  $\mu\text{g/ml}$  and 200  $\mu\text{g/ml}$  C-Ab, doubling the C-Ab concentration roughly doubles the quantity of INF- $\gamma$  captured. A similar trend was seen with Protein A concentration, but this was likely due to nonspecific binding to Protein A. The binding of the ELISA proteins directly to Protein A and the gold surface was a common trend throughout these experiments. This meant that BSA was relatively unsuccessful at blocking Protein A. Another issue was the adhesion of proteins to the silicon backside of the one-side gold-coated chips. Fortunately, the silicon signals were sufficiently smaller than the gold signals that the resultant conclusions were unaffected, but this does emphasize the importance of blocking the backside of cantilevers.

The second set of ELISA experiments was performed to examine the effectiveness of all the linkers and blocking procedures. In order to better perform this evaluation, a number of changes were made to the ELISA procedure. Firstly, the chips were coated on both sides with gold to prevent nonspecific binding of proteins to the silicon backside. Secondly, each linker experiment was performed using a standard curve in order to evaluate the linearity of the results for each linker. Thirdly, the ELISA from the C-Ab step to the HRP-streptavidin step was performed in the same set of wells in a 96-well plate to increase the reliability of the experiments. When the chips were removed for the colorimetric reaction these empty wells also provided a convenient control to confirm that the ELISA was performed correctly thus ensuring that any variance in the chip standard curves are due to the linking procedure.

The DSP and glutaraldehyde linkers both performed well, with reasonable linearity and little nonspecific binding. The DSP-PEG linker did not produce very good results. Although it produced the lowest nonspecific binding signal out of all the signals, there was a significant variation between the two series in both the individual and simultaneous linker experiments. Both Protein A and EDC/Sulfo-NHS did not perform very well either due to substantial amounts of nonspecific binding. This was at least partially due to the low C-Ab concentration used for the

linking comparison. In addition, neither produced very linear results. By far the best results were obtained with Prolinker B. The results were nearly identical, linear, and had the second lowest rate of nonspecific binding after the DSP-PEG. Also, it produced the only results which were greater than those of the empty control wells.

The blocking experiments were performed with DSP and Prolinker B respectively. Four blockers were examined: cC-Ab, BSA, PEG-thiol and PEG-silane. The cC-Ab performed well in both experiments, especially in the Prolinker B experiment. The BSA also performed well in the first experiment, though the second experiment showed that the amount nonspecific binding prevented by BSA on the gold surface is low or negligible. The PEG-thiol also performed well in both experiments, though considerable binding took place despite the PEG on the surface. This was particularly evident in the Prolinker B experiment where the PEG blocking step was performed before the linking step. The plain silane did not perform well. Substantial binding occurred in the DSP experiment and the blocking was very poor in the Prolinker B experiment. The thermal silanization method, which was recommended by the producer of the silane, led to substantially better results, though it was less effective than the PEG-thiol at the lower INF- $\gamma$  concentrations.

There are a number of recommendations that result from the ELISA experiments. Firstly, when designing experiments which include linkers and proteins, it is important to recognize that they will likely adhere to any surface despite the use of blocking methods. This is why dual-side coated gold chips are preferable over blocking the backside of silicon chips. Also, proteins frequently bind to other proteins as well, so it is important to examine how the component proteins interact. Overall, from both the fluorescent and ELISA experiments, Prolinker B is recommended as the best linker on gold surfaces by a significant margin. Also, cC-Ab performed well as a control molecule for the hC-Ab, especially in conjunction with Prolinker B. As for the blocking molecules, the thermal PEG-silanization procedure and PEG-thiol were both quite effective at reducing the adhesion of molecules to silicon and gold surfaces respectively.

The goal of the deflection cantilever array experiments was to develop a procedure to reliably and reproducibly measure INF- $\gamma$  concentration with commercially available components. This procedure could then be readily altered to measure many different proteins. There were numerous impediments to overcome, but the most significant issue was that the cantilevers do not deflect equally in buffer solution, and that the magnitude of this deflection was similar to the deflection produced by the specific INF- $\gamma$  C-Ab interaction. This made it challenging to produce results with consistent separation between the active and reference cantilever signals, let alone reproducible measurement of INF- $\gamma$ . Equilibration in buffer solution and elimination of the nontracking cantilevers through a heat test were attempted in order to reduce the problem, though without much success.

Instead of the equilibration and heat test methods, three background subtractions were tested to reduce the background deflection of the cantilevers. Two of the background subtractions were linear fits, and were performed during a still and flowing buffer period respectively. The linear background subtraction was a reasonable fit for the deflection in flowing buffer since the sample intake occurred immediately afterwards, and was relatively brief. For the still buffer background subtraction, the linear fit was less accurate, and a logarithmic fit was tested as it better reflects the deflection of the cantilevers in buffer solution.

In order to organize the data, the results were categorized into three groups based on the separation between the active and control cantilever series. The group I, group II and group III results are those where there is separation between all, the majority and less than the majority of the active and reference cantilevers over the greater part of the time period examined. The effectiveness of the background subtractions was based on whether the classification of the data was improved, unchanged or worsened following the subtraction. By percentage of the total number of data sets analyzed, the linear still background subtraction had the greatest rate of improvement, followed by the linear flowing background subtraction and the logarithmic background subtraction. The linear still background subtraction also had the greatest detrimental effect on the data

however, followed by the logarithmic and linear flowing background subtractions. Also, since the linear still background subtraction was a relatively poor fit to the background deflection curve, the linear flowing background subtraction was the most effective method tested.

Five linkers were used in the cantilever deflection experiments and three produced positive results. The Prolinker B linker produced the greatest number of group I results out of all the linkers, though most of these experiments were performed with only two active and reference cantilevers. The EDC/Sulfo-NHS linking procedure produced the best group I result out of all the INF- $\gamma$  experiments, but the result was irreproducible despite numerous attempts. The glutaraldehyde linker was the most reliable linker, as each experiment resulted in at least one group I result. Also, EZ-link was used to detect streptavidin, though as with the EDC-Sulfo/NHS, the positive results proved difficult to reproduce. The majority of the blocking methods tested led to positive results. The thermal silanization procedure was used in the majority of the group I results while PEG-thiol blocking of the gold backside was used successfully in two of the glutaraldehyde experiments.

There are a number of avenues which could be explored to improve the cantilever measurements. The most critical changes involve decreasing or eliminating the divergent deflection of the cantilevers in buffer solution. Firstly, the functionalization should be designed so that all the cantilevers can be functionalized simultaneously. This will ensure that environmental conditions affect all the functionalized cantilevers equally. Secondly, to prevent deposits or patterns from forming on the cantilever surfaces, the functionalization process must be refined. Improvements could be made by decreasing the functionalization time or modifying the functionalization solution in order to decrease evaporation. This would not solve the patterns which may form in a still solution. The best solution would be to design a new functionalization unit which allows the fluid to flow across the surface of the individual cantilevers, decreasing evaporation and the formation of patterns on the cantilever surfaces. Thirdly, increasing the maximum sample volume intake above 500  $\mu$ l would allow for a longer sample

intake, which would increase the rate of protein binding. This in turn would increase the rate of specific deflection due to the protein of interest, reducing the impact of the nonspecific deflection.

The next set of recommendations relate to the reproducibility of the experiments. Firstly, the Cantisens machine is not ideal for cantilever deflection measurements as the laser spot must be centered in exactly the same location on each cantilever for each measurement to provide reproducible results, something which with the current setup is very difficult to achieve. For this reason, modifications such as a position sensor for arrays in the Cantisens machine, or a different machine which allows for more reliable deflection measurements is recommended. Secondly, the cantilever measurements are very sensitive to the conditions, and small variations when using the same procedure can significantly impact the results. From the experiments which were performed and the literature review, it seems that reproducible measurement of proteins with cantilevers is the most feasible when multiple cantilevers are used to perform the measurement of a single protein. Therefore, while a measurement array with eight cantilevers may be sufficient to accurately measure a single protein, multiple arrays or arrays with many more cantilevers should be used to measure multiple proteins simultaneously. [62]

The final recommendations concern the chemistry used to link the C-Ab to the arrays and to block the arrays. The PEG-silane is recommended to block the silicon backside of cantilever arrays, but it is critical that the PEG-silane is fresh. Also, it is recommended that an antibody that is inert to the protein of interest is used as a control for the active antibody because other molecules like BSA and ethanolamine do not accurately reflect the behavior of an antibody due to environmental conditions. Regarding the linking procedures, Prolinker B is recommended for future experiments given the quality and reproducibility of the fluorescence, ELISA and cantilever data.

## References

- [1] Mattsson N, Zetterberg H, Hansson O, Andreasen N, Parnetti L, Jonsson M, *et al.* CSF Biomarkers and Incipient Alzheimer Disease in Patients With Mild Cognitive Impairment. *JAMA* 2009 Jul 22;302(4):385-93.
- [2] Diniz BS, Pinto Junior JA, Forlenza OV. Do CSF total tau, phosphorylated tau, and  $\beta$ -amyloid 42 help to predict progression of mild cognitive impairment to Alzheimer's disease? A systematic review and meta-analysis of the literature. *World Journal of Biological Psychiatry* 2008;9(3):172-82.
- [3] Hansson O, Zetterberg H, Buchhave P, Londos E, Blennow K, Minthon L. Association between CSF biomarkers and incipient Alzheimer's disease in patients with mild cognitive impairment: a follow-up study. *Lancet Neurology* 2006 Mar;5(3):228-34.
- [4] Blennow K. Cerebrospinal Fluid Protein Biomarkers for Alzheimer's Disease. *NeuroRx* 2004 Apr;1(2):213-25.
- [5] Weaver CT, Harrington LE, Mangan PR, Gavrieli M, Murphy KM. Th17: An Effector CD4 T Cell Lineage with Regulatory T Cell Ties. *Immunity* 2006 Jun;24(6):677-88.
- [6] Ishizu T, Osoegawa M, Mei FJ, Kikuchi H, Tanaka M, Takakura Y, *et al.* Intrathecal activation of the IL-17/IL-8 axis in opticospinal multiple sclerosis. *Brain* 2005 May;128(Pt 5):988-1002.
- [7] Karni A, Koldzic DN, Bharanidharan P, Khoury SJ, Weiner HL. IL-18 is linked to raised IFN-gamma in multiple sclerosis and is induced by activated CD4(+) T cells via CD40-CD40 ligand interactions. *Journal of Neuroimmunology* 2002 Apr;125(1-2):134-40.
- [8] Yamaoka-Tojo M, Tojo T, Wakaume K, Kameda R, Nemoto S, Takahira N, *et al.* Circulating interleukin-18: A specific biomarker for atherosclerosis-prone patients with metabolic syndrome. *Nutrition & Metabolism* 2011;8:3.

- [9] Yang L, Zhang Z, Sun D, Xu Z, Zhang X, Li L. The serum interleukin-18 is a potential marker for development of post-stroke depression. *Neurological Research* 2010 May;32(4):340-6.
- [10] Ajdukovic J, Tonkic A, Salamunic I, Hozo I, Simunic M, Bonacin D. Interleukins IL-33 and IL-17/IL-17A in patients with ulcerative colitis. *Hepato-Gastroenterology* 2010 Nov-Dec;57(104):1442-4.
- [11] Wu HP, Chen CY, Kuo IT, Wu YK, Fu YC. Diagnostic Values of a Single Serum Biomarker at Different Time Points Compared with Alvarado Score and Imaging Examinations in Pediatric Appendicitis. *Journal of Surgical Research*, 2011.
- [12] 2004 Global Immunization Data. [Webpage] 2005 [cited April 5, 2011]; Available from: <http://www.who.int/mediacentre/factsheets/fs288/en/index.html>.
- [13] Amanna IJ, Slifka MK. Wanted, dead or alive: new viral vaccines. *Antiviral research* 2009 Nov;84(2):119-30.
- [14] Amanna IJ, Slifka MK. Contributions of humoral and cellular immunity to vaccine-induced protection in humans. *Virology* 2011 Mar 15;411(2):206-15.
- [15] ELISA Kits. [cited April 5, 2011]; Available from: <http://www.rapidtest.com/products-elisakits.html>
- [16] Leca-Bouvier B, Blum LJ. Biosensors for Protein Detection: A Review. *Analytical Letters* 2005;38:1491-1517.
- [17] Lange K, Rapp BE, Rapp M. Surface acoustic wave biosensors: a review. *Analytical and Bioanalytical Chemistry* 2008 Jul;391(5):1509-19.
- [18] Schmid JH, Sinclair W, Garcia J, Janz S, Lapointe J, Poitras D, *et al.* Silicon-on-insulator guided mode resonant grating for evanescent field molecular sensing. *Optics Express* 2009 Sep 28;17(20):18371-80.
- [19] Chua JH, Chee RE, Agarwal A, Wong SM, Zhang GJ. Label-Free Electrical Detection of Cardiac Biomarker with Complementary Metal-Oxide Semiconductor-Compatible Silicon Nanowire Sensor Arrays. *Analytical Chemistry* 2009 Aug 1;81(15):6266-71.
- [20] Patolsky F, Zheng G, Lieber CM. Nanowire sensors for medicine and the life sciences. *Nanomedicine (London, England)* 2006 Jun;1(1):51-65.

- [21] Hooper IR, Rooth M, Sambles JR. Dual-channel differential surface plasmon ellipsometry for bio-chemical sensing. *Biosensors & Bioelectronics* 2009 Oct 15;25(2):411-7.
- [22] Hoffmann C, Schmitt K, Brandenburg A, Hartmann S. Rapid protein expression analysis with an interferometric biosensor for monitoring protein production. *Analytical and Bioanalytical Chemistry* 2007 Mar;387(5):1921-32.
- [23] Ellington AA, Kullo IJ, Bailey KR, Klee GG. Antibody-Based Protein Multiplex Platforms: Technical and Operational Challenges. *Clinical Chemistry* 2010;56(2):186-93.
- [24] Berg P, Zaghoul M, Tigli O, inventors; Multiplex Biosensor. United States. 2009.
- [25] Arruda DL, Wilson WC, Nguyen C, Yao QW, Caiazzo RJ, Talpasanu I, *et al.* Microelectrical sensors as emerging platforms for protein biomarker detection in point-of-care diagnostics. *Expert Review of Molecular Diagnostics* 2009 Oct;9(7):749-55.
- [26] Lee SY, Amsden JJ, Boriskina SV, Gopinath A, Mitropolous A, Kaplan DL, *et al.* Spatial and spectral detection of protein monolayers with deterministic aperiodic arrays of metal nanoparticles. *Proceedings of the National Academy of Sciences of the United States of America* Jul 6;107(27):12086-90.
- [27] Jenison R, La H, Haeberli A, Ostroff R, Polisky B. Silicon-based Biosensors for Rapid Detection of Protein or Nucleic Acid Targets. *Clinical Chemistry* 2001 Oct;47(10):1894-900.
- [28] Arntz Y, Seelig JD, Lang HP, Zhang J, Hunziker P, Ramseyer JP, *et al.* Label-free protein assay based on a nanomechanical cantilever array. *Nanotechnology* 2003 January 2003;14:86-90.
- [29] Ilic B, Yang Y, Aubin K, Reichenbach R, Krylov S, Craighead HG. Enumeration of DNA molecules bound to a nanomechanical oscillator. *Nano Letters* 2005 May;5(5):925-9.
- [30] Wu G, Datar RH, Hansen KM, Thundat T, Cote RJ, Majumdar A. Bioassay of prostate-specific antigen (PSA) using microcantilevers. *Nature Biotechnology* 2001 Sep;19(9):856-60.

- [31] Lequin RM. Enzyme Immunoassay (EIA)/Enzyme-Linked Immunosorbent Assay (ELISA). *Clinical Chemistry* 2005 Dec;51(12):2415-8.
- [32] Crowther JR. The ELISA Guidebook. *Methods in Molecular Biology* Clifton, NJ 2000;149:III-IV, 1-413.
- [33] *Fluorescence Imaging Principles and Methods*. Amersham Biosciences, 2002.
- [34] Legendplex Custom Luminex xMAP Multiplex Assays. [cited April 5, 2011]; Available from: <http://www.biosite.se/uploads/BioLegend/LEGENDplex.pdf>
- [35] Liew M, Groll MC, Thompson JE, Call SL, Moser JE, Hoopes JD, *et al*. Validating a custom multiplex ELISA against individual commercial immunoassays using clinical samples. *BioTechniques* 2007 Mar;42(3):327-8, 30-3.
- [36] Burkhardt M, LopezAcosta A, Reiter K, Lopez V, Lees A. Purification of soluble CD14 fusion proteins and use in an electrochemiluminescent assay for lipopolysaccharide binding. *Protein Expression and Purification* 2007 Jan;51(1):96-101.
- [37] Binnig G, Quate CF, Gerber C. Atomic Force Microscope. *Physical Review Letters* 1986 Mar 3;56(9):930-3.
- [38] Barattin R, Voyer N. Chemical modifications of AFM tips for the study of molecular recognition events. *Chemical Communications (Cambridge, England)* 2008 Apr 7(13):1513-32.
- [39] Waggoner PS, Craighead HG. Micro- and nanomechanical sensors for environmental, chemical, and biological detection. *Lab on a Chip* 2007 Oct;7(10):1238-55.
- [40] Bashir R, Hilt JZ, Elibol O, Gupta A, Peppas NA. Micromechanical cantilever as an ultrasensitive pH microsensor. *Applied Physics Letters* 2002;81(16):3091-3.
- [41] Dauksaite V, Lorentzen, M., Besenbacher, F., Kjems, J. Antibody-based protein detection using piezoresistive cantilever arrays. *Nanotechnology* 2007;18:125503-7.

- [42] Davila AP, Jang J, Gupta AK, Walter T, Aronson A, Bashir R. Microresonator mass sensors for detection of *Bacillus anthracis* Sterne spores in air and water. *Biosensors & Bioelectronics* 2007 Jun 15;22(12):3028-35.
- [43] Huber F, Hegner M, Gerber C, Guntherodt HJ, Lang HP. Label free analysis of transcription factors using microcantilever arrays. *Biosensors & Bioelectronics* 2006 Feb 15;21(8):1599-605.
- [44] Lai J, Perazzo T, Shi Z, Majumdar A. Optimization and performance of high-resolution micro-optomechanical thermal sensors. *Sensors and Actuators A: Physical* 1997;58(2):113-9.
- [45] Nugaeva N, Gfeller KY, Backmann N, Lang HP, Duggelin M, Hegner M. Micromechanical cantilever array sensors for selective fungal immobilization and fast growth detection. *Biosensors & Bioelectronics* 2005 Dec 15;21(6):849-56.
- [46] Seo H, Jung S, Jeon S. Detection of formaldehyde vapor using mercaptophenol-coated piezoresistive cantilevers. *Sensors and Actuators B: Chemical* 2007;126(2):522-6.
- [47] Stoney GG. The Tension of Metallic Films deposited by Electrolysis. *Proceedings of the Royal Society of London Series A* 1909;32:172–5.
- [48] Velanki S, Ji H. Detection of feline coronavirus using microcantilever sensors. *Measurement Science and Technology* 2006;17(11):2964-8.
- [49] Yi JW, Shih WY, Mutharasan R, Shih WH. In situ cell detection using piezoelectric lead zirconate titanate-stainless steel cantilevers. *Journal of Applied Physics Letters* 2003;93(1):619-25.
- [50] Miyatani T, Fujihira M. Calibration of surface stress measurements with atomic force microscopy. *Journal of Applied Physics Letters* 1997;81(11):7099–115.
- [51] Shekhawat G, Tark SH, Dravid VP. MOSFET-Embedded microcantilevers for measuring deflection in biomolecular sensors. *Science* 2006 Mar 17;311(5767):1592-5.
- [52] Calleja M, Nordstrom M, Alvarez M, Tamayo J, Lechuga LM, Boisen A. Highly sensitive polymer-based cantilever-sensors for DNA detection. *Ultramicroscopy* 2005 Nov;105(1-4):215-22.

- [53] Tang Y, Fang J, Yan X, Ji H-F. Fabrication and characterization of SiO<sub>2</sub> microcantilever for microsensor application. *Sensors and Actuators B* 2004;97:109–13.
- [54] Berger R, Delamarche E, Lang HP, Gerber C, Gimzewski JK, Meyer E, et al. Surface Stress in the Self-Assembly of Alkanethiols on Gold. *Science* 1997;276(5321):2021-4.
- [55] Fritz J, Baller MK, Lang HP, Rothuizen H, Vettiger P, Meyer E, et al. Translating biomolecular recognition into nanomechanics. *Science* 2000 Apr 14;288(5464):316-8.
- [56] Wu G, Ji HF, Hansen K, Thundat T, Datar R, Cote R, et al. Origin of nanomechanical cantilever motion generated from biomolecular interactions. *Proceedings of the National Academy of Sciences* 2001;98:1560-4.
- [57] McKendry R, Zhang J, Arntz Y, Strunz T, Hegner M, Lang HP, et al. Multiple label-free biodetection and quantitative DNA-binding assays on a nanomechanical cantilever array. *Proceedings of the National Academy of Sciences of the United States of America* 2002 Jul 23;99(15):9783-8.
- [58] Weaver Jr. W, Timoshenko SP, Young DH. *Vibration Problems in Engineering*. 5 ed. New York: Wiley-Interscience, 1990.
- [59] Hwang KS, Lee JH, Park J, Yoon DS, Park JH, Kim TS. In-situ quantitative analysis of a prostate-specific antigen (PSA) using a nanomechanical PZT cantilever. *Lab on a Chip* 2004 Dec;4(6):547-52.
- [60] Lee JH, Hwang KS, Park J, Yoon KH, Yoon DS, Kim TS. Immunoassay of prostate-specific antigen (PSA) using resonant frequency shift of piezoelectric nanomechanical microcantilever. *Biosensors & Bioelectronics* 2005 Apr 15;20(10):2157-62.
- [61] Wee KW, Kang GY, Park J, Kang JY, Yoon DS, Park JH, et al. Novel electrical detection of label-free disease marker proteins using piezoresistive self-sensing micro-cantilevers. *Biosensors & Bioelectronics* 2005 Apr 15;20(10):1932-8.

- [62] Yue M, Stachowiak JC, Lin H, Datar R, Cote R, Majumdar A. Label-Free Protein Recognition Two-Dimensional Array Using Nanomechanical Sensors. *Nano Letters* 2008 Feb;8(2):520-4.
- [63] Chen CH, Hwang RZ, Huang LS, Lin SM, Chen HC, Yang YC, *et al.* A Wireless Bio-MEMS Sensor for C-Reactive Protein Detection Based on Nanomechanics. *IEEE Transactions on Biomedical Engineering* 2009 Feb;56(2):462-70.
- [64] Milburn C, Zhou J, Bravo O, Kumar C, Soboyejo WO. Sensing Interactions Between Vimentin Antibodies and Antigens for Early Cancer Detection *Journal of Biomedical Nanotechnology* 2005 March 2005;1(1):9.
- [65] Grogan C, Raiteri R, O'Connor GM, Glynn TJ, Cunningham V, Kane M, *et al.* Characterisation of an antibody coated microcantilever as a potential immuno-based biosensor. *Biosensors & Bioelectronics* 2002 Mar;17(3):201-7.
- [66] Amritsar J, Stiharu I, Packirisamy M. Bioenzymatic detection of troponin C using micro-opto-electro-mechanical systems. *Journal of Biomedical Optics* 2006 Mar-Apr;11(2):021010.
- [67] Knowles TPJ, Shu W, Huber F, Lang HP, Gerber C, Dobson C, *et al.* Label-free detection of amyloid growth with microcantilever sensors. *Nanotechnology* 2008;19(38):384007-38411.
- [68] Montserrat Calleja JT, Maria Nordström, and Anja Boisen. Low-noise polymeric nanomechanical biosensors. *Applied Physics Letters* 2006;88(11):3.
- [69] Mukhopadhyay R, Sumbayev VV, Lorentzen M, Kjems J, Andreasen PA, Besenbacher F. Cantilever sensor for nanomechanical detection of specific protein conformations. *Nano Letters* 2005 Dec;5(12):2385-8.
- [70] Shu W, Laurenson S, Knowles TP, Ko Ferrigno P, Seshia AA. Highly specific label-free protein detection from lysed cells using internally referenced microcantilever sensors. *Biosensors & Bioelectronics* 2008 Oct 15;24(2):233-7.
- [71] Savran CA, Knudsen SM, Ellington AD, Manalis SR. Micromechanical Detection of Proteins Using Aptamer-Based Receptor Molecules. *Analytical Chemistry* 2004 Jun 1;76(11):3194-8.

- [72] Yen Y-K, Huang C-Y, Chen C-H, Hung C-M, Wu K-C, Lee C-K, et al. A novel, electrically protein-manipulated microcantilever biosensor for enhancement of capture antibody immobilization. *Sensors and Actuators B: Chemical* 2009;141:498-505.
- [73] Lam Y, Abu-Lail NI, Alam MS, Zauscher S. Using microcantilever deflection to detect HIV-1 envelope glycoprotein gp120. *Nanomedicine* 2006 Dec;2(4):222-9.
- [74] Backmann N, Zahnd C, Huber F, Bietsch A, Pluckthun A, Lang HP, et al. A label-free immunosensor array using single-chain antibody fragments. *Proceedings of the National Academy of Sciences of the United States of America* 2005 Oct 11;102(41):14587-92.
- [75] Shu W, Laue ED, Seshia AA. Investigation of biotin-streptavidin binding interactions using microcantilever sensors. *Biosensors & Bioelectronics* 2007 Apr 15;22(9-10):2003-9.
- [76] Dutta P, Sanseverino J, Datskos PG, Sepaniak MJ. Nanostructured Cantilevers as Nanomechanical Immunosensors for Cytokine Detection. *NanoBiotechnology* 2005;1(3):237-44.
- [77] Moulin AM, O'Shea SJ, Badley RA, Doyle P, Welland ME. Measuring Surface-Induced Conformational Changes in Proteins. *Langmuir* 1999;15:8776-9.
- [78] Lee Y, Lee EK, Cho YW, Matsui T, Kang IC, Kim TS, et al. ProteoChip: a highly sensitive protein microarray prepared by a novel method of protein immobilization for application of protein-protein interaction studies. *Proteomics* 2003 Dec;3(12):2289-304.
- [79] Oh SW, Moon JD, Lim HJ, Park SY, Kim T, Park J, et al. Calixarene derivative as a tool for highly sensitive detection and oriented immobilization of proteins in a microarray format through noncovalent molecular interaction. *The FASEB Journal express article* 2005;10.1096/fj.04-2098fje
- [80] Wang Z, Jin G. Feasibility of protein A for the oriented immobilization of immunoglobulin on silicon surface for a biosensor with imaging ellipsometry *Journal of Biochemical and Biophysical Methods* 2003;57(3):203-11

- [81] Gizeli E, Bender F, Rasmusson A, Saha K, Josse F, Cernosek R. Sensitivity of the acoustic waveguide biosensor to protein binding as a function of the waveguide properties. *Biosensors and Bioelectronics* 2003;18:1399-406.
- [82] Reimhult K, Petersson K, Krozer A. QCM-D analysis of the performance of blocking agents on gold and polystyrene surfaces. *Langmuir* 2008 Aug 19;24(16):8695-700.
- [83] human IFN- $\gamma$  Catalog Number: DY285. [cited February 10, 2011]; Available from: <http://www.rndsystems.com/pdf/dy285.pdf>
- [84] Mangeat T, Berthier A, Elie-Caille C, Perrin M, Boireau W, Pieralli C, et al. Gold/Silica biochips: Applications to Surface Plasmon Resonance and fluorescence quenching *Biophotonics* 2009;19(2):252-8.
- [85] Chen H, Kim YS, Lee J, Yoon SJ, Lim DS, Choi H-J, et al. Enhancement of BSA Binding on Au Surfaces by calix[4]bisazacrown Monolayer. *Sensors* 2007;7:2263-72.
- [86] Riquelme BD, Valverde JR, Rasia RJ. Kinetic study of antibody adhesion on a silicon wafer by laser reflectometry. *Optics and Lasers in Engineering* 2003;39(5):589-98.
- [87] Coen MC, Lehmann R, Groning P, Biemann M, Galli C, Schlapbach L. Adsorption and Bioactivity of Protein A on Silicon Surfaces Studied by AFM and XPS. *Journal of Colloid and Interface Science* 2001 Jan 15;233(2):180-9.
- [88] Yue M, Lin H, Dedrick DE, Satyanarayana S, Majumdar A, Bedekar AS, et al. A 2-D Microcantilever Array for Multiplexed Biomolecular Analysis. *Journal of Microelectromechanical Systems* 2004 April 2004;13(2):290-9.